U.S. Department of Transportation

Federal Railroad Administration

Prototype Design of a Collision Protection System for Cab Car Engineers

Office of Research and Development
Washington, DC 20590

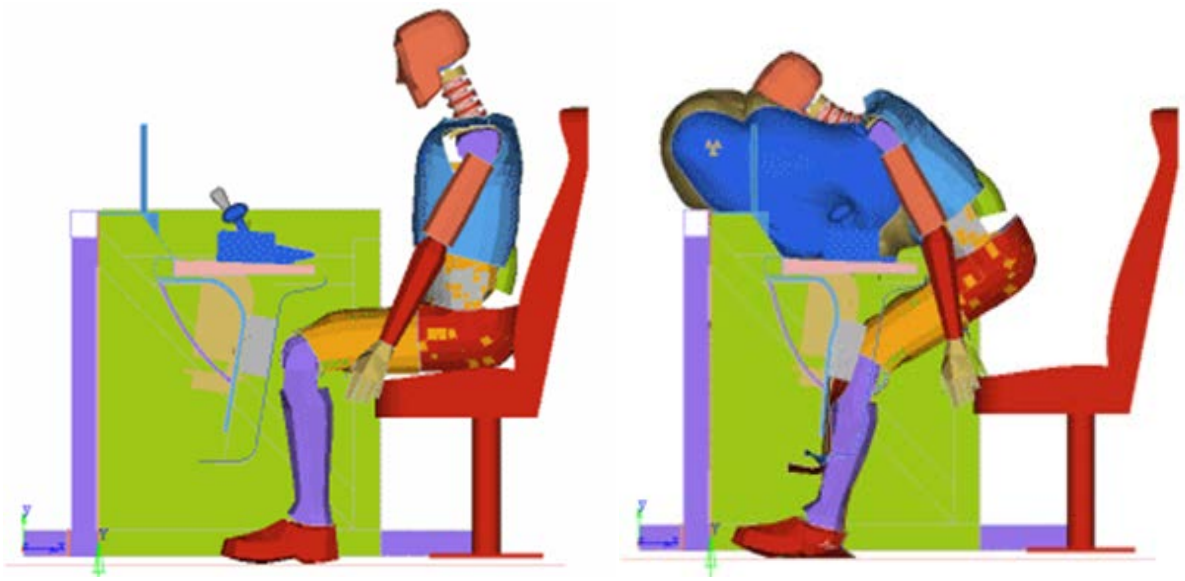

DOT/FRA/ORD-13/15

Final Report
March 2013

NOTICE

This document is disseminated under the sponsorship of the Department of Transportation in the interest of information exchange. The United States Government assumes no liability for its contents or use thereof. Any opinions, findings and conclusions, or recommendations expressed in this material do not necessarily reflect the views or policies of the United States Government, nor does mention of trade names, commercial products, or organizations imply endorsement by the United States Government. The United States Government assumes no liability for the content or use of the material contained in this document.

NOTICE

The United States Government does not endorse products or manufacturers. Trade or manufacturers' names appear herein solely because they are considered essential to the objective of this report.

REPORT DOCUMENTATION PAGE

Form Approved
OMB No. 0704-0188

1. AGENCY USE ONLY (Leave blank)	2. REPORT DATE	3. REPORT TYPE AND DATES COVERED
	March 2013	Final Report April 2012

4. TITLE AND SUBTITLE
Prototype Design of a Collision Protection System for Cab Car Engineers

5. FUNDING NUMBERS
RR28A2/HL022

6. AUTHOR(S)
Anand Prabhakaran, Som P. Singh, and Anand R. Vithani

7. PERFORMING ORGANIZATION NAME(S) AND ADDRESS(ES)
Sharma &Associates, Inc.
100 W. Plainfield Road
Countryside, IL 60525

8. PERFORMING ORGANIZATION REPORT NUMBER

9. SPONSORING/MONITORING AGENCY NAME(S) AND ADDRESS(ES)
U.S. Department of Transportation
Federal Railroad Administration
Office of Railroad Policy and Development
Office of Research and Development
Washington, DC 20590

10. SPONSORING/MONITORING AGENCY REPORT NUMBER
DOT/FRA/ORD-13/15

11. SUPPLEMENTARY NOTES
U.S. Department of Transportation
Research and Innovative Technology Administration
John A. Volpe National Transportation Systems Center
55 Broadway
Cambridge, MA 02142-1093

12a. DISTRIBUTION/AVAILABILITY STATEMENT
This document is available to the public through the FRA Web site at http://www.fra.dot.gov.

12b. DISTRIBUTION CODE

13. ABSTRACT (Maximum 200 words)

The objective of this project was to develop and analyze a passive system to protect a cab car engineer from secondary impact injuries that might be experienced due to impact with the cab console. The primary requirement for the system was the ability to compartmentalize and limit the injury indices for a 95th percentile Anthropomorphic Test Device (ATD). A baseline cab console was modified with an airbag and a crushable knee bolster to meet this objective. A computer model of an ATD impacting the cab console was validated using results from component-level tests. The modeling results indicate that the engineer protection system is capable of meeting the performance requirements. Subsequent work is planned to build and test the proposed system.

14. SUBJECT TERMS
Crashworthiness, cab console, secondary impact protection, airbags, energy absorption, crushable knee bolster, quasi-static testing, crash energy management, injury indices, finite element analysis

15. NUMBER OF PAGES
114

16. PRICE CODE

17. SECURITY CLASSIFICATION OF REPORT	18. SECURITY CLASSIFICATION OF THIS PAGE	19. SECURITY CLASSIFICATION OF ABSTRACT	20. LIMITATION OF ABSTRACT
Unclassified	Unclassified	Unclassified	Unlimited

NSN 7540-01-280-5500

Standard Form 298 (Rev. 2-89)
Prescribed by ANSI Std. 239-18
298-102

METRIC/ENGLISH CONVERSION FACTORS

ENGLISH TO METRIC	METRIC TO ENGLISH
LENGTH (APPROXIMATE)	**LENGTH (APPROXIMATE)**
1 inch (in) = 2.5 centimeters (cm)	1 millimeter (mm) = 0.04 inch (in)
1 foot (ft) = 30 centimeters (cm)	1 centimeter (cm) = 0.4 inch (in)
1 yard (yd) = 0.9 meter (m)	1 meter (m) = 3.3 feet (ft)
1 mile (mi) = 1.6 kilometers (km)	1 meter (m) = 1.1 yards (yd)
	1 kilometer (km) = 0.6 mile (mi)
AREA (APPROXIMATE)	**AREA (APPROXIMATE)**
1 square inch (sq in, in^2) = 6.5 square centimeters (cm^2)	1 square centimeter (cm^2) = 0.16 square inch (sq in, in^2)
1 square foot (sq ft, ft^2) = 0.09 square meter (m^2)	1 square meter (m^2) = 1.2 square yards (sq yd, yd^2)
1 square yard (sq yd, yd^2) = 0.8 square meter (m^2)	1 square kilometer (km^2) = 0.4 square mile (sq mi, mi^2)
1 square mile (sq mi, mi^2) = 2.6 square kilometers (km^2)	10,000 square meters (m^2) = 1 hectare (ha) = 2.5 acres
1 acre = 0.4 hectare (he) = 4,000 square meters (m^2)	
MASS - WEIGHT (APPROXIMATE)	**MASS - WEIGHT (APPROXIMATE)**
1 ounce (oz) = 28 grams (gm)	1 gram (gm) = 0.036 ounce (oz)
1 pound (lb) = 0.45 kilogram (kg)	1 kilogram (kg) = 2.2 pounds (lb)
1 short ton = 2,000 pounds (lb) = 0.9 tonne (t)	1 tonne (t) = 1,000 kilograms (kg) = 1.1 short tons
VOLUME (APPROXIMATE)	**VOLUME (APPROXIMATE)**
1 teaspoon (tsp) = 5 milliliters (ml)	1 milliliter (ml) = 0.03 fluid ounce (fl oz)
1 tablespoon (tbsp) = 15 milliliters (ml)	1 liter (l) = 2.1 pints (pt)
1 fluid ounce (fl oz) = 30 milliliters (ml)	1 liter (l) = 1.06 quarts (qt)
1 cup (c) = 0.24 liter (l)	1 liter (l) = 0.26 gallon (gal)
1 pint (pt) = 0.47 liter (l)	
1 quart (qt) = 0.96 liter (l)	
1 gallon (gal) = 3.8 liters (l)	
1 cubic foot (cu ft, ft^3) = 0.03 cubic meter (m^3)	1 cubic meter (m^3) = 36 cubic feet (cu ft, ft^3)
1 cubic yard (cu yd, yd^3) = 0.76 cubic meter (m^3)	1 cubic meter (m^3) = 1.3 cubic yards (cu yd, yd^3)
TEMPERATURE (EXACT)	**TEMPERATURE (EXACT)**
[(x-32)(5/9)] °F = y °C	[(9/5) y + 32] °C = x °F

QUICK INCH - CENTIMETER LENGTH CONVERSION

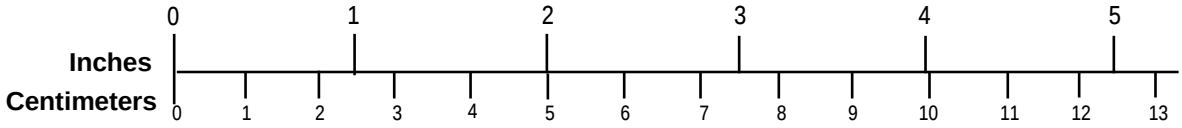

QUICK FAHRENHEIT - CELSIUS TEMPERATURE CONVERSIO

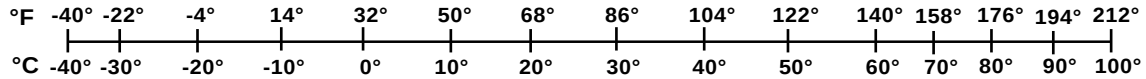

For more exact and or other conversion factors, see NIST Miscellaneous Publication 286, Units of Weights and Measures. Price $2.50 SD Catalog No. C13 10286

Updated 6/17/98

Contents

Illustrations

Tables

Executive Summary

Passenger trains are an extremely safe mode of travel in the United States. However, several train accidents over the last few years, coupled with the availability of newer technologies that could lead to safer rail travel, have prompted significant research into the science of train crashworthiness. The Federal Railroad Administration (FRA) has been funding crashworthiness research, and the John A. Volpe National Transportation Systems Center (Volpe) has been conducting pioneering research work in support of FRA. The research approach has been to propose strategies for improved crashworthiness and to apply analytical tools and testing techniques for evaluating the effectiveness of those strategies.

In a rail vehicle collision, the cab or locomotive engineer is in a vulnerable position at the leading end of the vehicle. In commuter train accidents with a conventional cab car leading, the control cab often suffers the most damage because there is little energy-absorbing structure between the occupied control cab and the front of the car. As cars with increased crashworthiness are introduced to the market, there is the potential to preserve survival space for the engineer. When sufficient survival space is preserved, the next objective is to protect the engineer from the injurious and potentially fatal forces and accelerations associated with secondary impact.

The objective of this project was to develop, analyze, fabricate, test, and validate a passive system to protect a cab car engineer from secondary impact injuries that might be experienced in moderate collision conditions. For this effort, the collision condition has been defined as a trapezoidal deceleration pulse with a peak of 23g and duration of 130 milliseconds (the 'Engineer Protection System (EPS) Test Pulse'). Below are the key functional requirements for the system:

- Compartmentalize and limit the injury indices for a 95th percentile Anthropomorphic Test Device (ATD) to values that are below those currently specified in Federal Motor Vehicle Safety Standards (FMVSS) 208
- Require no input or action by the engineer
- Allow for unencumbered exit of the engineer (current regulations, operating procedures, crew preferences, etc. do not allow the use of any seatbelt or like restraints)
- Be capable of being adapted or modified for existing cab cars and locomotives

To better understand the layout in cab cars and to avoid developing concepts and strategies that were too specific to any particular cab design, cab layouts from four agencies were studied: Metrolink in Los Angeles, CA; Metra in Chicago, IL; Long Island Railroad (LIRR) in New York; and Northern Indiana Commuter Transportation District (NICTD) in Chesterton, IN. The effort focused on identifying critical functional, operational, and ergonomic parameters such as space availability, locations of throttle and braking controls, instruments, seat position, etc., with a special emphasis on the location, size, and shape of exposed control levers (i.e. surfaces likely to pose an injury threat during a crash). The cab review also made it clear that the operator cab is a highly confined space with densely positioned equipment, which makes it hard to find room for new safety items or devices.

Based on the cab review, a composite cab layout was developed that was:

- Reasonably representative of existing cabs

- Consistent with cab occupant protection strategies, and
- Capable of meeting functional, safety, and ergonomic requirements.

As part of the preliminary research effort, the current standards, injury criteria, state-of-the-art technologies, and strategies of the automotive, heavy vehicle, and railway industry were reviewed. This effort provided critical insight into the applicability, strengths, and weaknesses of potential strategies and technology solutions. The protection strategies used in the automotive industry offered elements that could be adapted for railroad application. For example, while most current automotive strategies focus on protecting a belted occupant, the automotive industry has a long history of providing a nominal level of protection to unbelted occupants.

Several concepts that provide protection to the head, chest, torso, and femur areas were generated through a brainstorming process. Those concepts were evaluated with the following criteria in mind:

- Feasibility and acceptability
- Development timeframe
- Likelihood of success
- Contribution to overall success of strategy
- Injury index reduction
- Compartmentalization
- Egress
- Design simplicity
- Maintenance
- Comfort and ergonomics
- Weight increase
- Material and manufacturing costs

Generated concepts were ranked by a panel according to the above characteristics (weighted appropriately), and the following two were selected for further evaluation:

- Automotive passenger-style airbag with a crushable knee bolster
- Inflated Tubular Structures (ITS) with a knee airbag or crushable knee bolster

The potential effectiveness of each concept was evaluated using preliminary MADYMO™ sled test simulations with the specified EPS test pulse and a 95^{th} percentile ATD in the seat. A baseline case with no passive occupant protection features was also evaluated for benchmarking purposes.

For the baseline case, the simulations predicted injury indices well in excess of the prescribed limits. As expected, both concepts showed significant improvements in injury indices compared to the baseline case. Concept 1 (passenger-style airbag with knee bolster) showed better injury prevention or mitigation performance compared with Concept 2 (ITS with knee airbag/knee bolster), including the potential for injury indices to be within 80 percent of the limits and improved ATD kinematics. Therefore, for this project, Concept 1 was selected for further design and development efforts.

Concept 1 was then developed into a detailed design and subsequently integrated into the composite cab layout. After several design iterations, a promising arrangement for the knee bolster was determined to be a combination of a honeycomb structure and a pair of deformable brackets. The airbag was a custom design similar to those typically used in the passenger side of an automobile. It was placed with the inflator and airbag housing in the operator's desk, which allowed for optimum protection for a range of occupant positions.

This design was then modeled in detail using RADIOSS, an explicit solver, and evaluated under the prescribed 23g pulse. These detailed simulations showed that the design would meet the safety performance goals with a comfortable margin. Various properties of the airbag and knee bolster system had been defined using theoretical design values. In order to gain confidence in the simulation results, the airbag, honeycomb, and deformable brackets were tested individually and compared with individual FE simulations that replicated the corresponding tests. This provided a set of verified properties for individual elements of the protection system.

The final design of the EPS, which incorporated the airbag and knee bolster data from the characterization tests, was evaluated with a 95th percentile ATD under the specified 23g crash pulse using an updated RADIOSS model. The simulation results (presented in the table below) show that the proposed cab EPS is expected to meet the targeted safety performance with comfortable margins.

Table 1. Performance of the Engineer Protection System (EPS)

Injury Parameter	Index Limit	Calculated Injury Indices (RADIOSS Model)		
		Base Case	Pre-Component Characterization Test	Post-Component Characterization Test
HIC_15	700	9,661	104	87
Chest 3ms (g)	60	38	38	35
Femur Left (N)	10,000	20,307	7,611	7,318
Femur Right (N)	10,000	20,236	7,743	6,924
Neck Tension (N)	4,170	5,089	2,177	2,504
Neck Compression (N)	4,000	2,525	934	543
Neck Injury Criterion (Tension-Extension), N_{te}	1.0	1.39	0.60	0.77
Neck Injury Criterion (Tension-Flexion), N_{tf}	1.0	1.07	0.25	0.29
Neck Injury Criterion (Compression-Extension), N_{ce}	1.0	0.28	0.26	0.18
Neck Injury Criterion (Compression-Flexion), N_{cf}	1.0	0.82	0.26	0.25

The system is expected to add approximately 30 pounds (lb) to the car weight, which is minimal considering the safety benefits offered. The cost of these systems is likely to vary significantly depending on volume. For small volumes (100 or fewer units per year), initial estimates of material cost indicate that the system is likely to add about $3,000 per equipped cab.

The results, and the rigorous process followed to arrive at this concept, provide reasonable confidence in the value of proceeding to the next phase of the protection system development. Also, simulation results from various intermediate configurations indicate that the resulting injury indices are not overly sensitive to minor variations in properties of design elements. In other words, reasonable design flexibility is available to achieve the specified injury protection criteria. Therefore, the protection system can be adjusted to accommodate other considerations, such as ATD categories, car designs, etc.

We recommend that the performance of the proposed system be verified through a full-scale sled test and subsequent model validation in the next phase of the effort.

1. Background

Although passenger trains are an extremely safe mode of travel in the United States, several train accidents over the last few years, as well as the availability of newer technologies that could lead to safer rail travel, have prompted significant research and development into train crashworthiness. This research program was sponsored by FRA's Office of Research and Development in support of improved safety standards for passenger rail vehicles.

In a rail vehicle collision (i.e., a passenger train accident), the cab or locomotive engineer is in a vulnerable position at the leading end of the vehicle. In accidents with a conventional cab car leading, the control cab often suffers the most damage given that there is little energy-absorbing structure between the occupied control cab and the front of the car. As cars with increased crashworthiness are introduced to the market, there is potential for preserving occupant space for the engineer. In particular, full-scale impact tests have demonstrated that the engineer's space can be preserved at closing speeds up to 30 mph.

When sufficient survival space is preserved, the next imperative is to protect the engineer from the forces and accelerations associated with secondary impact. Secondary impact occurs when the rail vehicle decelerates or accelerates suddenly due to collision forces and the occupants of the rail vehicle strike some part of the interior. Given the hard surfaces and protruding knobs and controls in an operator cab, even a low speed collision can result in large, concentrated forces acting upon the engineer.

Hence, there is a significant need to develop 'Engineer Protection Systems' that can protect cab car engineers in frontal collisions (a common mode of train collision) from secondary impact injuries. Given the particular vulnerability of cab cars under these collision conditions, the initial focus is on cab cars. However, the concepts developed through this effort and the process followed could be extended in the future to freight and passenger locomotives.

The intent of this effort has been to develop a passive (i.e. without active input from the engineer) interior protection strategy for cab car and locomotive engineers, assuming that the rail car structure can preserve adequate survival space for the engineer. The occupant protection strategy should protect engineers from the secondary impact that occurs when the engineer strikes the control console.

2. Objectives and Scope

The objective of this project was to develop, analyze, fabricate, test, and validate injury prevention and mitigation strategies to protect a cab car engineer under collision conditions similar to those of the full-scale multilevel car test. The selected strategy and corresponding design will have the following key characteristics:

- Protect engineers from the secondary impact that occurs following a frontal train collision when the engineer strikes the control console.
- Require no action from the operator to trigger the system.
- Allow for unencumbered exit of the engineer. Seatbelts or other systems that must be disengaged before the operator can flee the cab will not be incorporated into the design. A successful protection strategy must not inhibit the engineer from emergency egress.
- Provide compartmentalization of a 95th percentile anthropomorphic test device (ATD) and measured injury criteria for the ATD's head, chest, neck, and femur that are below the limits currently specified in the Federal Motor Vehicle Safety Standards (FMVSS) 208 [1], when tested under the EPS Test Pulse (see figure 1).

2.1 Scope

The scope of this project is to develop a passive (i.e. not requiring operator input) safety system for a train engineer in a cab car, and includes the following objectives:

- Develop a representative and generic control stand geometry, applicable to cab cars, with the appropriate material and space representations.
- Develop design concepts to protect the engineer from secondary impacts, following the key criteria outlined above.
- Identify the most promising design concept in consultation with Volpe and develop the concept into a design suitable for evaluation.
- Evaluate the performance of the selected concept for compliance with FMVSS criteria, using the appropriate analytical techniques, and refine the design as needed to meet those requirements.
- Develop, build, and characterize by test, the individual components that make up the system, and update the analytical models based on the test results.
- Re-evaluate system performance using the revised component models, and update the design, if needed, to meet FMVSS performance requirements.

2.2 Performance Requirements

The occupant protection system shall be designed to limit human injury to a 95th percentile, Hybrid III, male ATD, to the injury criteria values outlined in section 2.2.2, when subjected to the EPS test pulse defined in section 2.2.1. The system shall also effectively compartmentalize the occupant as outlined in 2.2.3. System performance shall be demonstrated under dynamic sled test conditions performed in accordance with 49 CFR Part 572, Subparts B and E, with the

ATD positioned in accordance with SAE AS8049. An analytical demonstration is intended under this (currently reported) phase of the effort, and a physical demonstration is planned under the next phase.

2.2.1 Cab Performance

The occupant protection system should be designed to be effective when subjected to the acceleration pulse and the corresponding secondary impact velocity (SIV) profile shown in Figure 1. This test pulse has an SIV similar to the SIV from the multilevel single car test [2]. The crash pulse is hereinafter referred to as the 'EPS Test Pulse' and is outlined in Table 2.

Table 2. Test Crash Pulse

Time (s)	Acc. (g)
0.00	0.0
0.01	23.0
0.03	23.0
0.13	0.0

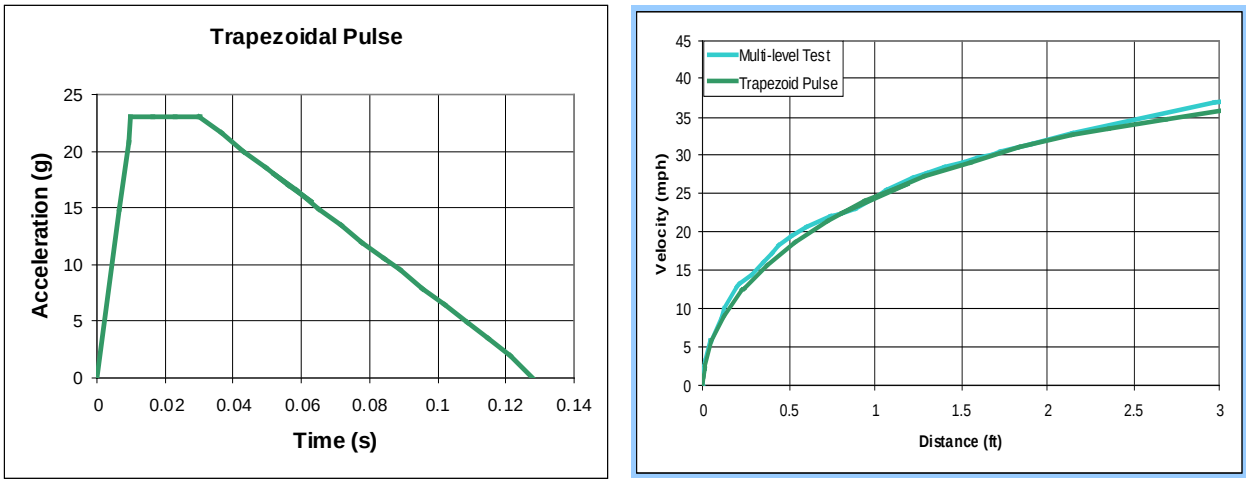

Figure 1. Crash Acceleration Pulse and Secondary Impact Velocity for EPS Test Requirements

2.2.2 Occupant Response

The injury measurements taken by the ATD must meet the following criteria, which are derived from CFR 49 Part 571, Standard No. 208; Occupant crash protection.

Table 3. Limiting Injury Indices

Injury Criterion	Limiting Value
HIC_{15}	<700
N_{ij}	<1.0
Neck Tension	<937 lbf (4,170 N)
Neck Compression	<899 lbf (4,000 N)
Chest Deceleration	<60g over a 3ms clip
Axial Femur Loads	<2,250 lbf (10,000 N)

2.2.3 Compartmentalization

Occupant kinematics should demonstrate that the occupant is effectively compartmentalized within the cab area by the occupant protection system. For this effort, compartmentalization is a design strategy that aims to contain the engineer between his or her seat and the console during a collision, preventing the engineer from traveling over consoles and impacting other hostile objects. During sled testing, ATD compartmentalization is evaluated up until the point of maximum forward progress of the ATD. The ATD must be confined between the console (potentially deformed) and the seat until the ATD begins to rebound and move away from the impacted console.

The following sections address and describe these tasks along with the underlying approach used to achieve the associated objective(s) and the results accomplished.

3. Development of a Baseline Cab Layout

As noted, the focus of this study is on developing concepts to improve the survivability of engineers in cab cars under a frontal collision scenario. Traditionally, cab cars have a relatively cramped operator layout with a high probability for impact with hostile surfaces during an accident. While most cab car configurations use a desk style control stand, there are significant variations in layout. To avoid developing a concept too specific to one design or layout, we conducted a comprehensive review of several existing cab car configurations used in commuter train operations. The goal of these reviews was to gather information and data on cab layout and cab designs that are currently in use, with respect to engineer seating, control layout, spatial considerations, etc. These data describe the overall cab layout, including geometry, protrusions, materials, seat layout, measurements, and photographs. Subsequently, key and common elements of the design were extracted to develop a 'baseline' cab, on which subsequent work was based.

3.1 Cab Studies and Measurements

Cab information was gathered from four large commuter rail operators:

1. Metrolink in Los Angeles, California
2. Metra in Chicago, Illinois
3. Long Island Railroad (LIRR) in New York
4. Northern Indiana Commuter Transportation District (NICTD) in Chesterton, Indiana

The Metra cab car and the NICTD EMU car were manufactured by Nippon Sharyo. LIRR cab cars were built by Kawasaki Heavy Industries, Ltd. Metrolink cab cars were built by Bombardier, Inc. Photographs of the cabs for the LIRR, Metrolink, and Metra cabs are shown in Figure 2, Figure 3, and Figure 4, respectively.

Figure 2. Engineer Chair, Console, and Control Panel Layout for the LIRR Cab Car

Figure 3. Metra Car Cab Console Views – Top of and Underneath the Engineer Desk

Figure 4. Metrolink Car Cab Console Views

3.2 Key Measurements

To facilitate a comparative evaluation of the cab from architectural, spatial, and construction perspectives, measurements of cab dimensions, location of throttle and brake controls, engineer seat height and location relative to the console and cab walls were made. Information was collected on the materials used for various cab elements. The architectural, geometry, and material data are shown in the following tables.

Table 4. Summary – Control Desk Architecture of the Surveyed Cabs

	LIRR	Metra	Metrolink	NICTD
Has overhead console?	No	Yes	Yes	Yes
Has left control panel?	Yes	Just an LCD screen	Yes	Yes
Has right control panel?	Yes	No	No	No
Has footrest?	Yes	No	Yes	No
Exposed equipment under desk?	Sparsely populated	Densely populated	Sparsely populated	Sparsely populated
Throttle controller location	Control desk – center	Control desk – center	Control desk – right	Control desk – center right
Brake controller location	Control desk – center	Control desk – right	Control desk – left	Control desk – center right
Has foot operated switches?	Yes, both feet	Yes, left foot	Yes, left foot	Yes, left foot
Has armrests on seats?	No	Yes	No	Yes

It may be noticed from Table 4 that, generally, cabs have extensive equipment under the desk protruding into the engineer's knee area. The throttle controller is generally either in the center or right of the engineer's seat. In some cases, the brake controller is located with the throttle controller in the center. The armrest and footrest are not standard features.

The geometric dimensions of the four cabs are shown in Table 5. The most important dimensions in the table in terms of injury potential from secondary collision are seat base to desk edge clearance, height of desk edge from cab floor, and the clearance from the engineer's torso position to the desk edge. These parameters range from 13.5 to 18.5 inches (in), 26.5 to 30.63 in, and 5 to 14.7 in, respectively. The wide range of the torso to desk edge clearance is due to the 6 in longitudinal adjustment to the engineer's seat to accommodate a range of femur lengths.

Table 5. Spatial Layout Summary of the Surveyed Cabs

	LIRR	**Metra**	**Metrolink**	**NICTD**
Chair base column to edge of control desk	18.5 in	13.5 in	14 in	13.5 in
Longitudinal seat adjustment range	6 in	6 in	No Data	6 in
Chair base column to right wall	15.25 in	15.5 in	14 in	15.5 in
Height of desk leading edge from floor	29.5 in	30 in	26.5 and 30.63 in	30 in
Height of desk edge on the far side	36.5 in	35.5 in	38 in	36 in
Torso – desk longitudinal clearance**	12.5– 18.5 in	5– 11 in	8.7– 14.7 in	5– 11 in
Torso – controller longitudinal clearance**	13– 19 in	7.5– 13.5 in	7– 13 in	12– 18 in
Knee – desk longitudinal clearance*	-1– 5 in	-2– 4 in	-2– 4 in	-3– 3 in
Chair base column to edge of control desk	18.5 in	13.5 in	14 in	13.5 in

* Seat adjustment range assumed to be 6 in
** Clearances are approximate and based on a sitting position with feet on the floor and thighs parallel to the floor.

The materials used in the cabs for the control desk, left and right control panel, seat and footrest are listed in Table 6. In all cases, the control desk and engineer seat base are constructed of steel. The seat bottom and back are made of foam and the control panels are made of plastic with housing constructed of steel.

Table 6. Summary – Cab Construction Materials

	LIRR	**Metra**	**Metrolink**	**NICTD**
Left control panel	Mainly steel, bank of plastic coated switches	LCD screen in steel housing	Mainly steel, bank of plastic coated switches	LCD screen in steel housing, steel panel
Right control panel	Mainly steel, bank of plastic coated switches	N/A	N/A	N/A
Control desk	Steel	Steel	Steel	Steel
Footrest	Steel	N/A	Steel	NA
Seat	Steel base and column, foam seat	Steel base and column, foam seat	Steel base and column, foam seat	Steel base and column, foam seat

To help develop an overall perspective for these cab layouts, Computer Aided Design (CAD) models were developed using the geometric measurements listed in Table 5. The CAD models permitted the team to study the layouts from various views—plan, end, side, and cross sections—at different positions along the longitudinal direction. These CAD models are presented in Figure 5.

Metrolink

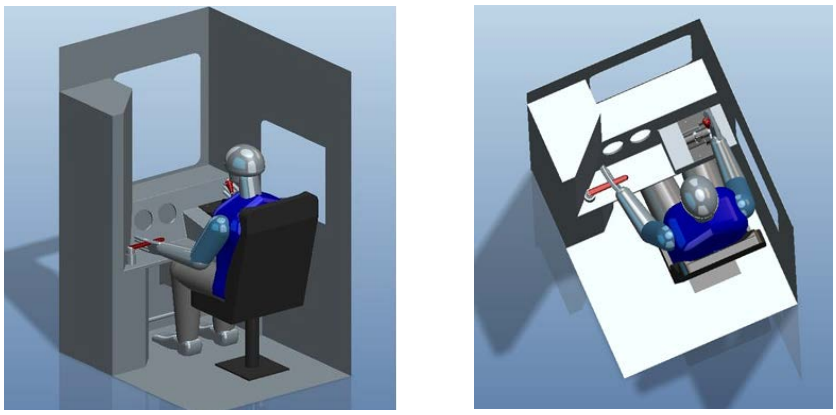

Metra

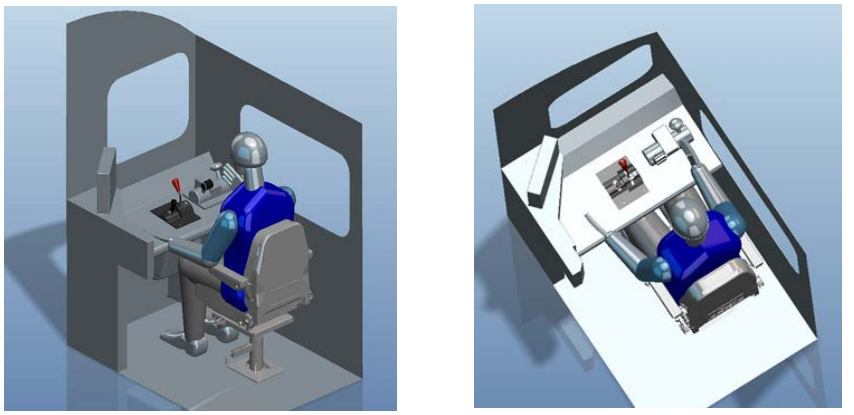

LIRR

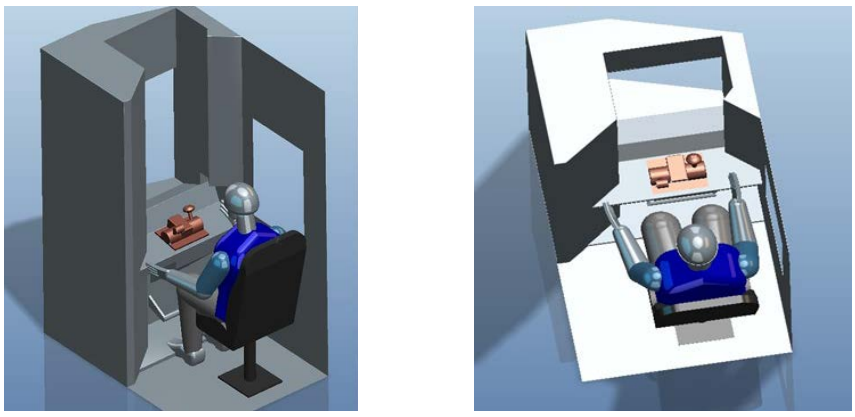

NICTD

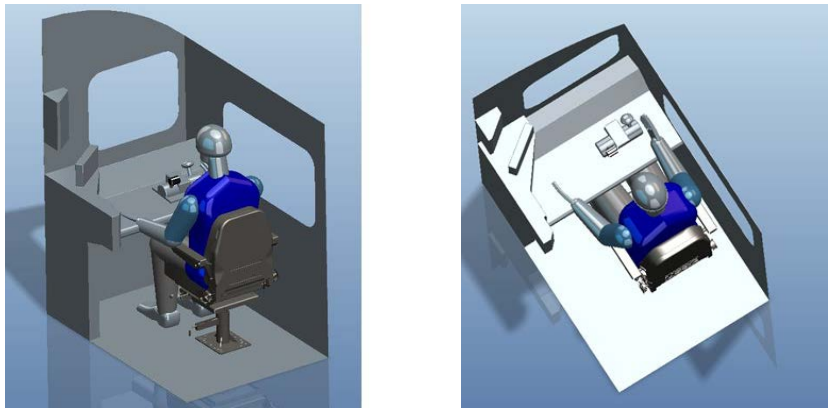

Figure 5. CAD Representations of Measured Cab Consoles

3.3 Baseline Composite Cab Layout

Critical functional, operational, and ergonomic parameters, such as throttle and braking controls, instruments, seat position, etc., were reviewed to develop the composite baseline cab. Special focus was placed on location, size, and shape of exposed control levers, as well as on surfaces likely to pose injury potential during a crash. To develop a composite cab layout amenable to a cab occupant protection strategy, the following requirements regarding functionality, safety, ergonomics, and overall cab space, were applied:

- All existing functionality shall remain unchanged.
- Any new geometry, instrument, lever, or surface feature introduced shall not interfere with safe operation of the equipment.
- Any new geometry, instrument, lever, or surface feature introduced shall not create potential for injury during crash.
- Frontal and side vision fields shall not be impacted.
- Control levers, handles, buttons, and knobs shall be within operational reach of 5^{th} percentile adult female to 95^{th} percentile adult male.
- Cab occupant space shall not be adversely affected.

With the criteria listed above, desk architecture (throttle and brake control levers and panels), desk geometry (height, width, and depth), and engineer seat position were selected. These are presented in Table 7 and compared with existing cab designs in Figure 6.

Table 7. Proposed Cab Geometry Dimensions

Dimension	Value	Selected Style Basis	Remark
Desk Height	30.0 in	LIRR, Metra, NICTD	Floor to Desk Top Leading Edge
Desk Depth	24.0 in	Metra, NICTD	Window Wall to Top Leading Edge
Desk Width	41.0 in	Metra, Metrolink, NICTD	
Desk Console Thickness	2.25 in	NICTD	Leading Edge Side
Desk Leading Edge to Chair Base Column	13.5 in	Metra, Metrolink, NICTD	Leading Edge Side

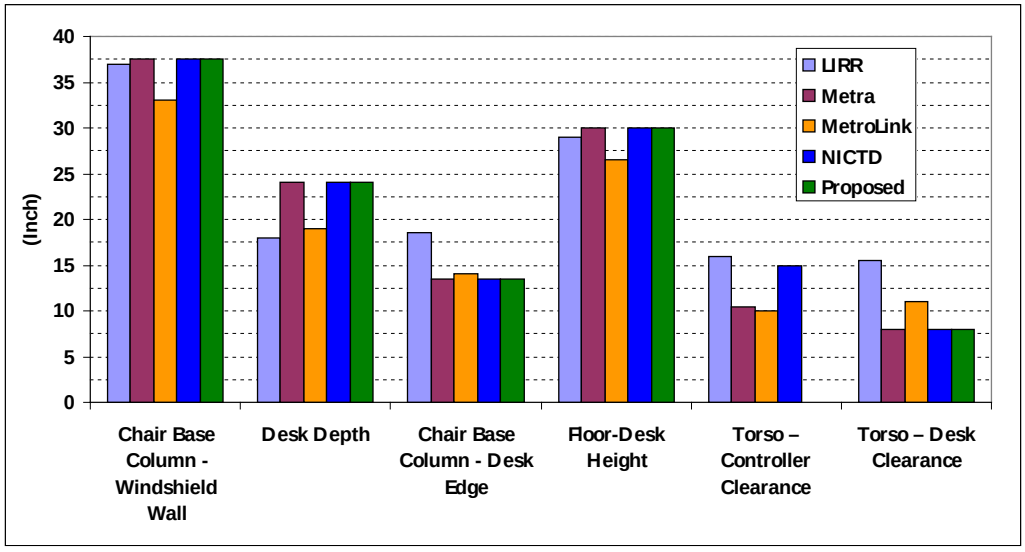

Figure 6. Summary of the Reviewed Cab Geometric Dimensions and the Proposed Cab Parameters

The selection of these values reflects general practice in the industry for desk geometries. However, the location of throttle and brake controllers was chosen to accommodate the need for an occupant protection system—most likely to be installed on the desk. The presence and location of other items such as radio, console, and footrest, and their selection rationale are listed in

Table 8. The throttle and reverser control was placed right of center to keep the top and under desk center free for head, chest, torso, and knee protection system(s). The baseline design did not incorporate a footrest or pedal in order to eliminate the potential for foot injury.

Table 8. Cab Equipment

Feature/Item	Location	Selected Style Basis
Throttle and Reverser	Right of Center	Metrolink
Brake Control Lever	Left of Center	Metrolink
Telephone/Radio Cradle	Left	LIRR, Metrolink, Metra
Overhead Console	Yes	LIRR, Metra, Metrolink, NICTD
Right Console	No	LIRR, Metra, Metrolink, NICTD
Left Console	Yes	LIRR, Metrolink, NICTD
Foot Rest	None	
Foot Operated Switch	Left	LIRR, Metrolink, NICTD

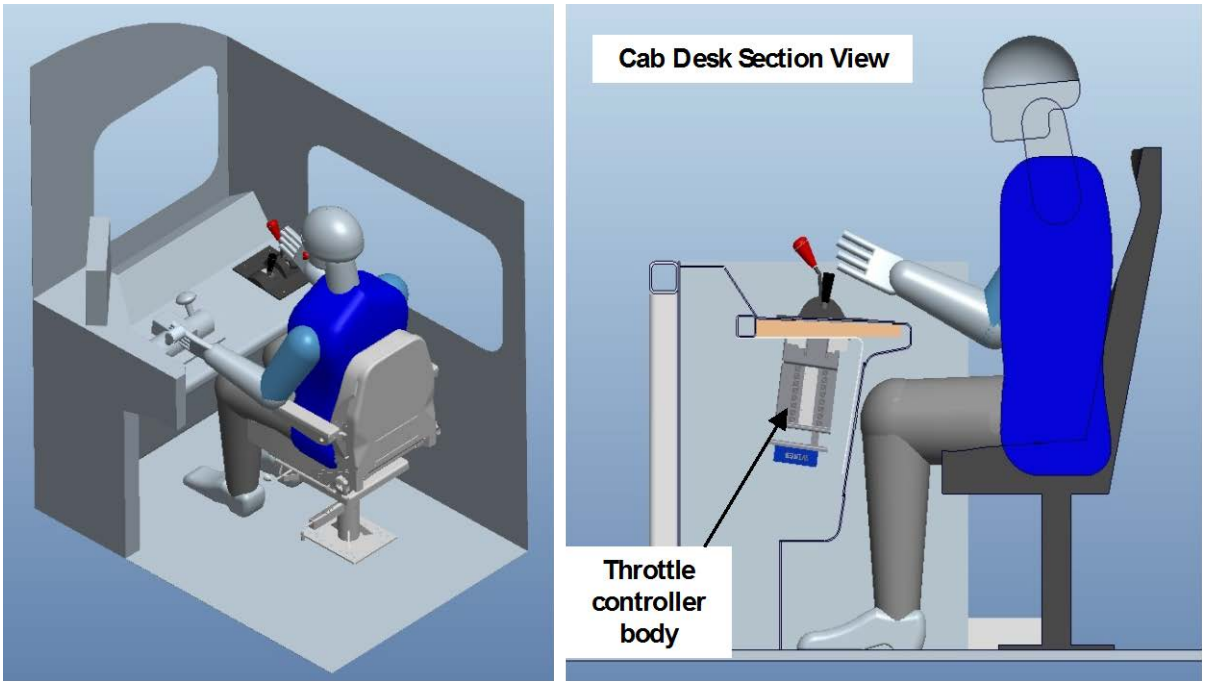

Figure 7. Composite Cab Layout

3.4 Summary

Based on a detailed review of four cabs from four different transit agencies, the project team developed a baseline cab design that represented a fair composite of the reviewed cabs, provided functionality, space, and ergonomics that was similar to the reviewed cabs, and provided opportunities for accommodating EPS components.

The baseline cab concept was subsequently developed into a detailed design, suitable for fabrication, using appropriate CAD software.

4. Review of Protection Strategies and Standards

To guide the process of developing an EPS, the project team conducted a detailed review of literature, standards, and state-of-the-art technologies for occupant protection systems used in the automobile, heavy vehicle (bus and truck), and railroad industries.

A key goal of this effort was to understand the approach, strategy, and protection system elements used in other industries—particularly, the automobile industry, and to consider the potential applicability to this cab engineer protection effort.

Another goal was to review the injury criteria and standards used for occupant protection to ensure that we were working towards the appropriate injury index targets in this effort.

This review is presented in detail in Appendix A. This section summarizes the key findings.

The protection strategies used in the automotive industry offer elements that can be adapted for railroad application. Large airbags, similar to those used on the passenger side of automobiles, offer good protection for the cab engineer's head and upper torso under frontal impact. Furthermore, the knee airbag or knee bolster type arrangement used for the automobile driver positions can also be adapted to protect the cab engineer's knee against impact forces resulting from the unbelted engineer moving against the desk and the knees impacting equipment protrusions under the desk.

Table 9 presents the rail industry standards that were reviewed as part of this effort, and Table 10 presents the automotive and heavy vehicle standards that were reviewed. The review indicated that although the impact and crash scenarios, the resulting crash pulses, and the sled test requirements for the automobile and railway industry are prescribed differently, the limiting injury criteria used are quite comparable.

The review also established that the set of limiting injury indices adopted for this effort was reasonable and consistent with other efforts, thereby providing additional confidence in the requirements laid out.

Table 9. Summary of the Railway Vehicle Interior Design and Occupant Protection Recommended Practices and Standards

Document	Type	Description	Effective	Region/ Country	Governing Body
49 CFR PART 238		PASSENGER EQUIPMENT SAFETY STANDARDS		USA	U.S.-DOT-FRA
49 CFR PART 238.233	S	Subpart C – Specific Requirements for Tier I Passenger Equipment - Interior Fittings and Surfaces	1999	USA	U.S.-DOT-FRA
49 CFR PART 238.435	S	Subpart E – Specific Requirements for Tier II Passenger Equipment Section - Interior Fittings and Surfaces	1999		
49 CFR PART 238.447	S	Subpart E – Specific Requirements for Tier II Passenger Equipment	1999		
AAR-MSRP Section M - RP-5104	RP	Locomotive Cabs	1974		AAR
AAR-MSRP Section M - RP-5128	RP	Diesel Locomotive Control Stand for New Locomotives	1975		
AAR-MSRP Section M - RP-5132	RP	Rounding All Possible Exposed Convex Edges and Corners	1971		
APTA SS-C&S-011-99 Rev.1 (3-22-04)	S	Standard for Cab Crew Seating Design and Performance	1999		APTA
APTA SS-C&S-016-99 Rev.1 (3-22-04)	S	Standard for Row-to-Row Seating in Commuter Rail Cars	2004		
APTA SS-C&S-016-99 Rev.2	S	Standard for Passenger Seats in Passenger Rail Cars	2010		
EN12663, July 2000	S	Structural Requirements for Railway Vehicles	2000	Europe	European Committee for Standardization
EN15227 Final Draft 2007	S	Crashworthiness Requirements of Railway Vehicle Bodies	2009	Europe	European Committee for Standardization
AV/ST9001, Issue One, February 2002	S	Vehicle Interior Crashworthiness – ATOC Vehicle Standard	2002	UK	Association of Operating Companies
GM/RT2100, Issue One, July 1994	S	Structural Requirements for Railway Vehicles	1994		Safety & Standards Directorate
GM/RT2100, Issue Four	S	Requirements for Rail Vehicle Structures	2010		Railway Safety and Standards Board
SAF/STD/0057/RSK, Version 2.1, Dec. 2004	S	Rolling Stock Structural Requirements	2009	Australia	Queensland Railway Governance and Management Framework

S: Standards, RP: Recommended Practices

Table 10. Summary of Automotive Crashworthiness Standards

Document	Description	Effective	Region/ Country	Governing Body
ECE R-80	Seats of Large Passenger Vehicles	1989, 2009 (Rev 2)	Europe	Economic Commission for Europe (ECE)
ECE R-29	Protection of the Occupants of the Cab of Commercial Vehicles	1993, 2007 (Rev 1)	Europe	ECE
ECE R-33	Vehicle Structure in Head-On Collision	1995, 2008 (Rev 3)	Europe	ECE
ECE R-66	Strength of the Superstructure of Large Passenger Vehicles	1995, 2008 (Rev 1)	Europe	ECE
FMVSS 201	Occupant Protection in Interior Impact	1968, Rev. 2008	USA	U.S.-DOT
FMVSS 222	Passenger Protection in Commercial Vehicles (Used for School Buses)	1968, Rev. 2008	USA	U.S.-DOT
FMVSS 208	Occupant Crash Protection	1977, Rev. 2008	USA	U.S.-DOT
ADR 69	Vehicle Standard (Australian Design Rule 69/00 – Full Frontal Impact Occupant Protection) 2006 Compilation 1	2007	Australia	Australia DOT and Regional Services
ISO 3471	Rollover Protection in Construction Equipment	1986, Rev. 2008	Worldwide	

5. Concept Development

Based on the requirements identified earlier, review of cab configurations, and knowledge of strategies employed elsewhere, several concepts to provide occupant protection in impact situations were developed. The viability of these various concepts was then evaluated using a set of objective criteria; subsequently, top ranked concepts were qualitatively analyzed using the appropriate simulation tools. The activities are described in the following subsections.

5.1 Development of Concepts

To initiate the concept development effort, the project team conducted a brainstorming session. The brainstorming session included staff from Volpe, Sharma & Associates, and Altair (occupant protection system design and simulation experts). The team identified several ideas for occupant protection focused on providing protection individually to the head, chest, torso and femur areas.

Ideas to protect the head included passenger-style airbags, deployable nets, local softening of contact surfaces, recessed control levers, drop down bolsters, neck braces, etc. Similarly, chest protection ideas included shaping of the console, use of honeycomb, airbags, a desk with an energy absorbing longitudinal stroke, knee activated torso bolster, ITS, relocation of controls, etc. Femur protection ideas included deformable bracket, honeycomb, knee airbags, inflated tubular structures, hydraulic dampers, etc. A complete list and associated descriptions for these ideas are included in Appendix B.

Each idea was rated with respect to the following four (4) criteria with a rating of high (H), medium (M) or low (L) by each team member:

- Feasibility and acceptability
- Development timeframe
- Likelihood of developing successful design
- Contribution to overall goals (success)

The ideas that were ranked near the top were then paired and combined to develop nine possible concepts for the head and chest protection and six ideas for femur protection. These fifteen elements were rated using the nine weighted criteria listed in Table 11.

Table 11. Evaluation Criteria and Weights for Cab Occupant Protection System Concepts

Weight	Criteria	Comment
5	Injury Index Reduction	Can the concept contribute significantly towards limiting injury criteria?
5	Compartmentalization	Can the concept help to keep the operator in his/her seat?
5	Affect Egress	Does the concept allow reasonable egress?
4	Feasibility	Is the concept feasible to develop and implement within the time constraints of this project?
3	Simplicity of Design	Does it have complex mechanisms or are there many variables to control?
3	Maintenance	Does the concept increase maintenance time or add new inspection requirements?
3	Comfort and Ergonomics	Is operator comfort or control ergonomics likely to be affected by the concept?
1	Weight Concerns	Will the concept adversely increase the weight of the cab?
1	Material Costs	Are material costs comparable to other concepts?
1	Manufacturing Costs	How easily can the system (desk, seat, and protection elements) be manufactured?

The weighted score was then used to rank the more viable options. The overall scores and ratings are shown in Appendix C and the resulting rankings are listed in Table 12.

Table 12. Selected Concept Elements for Head, Torso, and Femur Protection

Concept Element	Score Rank
Head and Chest	
Passenger Style Airbag	1
Passenger Style Airbag + Tethers	2
ITS (Inflatable Tube Structures)	3
Shaping the Console	4
Crushable Console (Honeycomb or Foam)	5
Local Softening	6
Cantilevered Bolster	7
Dropdown Bolster + Shaping the Console	8
Rotating Frame + ITS	9
Femur	
Honeycomb or Foam	1
Knee Airbag	2
Deformable Beam Bracket + Honeycomb/Foam	3
ITS	4
Tube in Tube	5
Hydraulic Damper	6

To develop the overall protection system, the following three concepts were formulated based on the elements listed in Table 12:

- Passenger Style Airbag + Knee Bolster
- ITS + Knee Airbag (or Knee Bolster)
- Crushable Desk + Crushable Knee Bolster

Analysis of the third concept by the Volpe team using a simplified MADYMO model concluded that it was not a viable solution. Based on preliminary simulations, it was not possible to protect the head and neck adequately without an airbag. Therefore, subsequent effort was focused on the first two concepts. CAD representations of the two concepts are shown in Figure 8 and Figure 9.

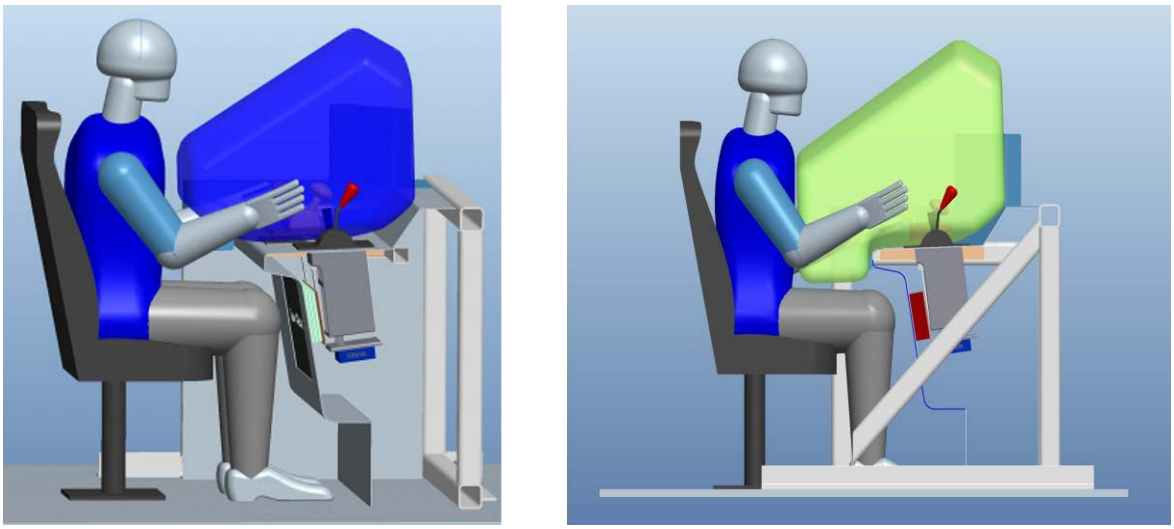

Figure 8. Occupant Protection System - Concept 1 – Airbag + Knee Bolster

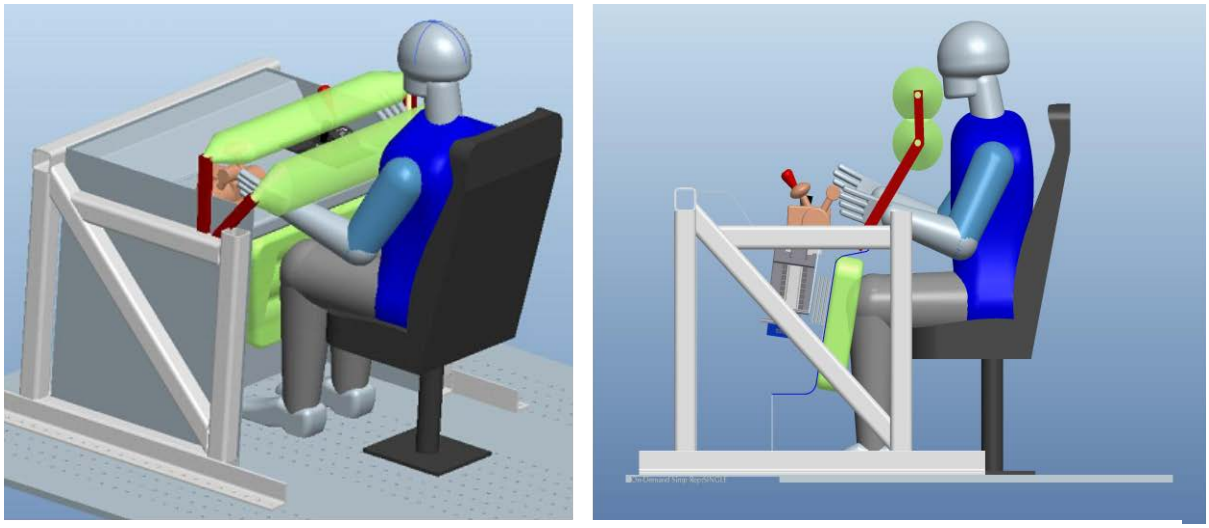

Figure 9. Occupant Protection System - Concept 2 – ITS + Knee Airbag

5.2 Preliminary Evaluation of Concept Viability

The intent of these preliminary simulations was to identify the strengths and weakness of the concepts, thereby helping to select a configuration for further development and detailed design. MADYMO [3] models of the two concepts were developed, including an ATD in the cab seat, and a desk with the deployable elements. For this initial modeling, typical passenger-style airbag and knee bolster properties from an automotive application were used. The initial properties were intended to serve as starting points for the analysis, not design targets. The EPS test pulse shown in Figure 1 and a 95th percentile adult male ATD were used. A baseline run was made with no head, torso, or knee protection system. Several variants of the two concepts were investigated, and a detailed description of this preliminary modeling effort is presented in Appendix D. The following section highlights the key findings.

5.2.1 Key Results

Injury indices for selected cases are presented in Table 12. Results show that the baseline case (no occupant protection system) produces injury indices for head, chest, neck, and femur, which are significantly higher than the prescribed limits. A quick review of the kinematics shows the ATD knees making the first contact below the console resulting in high femur loads, followed by the torso and then the head striking the console with significant force.

Several variants of Concept 1 (airbag + knee bolster) yielded positive results, and the target injury criteria were met in these cases. Improved performance was observed when airbag venting was eliminated to provide better resistance to occupant head travel, reducing the injury indices to below 80 percent of the limits. Kinematics show an initial knee hit against the deformable knee bolster with nominal femur loads, followed by rotation of the upper torso and head about the pelvis, with the head and torso striking the airbag and riding down with low acceleration (see appendix D); the moderate HIC values were the result of a late head strike against the console. As the design was further developed, better airbag design and deployment was implemented, eliminating the head strike, and resulting in improved HIC values (under 200). The peak neck injury values, while within limits, were also observed during the late head strike.

Concept 2 also offered significantly better performance than the base case, with significant reductions in injury indices. However, depending on the particular design variation, one or the other injury criteria was close to the target limit. Table 12 presents one case (with no vents and the ITS units moved back) that showed reasonable injury results. The kinematics generally consisted of initial knee contact with nominal femur loads followed by near simultaneous contact of the head and torso with the ITS systems with relatively high (but below the limit) HIC and chest accelerations. Additionally, it was felt that the kinematics of the ATD were less than ideal, due to the rebounding seen after impact.

Table 13. MADYMO™ Simulation Results for the Two Concepts and the Baseline

Injury Response	Requirements 95th% ATD	Baseline		Concept 1 (Airbag + Knee Bolster)		Concept 2 (ITS + Knee Bolster)	
		No Protection	% of Target	W/O Front Wall Contact and No Vents	% of Target	No Vents	% of Target
HIC_15	700	84,318	**12,045 %**	531	76%	617	**88%**
Chest 3ms (g)	60.0	75.3	**126%**	43.3	72%	60.0	**100%**
V*C (m/s)	1.0	0.44	44%	0.45	45%	0.70	70%
Femur Left (N)	10,000	15,556	**156%**	5,825	58%	6,308	63%
Femur Right (N)	10,000	15,554	**156%**	5,826	58%	6,919	69%
Neck Tension (N)	4,170	11,262	**270%**	2,495	60%	1,210	29%
Neck Comp. (N)	4,000	4,509	**113%**	113	3%	473	12%
N_{te}	1.00	3.44	**344%**	0.75	75%	0.62	62%
N_{tf}	1.00	1.95	**195%**	0.70	70%	0.43	43%
N_{ce}	1.00	0.27	27%	0.13	13%	0.04	4%
N_{cf}	1.00	2.15	**215%**	0.03	3%	0.32	32%

xx Exceeds 100% of requirements
x Exceeds 80% of requirements

5.3 Summary

Two concepts for cab engineer protection were developed using a rigorous process and with careful consideration of all parameters. The developed concepts, as well as a baseline (no protection) version, were further evaluated using MADYMO simulations.

For the baseline case, the simulations predicted injury indices well in excess of the prescribed limits.

As expected, when compared with the baseline case, both protection concepts showed significant improvements for all injury indices. Concept 1 (passenger-style airbag and knee bolster) showed better performance compared with Concept 2 (ITS with knee bolster), offering better ATD kinematics and the potential for all injury indices to be within 80 percent of the limits. For Concept 2 (ITS), chest injury index values were close to the limits, in addition to having

unfavorable rebounding kinematics of the occupant due to the lack of energy absorption for the upper torso in that concept. Therefore, for this project, Concept 1 was selected for further design and development efforts.

6. Detailed Design

The EPS identified as Concept 1 (Airbag + Knee Bolster) was then developed in detail, with subsequent evaluation and refinement. Upon successful evaluation of the system's effectiveness, the design was documented using engineering drawings.

The selected concept consisted of two main modules: an automotive passenger-style airbag for head and torso protection, and an energy absorbing knee bolster for knee protection. The airbag model was derived from an existing passenger-style airbag commonly used in the automotive industry, which was enlarged for this application. The energy absorbing knee bolster was developed after evaluating several different concepts and iterations for each concept.

6.1 Airbag System Design

The airbag system is composed of an airbag and an inflator, both of which are housed in a standard automotive packaging format. The proposed system uses a relatively large, custom-design airbag similar to an automotive 'passenger-style' airbag, and an off-the-shelf inflator model # PH-5 from Key Safety Systems (KSS). The airbag cushion is 28 in (700 mm) long and 18 in (450 mm) wide, with a volume of 5.5 cubic feet (155 liters), and two sets of internal tethers to control the desired deployed shape. The airbag dimensions and other key details of the system are presented in Figure 10 and Figure 11.

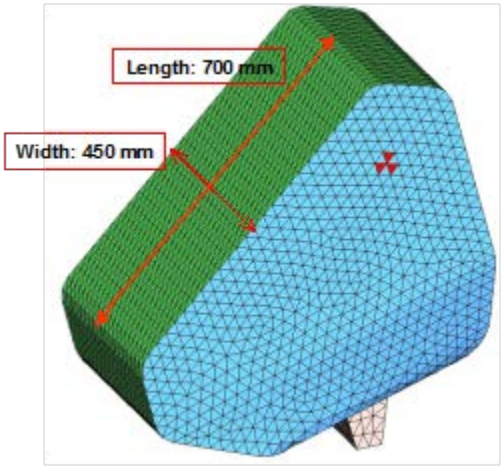

Figure 10. Airbag Shape

Airbag Configurations;

- **700mm length cushion**
- **450mm width cushion**
- **155 liters cushion volume**
- **upper / lower tether (510 / 400 mm)**
- **No vents / 2 x 10mm vents**
- **PH-5 inflator, 700kPa (10ms time delay)**

Description Airbag Module:
• Single occupant, automotive passenger style
• Production-based design
• Module weight approx. 3.9kg

Inflator:
• Hybrid or pyrotechnic technology. 12 V connection
• Single or dual-stage inflator (700 - 500KPa)

Cushion:
• 155 liter tethered cushion. Sewn construction
• Material un-coated 630 denier PA6.6 nylon fabric

Housing:
• 1008/1010 Steel

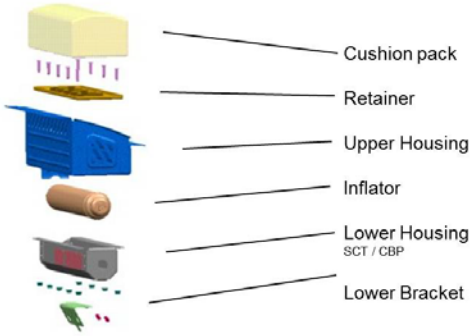

Figure 11. Airbag Module Details

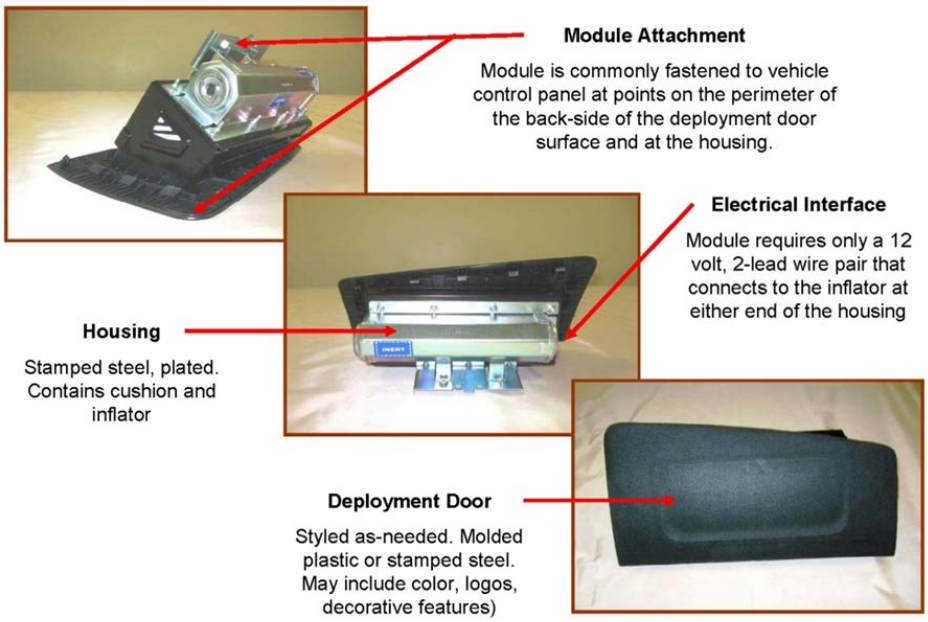

Figure 12. Airbag Assembly Components

The airbags are generally triggered by an external trigger control module. On an actual automobile (or future railcar application), the trigger module receives input from acceleration sensors, and based on the appropriate severity of the sensor input, triggers the deployment of the airbag. For a sled test application, the trigger module is contained in the sled test apparatus, and is triggered based on a preset Time-To-Fire (TTF).

On a future rail car application, the expected deceleration pulses under a nominal set of actual impact conditions would be reviewed to determine car design-specific TTF characteristics. Analytical system performance using a validated model under these nominal crash pulses would be used to further refine the TTF design. In the final implementation, TTF can be controlled to best suit design intent through either a predefined time following pulse detection, or an acceleration magnitude trigger with delay.

The airbag housing is generally constructed of steel (stamped and plated) and houses the airbag and the inflator (see Figure 12). The housing is commonly fastened to the vehicle control panel at various distributed points. Note that this picture shows an example airbag assembly and that the deployment door design will need to be different in its final implementation for the current application. Figure 13 provides overall dimensions of the airbag housing.

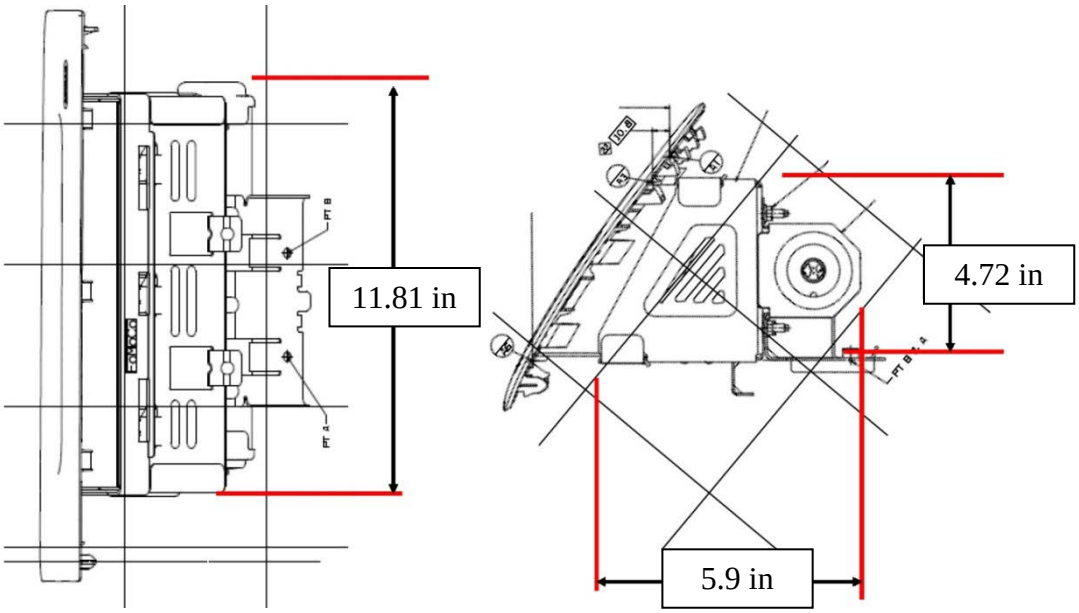

Figure 13. Airbag Housing Dimensions

The inflator selected (model: PH-5) is a dual stage model with a pressure rating of 700kPa (101.4 psi), and a diameter of 45 mm (1.77 in). Figure 14 below shows an image of the PH-5 inflator.

Figure 14. PH-5 Inflator

A dual stage inflator can receive two successive trigger signals to initiate full deployment. In certain automotive crash conditions, such as a child being seated facing the airbag, only the first of two stages may be triggered. Modern airbag inflators are generally two stage inflators as required by recent standards and regulations in the automotive industry. The two stages are usually phased 10 milliseconds (ms) apart in a deployment.

Inflators are characterized using an automotive industry standard "Constant Volume Inflation Test." In this test, full flow from the inflator is directed towards a constant control volume (pressure vessel) with a volume of 60 liters. The pressure rise in this control volume is monitored continuously. The time history of pressure rise in this control volume is the test output, which is a measure of the flow rate and capacity of the inflator. Most simulation codes take the output of this test as direct input into the airbag module. Off-the-shelf inflators are pretested and are supplied with this information by the airbag system suppliers. A standard test result for the PH-5 inflator is presented in Figure 15.

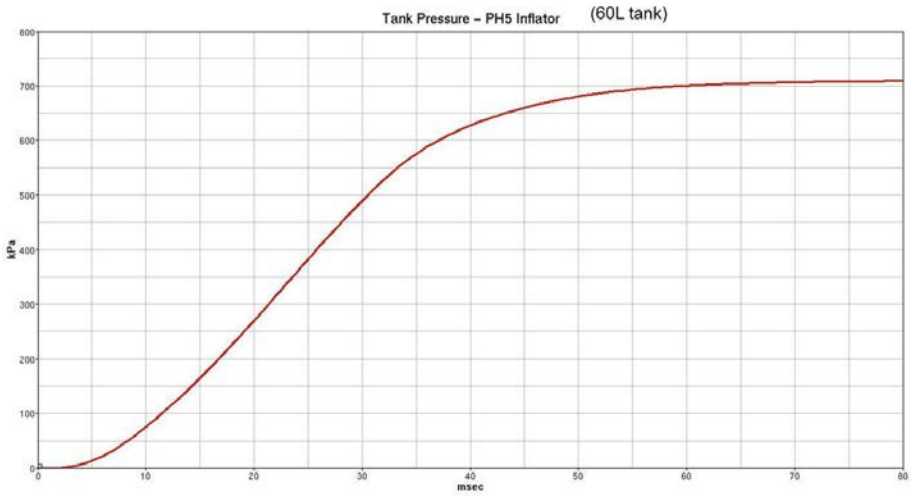

Figure 15. Output from a 60 Liter Inflation Test – PH5 Inflator

6.2 Knee Bolster Design

Unlike the airbag module, the knee bolster module is not a standardized module. The automotive industry uses a combination of deformable metal brackets and deformable plastic or composite cover panels on the dashboard.

To develop the knee bolster design, a detailed finite element (FE) model of the baseline cab structure was created in RADIOSS [4], incorporating all relevant details about the desk and console. Figure 16 below shows the baseline cab structure FE model used in simulations. The force-deflection (F-D) response of the knee bolster module was then derived using a quasi-static, nonlinear analysis by applying the load through two knee-form surfaces and calculating the displacement response.

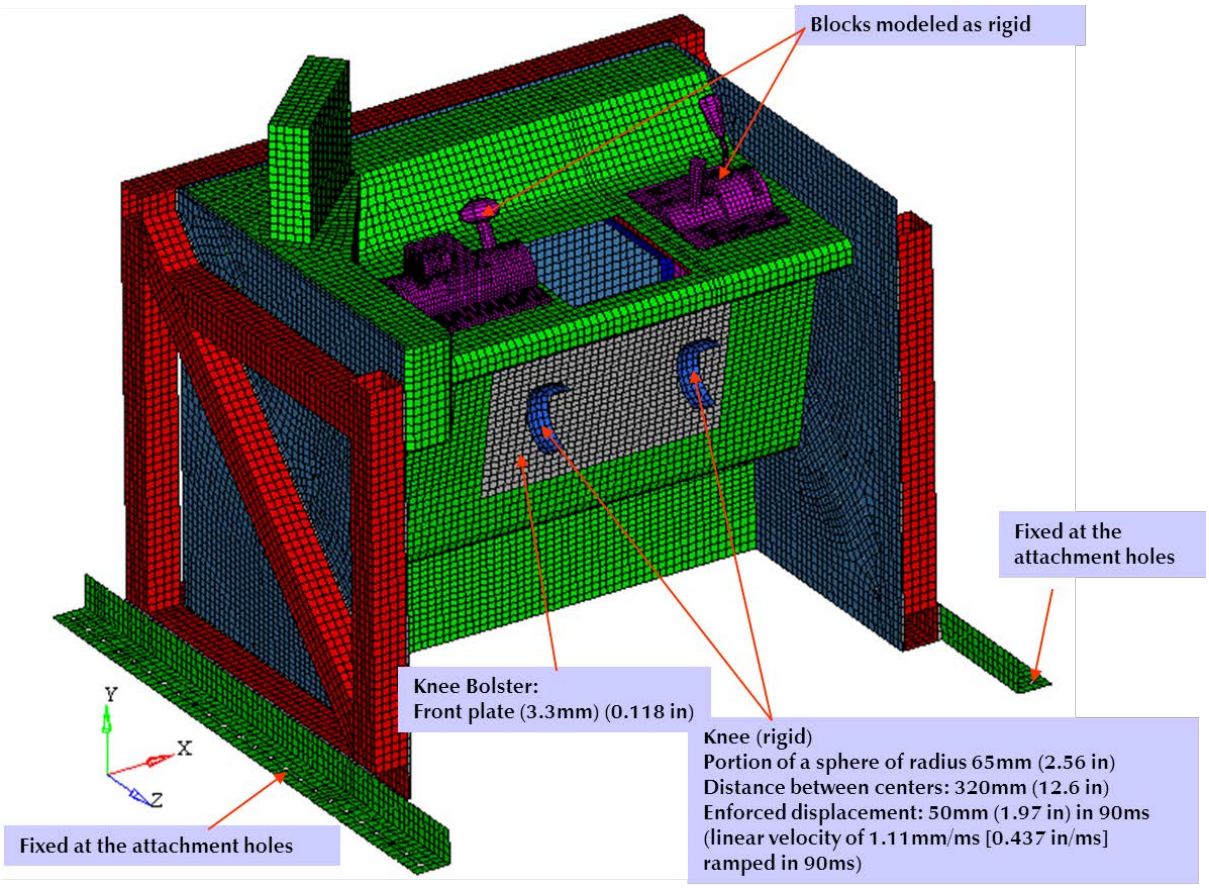

Figure 16. Baseline Cab Structure Finite Element Model

The initial target curve for the knee bolster F-D response was the assumed curve used in the preliminary MADYMO models, which was based on a typical automotive style knee bolster. This served as the initial target not because it was 'ideal', but because it had shown reasonable performance in the preliminary MADYMO simulations.

To derive a detailed design for the knee bolster, several configurations were simulated in RADIOSS and the F-D responses were compared with the assumed target curve. In cases where the configuration showed an acceptable match with the target F-D curve, the properties of the configuration were transferred to the MADYMO model for a quick assessment of the configuration's efficacy in meeting the injury criteria. This iterative process resulted in a promising knee bolster configuration, shown in Figure 17, which matched the target curve reasonably well.

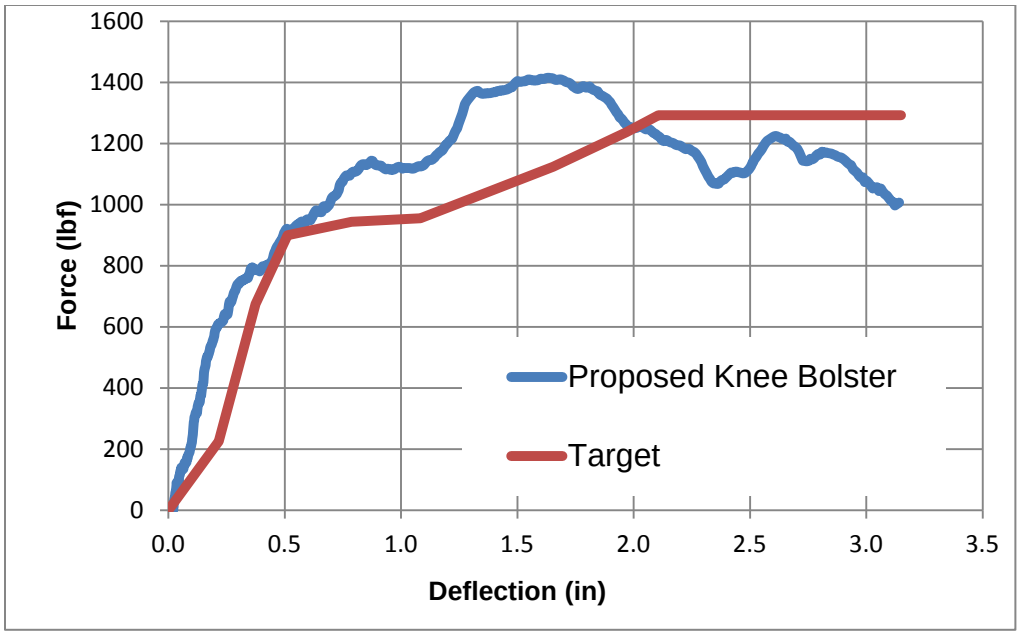

Figure 17. Force versus Deflection – Preliminary Knee Bolster Design

Preliminary configuration consisted of a honeycomb block working in series with a pair of deformable stamped brackets. The system consists of a front plate, honeycomb, back plate, and energy absorbing brackets, as shown in Figure 18. For ease of manufacturability and prototyping, the deformable brackets were revised to use flat bar stock (⅜ in) that provided equivalent bending strength. Crushing of the honeycomb in combination with controlled failure of the knee bolster brackets provided the desired energy absorption, as well as the appropriate ATD kinematics. Figure 18 and Figure 19 highlight the key characteristics and dimensions of the final configuration.

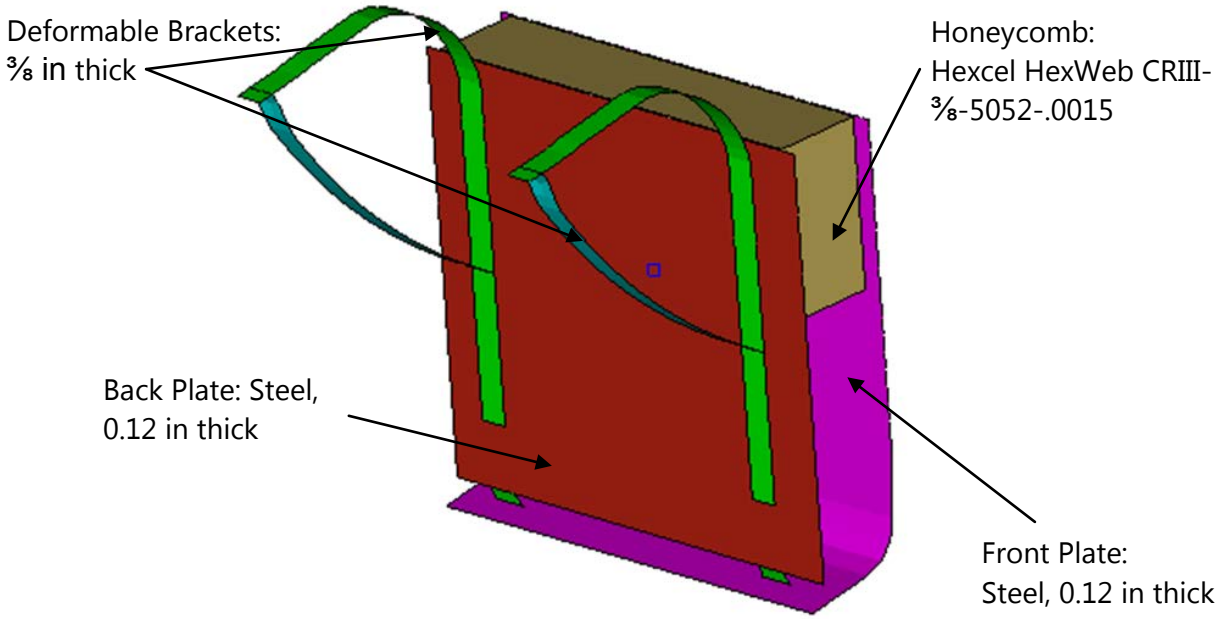

Figure 18. Knee Bolster System Assembly (Left)

The honeycomb material in the proposed knee bolster system is a HexCel Corporation product HexWeb CRIII-⅜-5052-0015N-2.3. This model is made up of ⅜ in hexagonal cells from 5052 aluminum with a nominal foil thickness of 0.0015 in and published crush strength of 75 psi. The knee bolster brackets are made of ASTM A36 steel with a minimum yield strength of 36 ksi, a minimum ultimate strength of 50 ksi, and the dimensions noted in Figure 19.

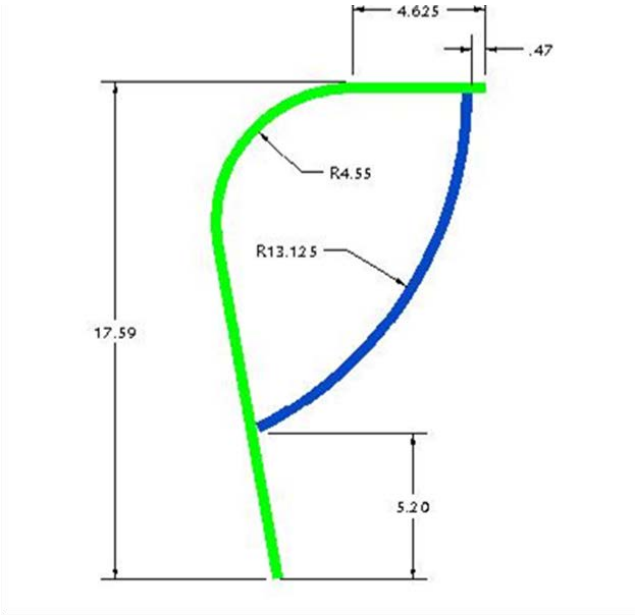

Figure 19. Dimensions of Knee Bolster Bracket

6.3 Design Evaluation

The detailed airbag and knee bolster information was then applied to the baseline console to prepare a sled test FE model, which included an accurate representation of the desk geometry, controls, and protection system. This model included a detailed representation of a 95th percentile Hybrid III ATD. To simulate a crash scenario, a 23 g crash pulse was imparted to the sled model. Forces and displacements of the ATD's knees, as well as all measurable injury indices, were tracked throughout the simulations. Figure 20 shows the full FE model used in the simulations.

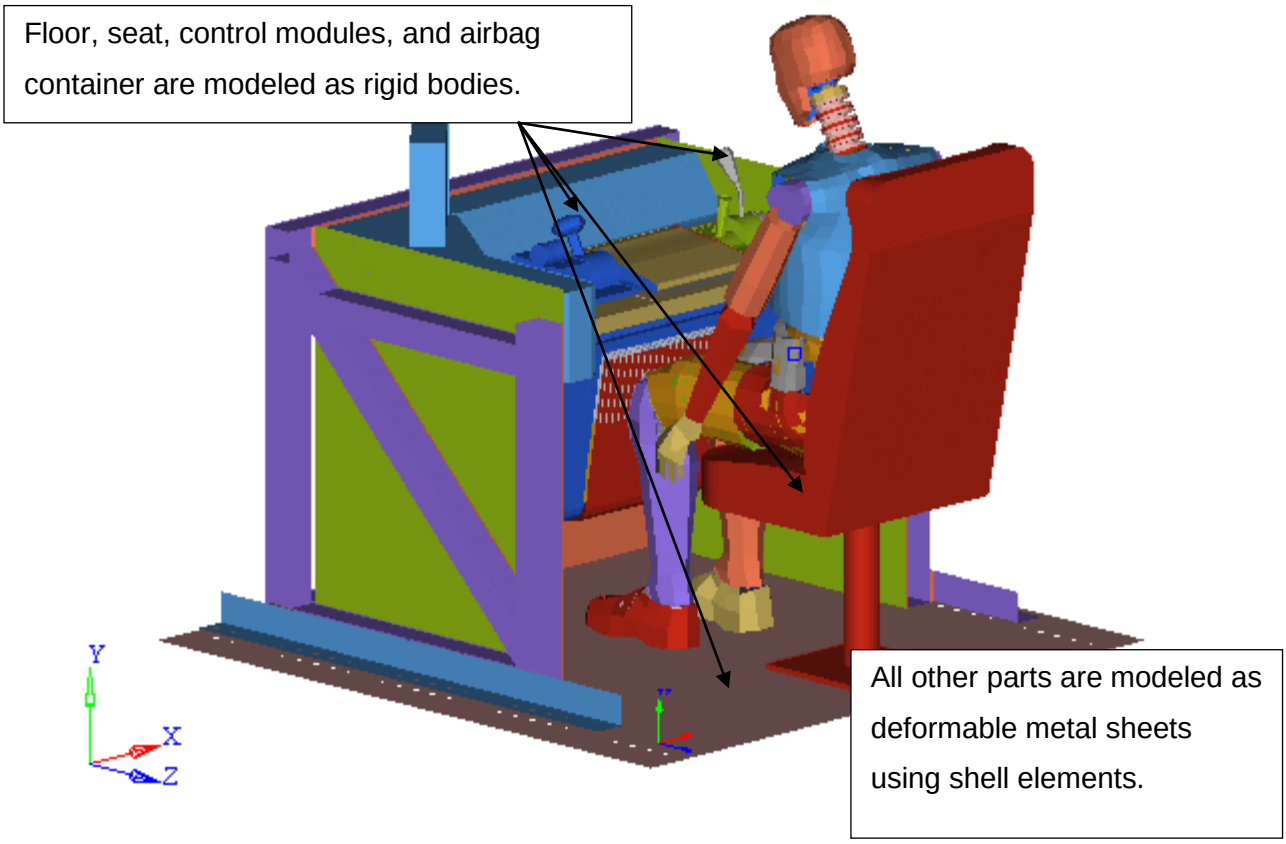

Figure 20. Baseline Sled Test Finite Element Model

The airbag cushion was defined as a RADIOSS monitored volume. Two control vents were defined to account for fabric permeability, stitching leakage, and actual bag vents. The first vent represents the fabric permeability and stitching leakage. A second vent in the airbag model that represents actual vents on the airbag was also defined; this vent could be turned 'on' or 'off' depending on the airbag design. Inflator characteristics were defined using the tested and published flow curves for the PH-5 inflator.

A RADIOSS 95th percentile Hybrid III deformable dummy FE model for frontal impact was positioned into the model. This is a calibrated model that is supplied, under license, by the ATD manufacturer, and has been certified by the manufacturer under a variety of test conditions including head drop, neck flexion, knee impact, knee slider, and chest impact.

Multiple simulations using different airbag widths and alternate inflator characteristics were conducted to fine tune the performance of this system. The airbag widths tried were 400 mm and 450 mm; while the kinematics and injury indices were similar, the 450 mm bag was selected for the final design because it offered better coverage for a wider range of conditions. In addition to the standard PH-5 inflator, a theoretical inflator with increased flow capacity (in the ratio of 450 mm to 400 mm) was tried for the 450 mm bag. As the enhanced capacity inflator did not seem to offer any performance benefits, the standard inflator, a pretested, off-the-shelf item, was retained for the final design.

6.3.1 Simulation Results

The predicted injury indices from the selected design are presented in Table 14. The results show that the design was effective in providing the required level of safety.

Table 14. Injury Indices – Design System (Pre-Characterization) Sled Test Model

Injury Index Parameter		Allowable Limit	Predicted Injury Index
HIC_15		700	104
Chest 3ms (g)		60	38
Femur Loads (N)	Left	10,000	7,611
	Right	10,000	7,743
Neck Loads (N)	Tension	4,170	2,177
	Compression	4,000	934
Neck Injury Criteria	N_{te}	1.0	0.60
	N_{tf}	1.0	0.25
	N_{ce}	1.0	0.26
	N_{cf}	1.0	0.26

Figure 21 shows two screen shots of the simulation—one at the beginning and the other at the end of maximum excursion of the ATD. The ATD kinematics are as follows: initial contact is between the femur and the knee bolster; as the femur loads rise, the torso pitches forward slightly, followed by contact between the chest and the airbag, followed almost immediately after by contact between the head and the airbag (this being coincident with the rise in neck loads). The knees then start straightening out and the head and torso ride down with the airbag. The relatively high HIC values seen in the preliminary (MADYMO) analyses were reduced by effective airbag design and timing that prevented the late head strike seen in the preliminary effort, resulting in significantly lower HIC values. Figure 22 provides the time histories of head acceleration, femur loads, thorax acceleration, and various neck loads.

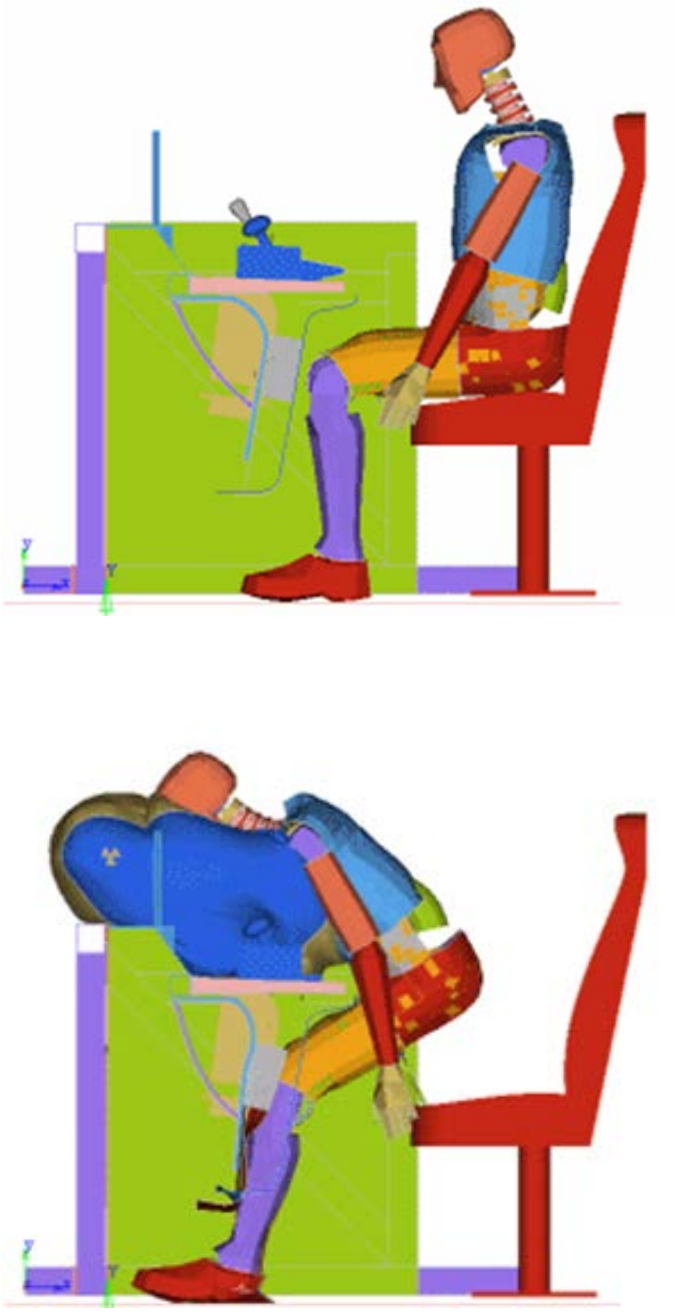

Figure 21. Designed System (Pre-Characterization) – Simulation Screen Shots

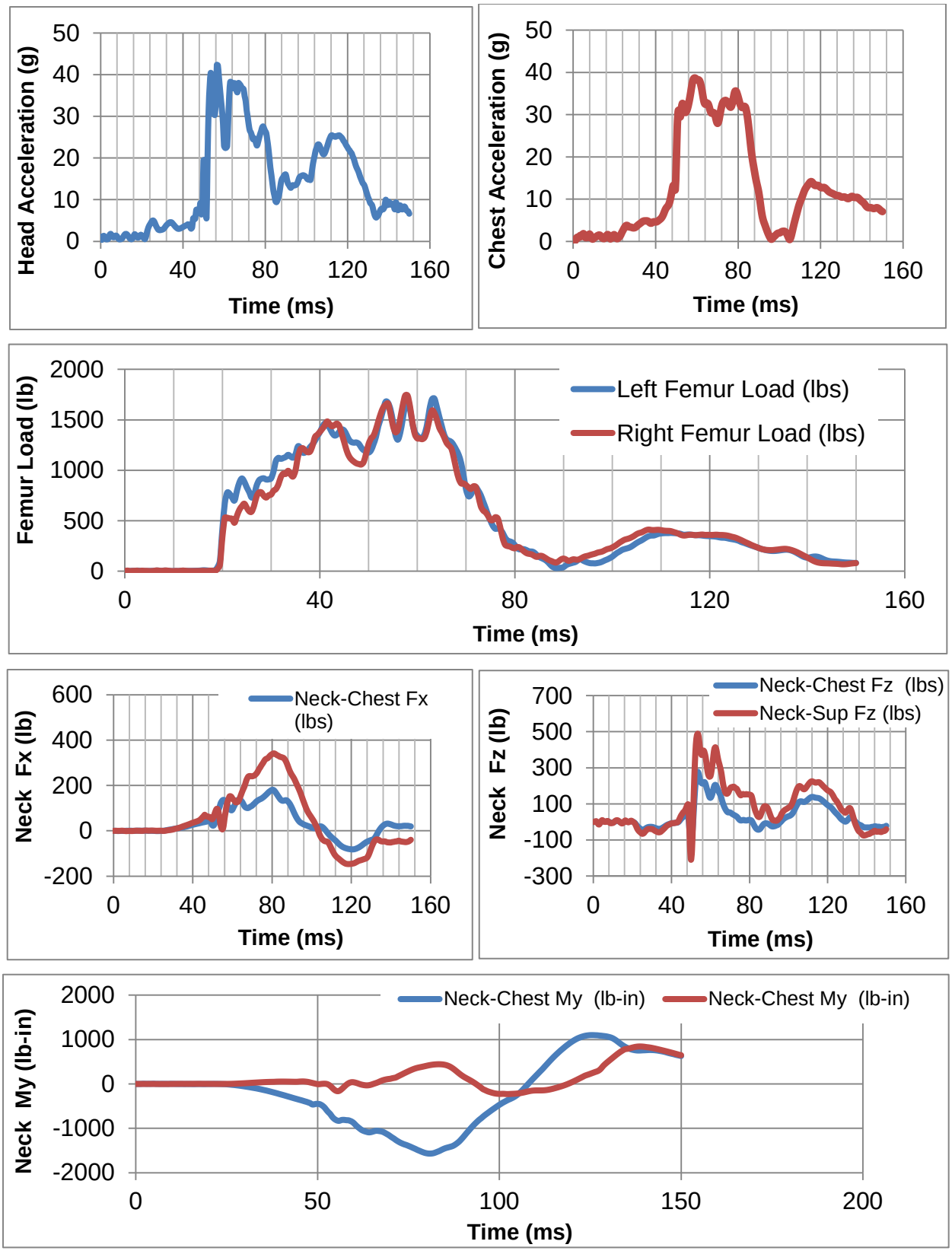

Figure 22. Simulation Results – Designed System (Pre-Characterization)

6.4 Weight and Cost

The system is expected to weigh about 30 lb, which is quite reasonable given the safety benefits offered. Table 15 below provides a brief breakdown of component weights.

Table 15. Component Weights

Component	Weight (lb)*
Airbag Module	9
Knee Bolster (KB) – Brackets (2)	8
KB – Honeycomb	1
KB – Front Plate	3
KB – Back Plate	9
Total	**30**

*Rounded up to the nearest whole lb

System costs can vary significantly based on order quantities. Based on an annual order quantity of 100 units or fewer, the cost of the system is estimated to be around $3,000 per equipped cab. A material cost breakdown is provided in Table 16.

Table 16. System Material Costs

Component	Cost*
Airbag Module	$ 2,500
Knee Bolster (KB) – Brackets (2)	$ 100
KB – Honeycomb	$ 250
Misc. Fabrication, Sheets, etc.	$ 150
Total	**$ 3,000**

*Based on an annual quantity of 100 or fewer

6.5 Summary

The previously chosen concept (passenger-style airbag with a deformable knee bolster) was developed into a detailed design. Specifically, airbag details and knee bolster details (characteristics) were defined.

Subsequently, this detailed design was developed into a full FE model, and the performance of the system was evaluated using RADIOSS under the prescribed EPS Test pulse and a 95th percentile male ATD.

The results showed that the design was effective in providing the safety benefits expected.

7. Component Characterization

To gain confidence in the modeling and simulation results, individual elements of the protection system were tested and characterized. The prototype protection system uses two deformable subsystems, a 'passenger-style' airbag (A/B) and an energy absorbing knee-bolster (K/B) to provide the desired level of safety. The goal of this effort was to conduct the tests needed to characterize both systems through the deployment and deformation range expected in this application.

The following sections describe the tests conducted on the airbag and knee bolster components and the subsequent characterization based on those test results. The goal of the testing was not to verify whether the individual components met a desired target performance; rather, it was to quantify how they performed and then to update the full system analytical model to use those tested characteristics. This approach was chosen because performance targets for this effort were defined at the system level (injury indices, compartmentalization, etc.) and not at the individual component level. In other words, specific pass-fail or other target criteria were not defined at the subsystem level, but at the full system level.

7.1 Airbag Characterization

The airbag system is composed of the airbag and the inflator, which are both housed in a standard automotive packaging format. The proposed system uses a custom version of an automotive 'passenger-style' airbag and an off-the-shelf inflator (model # PH-5) from Key Safety Systems (KSS). Airbag performance can be fully characterized by its deployed shape and volume and its leakage under load. The intent of the airbag tests was to develop the shape and leakage characteristics, either directly or indirectly. The automotive industry has developed standardized test sequences that are used to characterize and quantify these elements. These standard tests include the following:

1. Static Deployment Test – characterizes deployed shape and verifies integrity
2. Drop Tower Test – characterizes airbag leakage, and deformation (under load)

7.1.1 Airbag Static Deployment Tests

Two airbag static deployment tests were conducted to establish the airbag's deployed shape, deployment height, and overall bag integrity. These preliminary tests also establish the height of the fully deployed airbag (which is a parameter that then flows into the drop tower test setup), and are used to confirm that the internal tethering works as intended.

Test Input Parameters

The only input parameter for the static deployment test is the time gap between the primary and secondary triggers, which was set to 10 ms as per the design of the inflator.

Expected Test Output

- Visual confirmation of deployed shape, including deployed height
- Visual confirmation of airbag integrity

Test Sequence

Each specimen airbag was deployed with its paired inflator, with the intended inflation sequence. Timed electrical signals were sent to the airbag inflator to deploy the bag. The control modules for these electrical signals are called squibs. There was no external energy or force applied to the bag. The process of inflation, time of inflation, etc. were monitored with high-speed video cameras to capture the airbag's final deployed shape, deployment height, and integrity. Inflation pressure was also observed for one bag. Post deflation, the bags were examined for any integrity issues, such as tears. Two airbags—one unvented and one vented with two 10 mm diameter vents—were tested.

Figure 23 shows the airbag test fixture used for these tests. The triggering system consisted of two squibs, with the second one being triggered 10 ms after the first one. Two high-speed video cameras were used to record the deployment sequence with a front and a side view.

Figure 24 shows the inflation sequence of the vented airbag. The results are as follows:

- No cushion integrity issues were observed either during or after the test.
- Cushion kinematics seemed favorable, as seen in Figure 24.
- Tethering worked as intended.
- The deployed height of the airbag was 23 in.
- The deployed shape was as expected.
- There were no anomalies in the pressure signal.

Figure 23. Drop Tower Test Setup

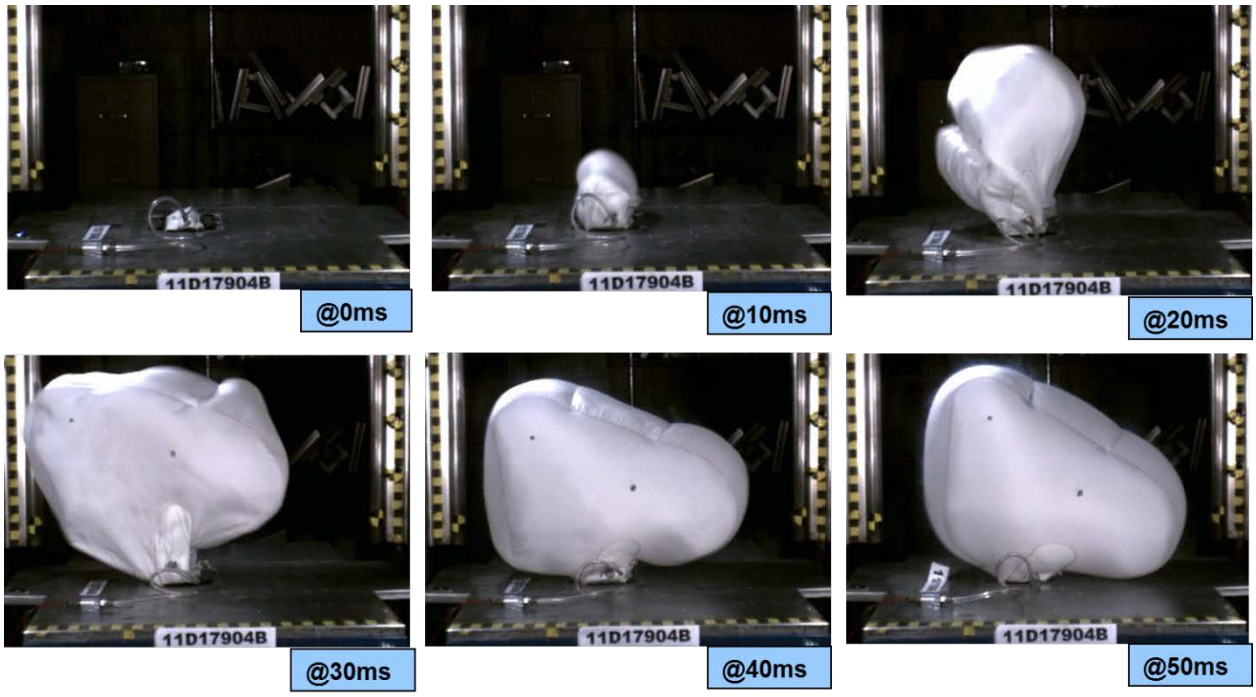

Figure 24. Sequence of Airbag Inflation for Static Deployment Test

7.1.2 Airbag Drop Tower Tests

Airbag drop tower tests are conducted to derive the leakage parameters needed to develop input for the analytical airbag model. These are 'indirect tests' (i.e., the key parameters derived from this test, such as leakage and airbag stiffness, are not measured directly). The test sequence is modeled using an analytical program such as RADIOSS/MADYMO™ with several known parameters (mass, drop height, flow rate into airbag, inflator trigger sequence, etc.) and several assumed parameters (fabric leakage, seam leakage, etc.). Post-test, the assumed parameters are adjusted so that the measured response (acceleration, velocity, and displacement of the dropping mass) matches the model response.

Test Description

During this test sequence, a known mass was dropped from a defined height onto a fully inflated airbag that is triggered and deployed during the test. The mass and the drop height were selected based on the energy input needed to adequately characterize the airbag system. The energy levels chosen were consistent with the expectations of airbag energy input from prior simulations.

Test Input Parameters

The key input to the test is the energy input, which is defined as a product of the weight of the drop mass and the height of the drop. The target value of 520 J (minimum) was taken from prior MADYMO simulations of a 95th percentile ATD under the EPS test pulse. The test input parameters are defined in Table 17. The target energy can be achieved with a 57 in drop height

and an 80-pound mass, if there is no friction in the guide rods. Based on experience, a value of 66 in was chosen to ensure that the target energy minimum was comfortably met and to account for guide rod friction.

Expected Test Output

- Acceleration of the drop mass measured by two accelerometers (0–50 g range)—left and right on the drop mass
- Trace of the two ignition (squib) signals for confirmation—one on each squib used to ensure that the inflator triggers sequence and timing are correct
- High-speed video of the event using two high-speed video cameras—one side view and one oblique view

Test Sequence/Details

A defined mass was dropped from a predetermined height onto a fully inflated airbag that is triggered and deployed during the test. The drop tower test fixture consists of mechanisms by which a vertically guided impactor with a defined mass can be dropped from a defined height onto a fully inflated airbag. Timed electrical signals are sent to the airbag inflator to deploy the bag, with the dropping of the mass synchronized with the inflation time of the airbag.

Table 17. Drop Tower Test Parameters

Parameter	Value	Remarks
Target Energy (Minimum)	520 joules (J)	Derived from prior MADYMO simulations of the proposed concept for a 95th percentile male ATD under the EPS Test pulse
Weight of Drop Mass	80 lb	Effective weight for 95th percentile male ATD impacting an airbag, as determined by previous automotive analyses
Drop Height + Airbag Deployed Height	66 in + 23 in = 89 in	Based on the deployed airbag height established in the Static Deployment Test , target energy to be absorbed by the airbag, and estimated friction at the guide rods
Data Acquisition System Trigger Height	40 in	Commensurate with the drop mass speed corresponding to the target energy, and timed to capture full event
Trigger Time for Primary Squib	45 ms	Timed to ensure full inflation
Trigger Time for Secondary Squib	55 ms	Timed to ensure full inflation

Figure 25 and Figure 26 present a schematic and a picture of the drop tower test setup. A total of four airbags were tested—two unvented airbags and two vented airbags (each bag with two 10 mm diameter vents).

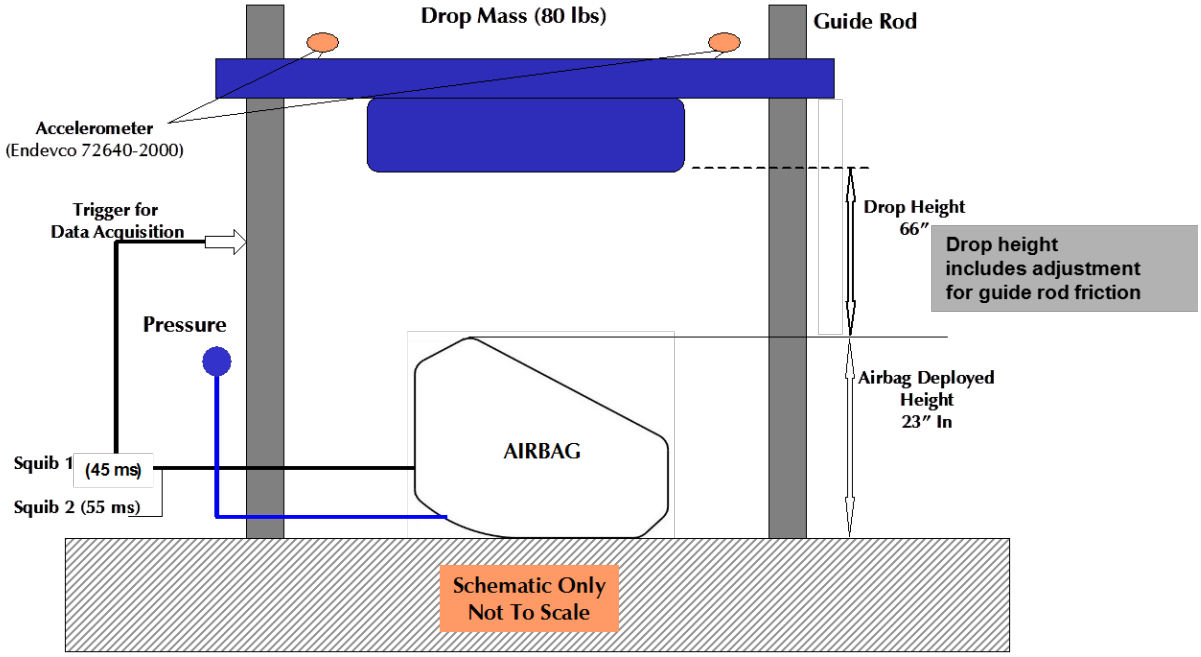

Figure 25. Airbag Drop Tower Test Frame

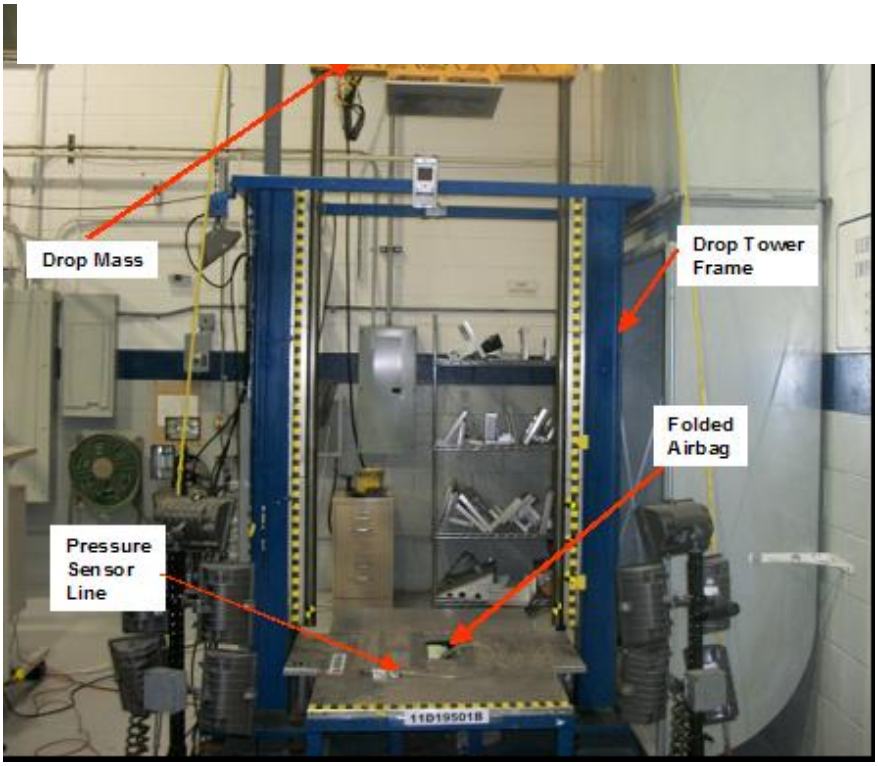

Figure 26. Airbag Drop Tower Test Frame

Drop Tower Test Results

Measured accelerations, computed forces, velocities, and displacements are presented in Figure 27 and Figure 28 for the two sets of drop tower tests conducted. Airbag resistive force is computed from the known drop mass and its recorded acceleration. Airbag kinematics are presented in Figure 29.

The following observations were made:

- No cushion integrity issues were observed either during or after the test.
- No unusual cushion kinematics were observed.
- Acceleration data and calculated velocity seemed reasonable.
- The expected energy input (~ 520 J) was imparted to the bags.

The measured data was used for developing a characterized airbag model.

Acceleration (g) versus Time (ms)

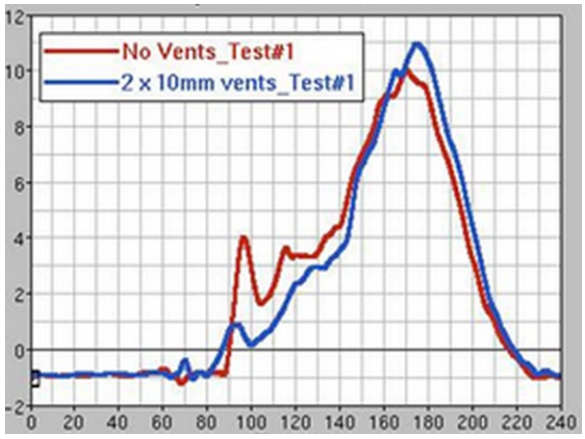

Velocity (m/sec) versus Time (ms)

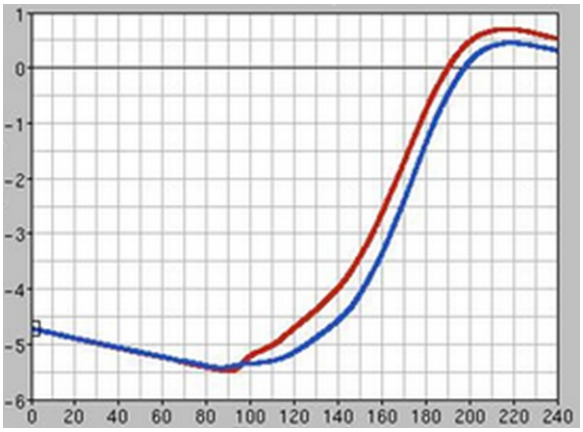

Displacement (m) versus Time (ms)

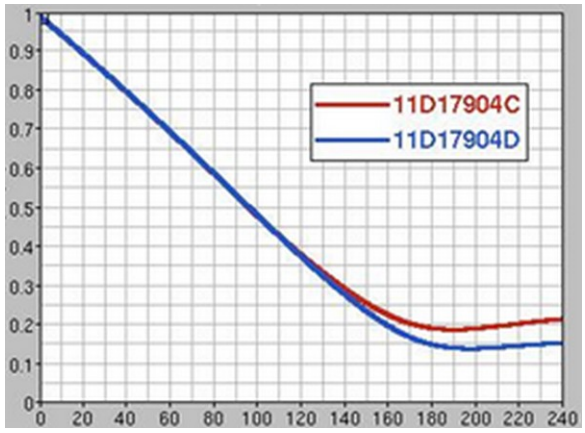

Impact Force (N) versus Time (ms)

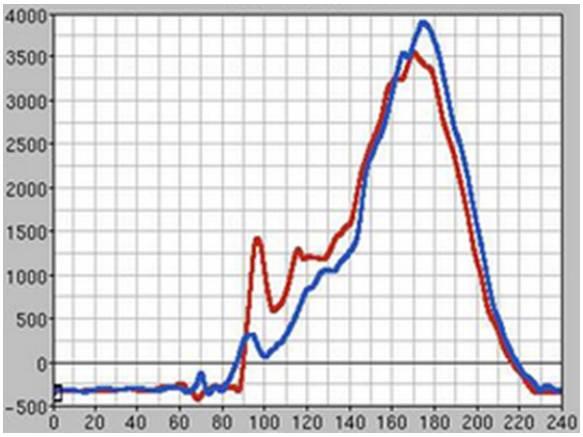

Force (N) versus Deflection (mm)

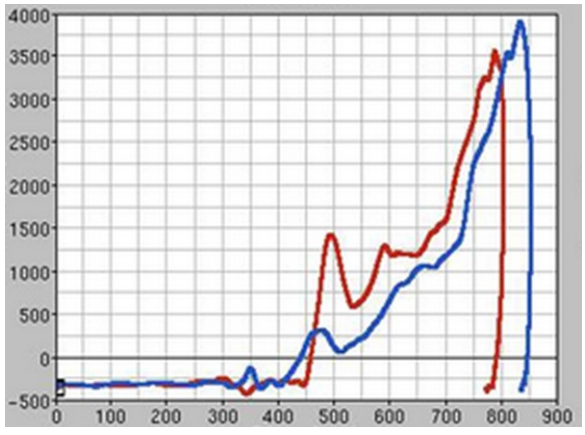

Kinetic Energy (Nm) versus Time (ms)

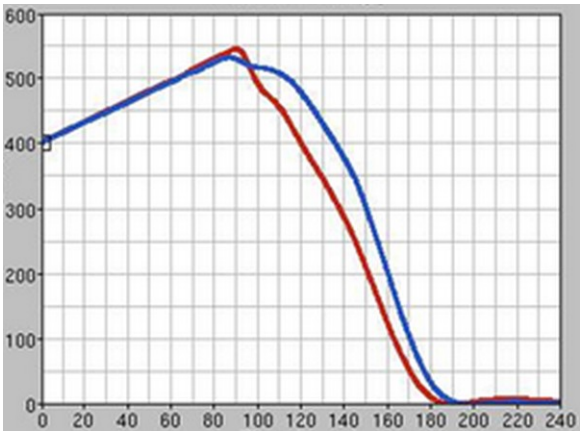

Figure 27. Measured and Computed Data – Drop Tower Test #1

Acceleration (g) versus Time (ms)

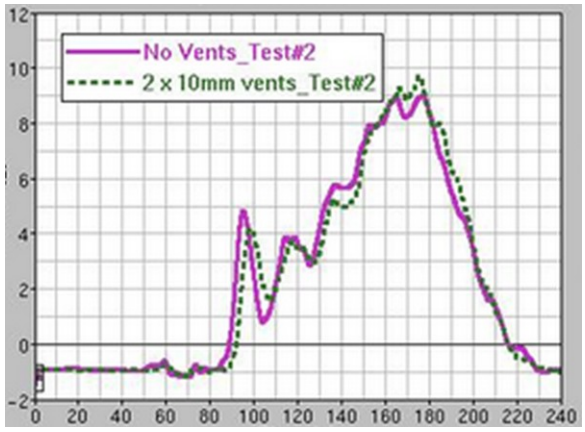

Velocity (m/sec) versus Time (ms)

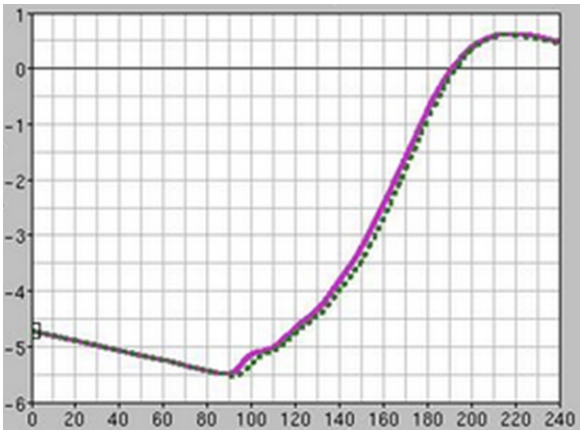

Displacement (m) versus Time (ms)

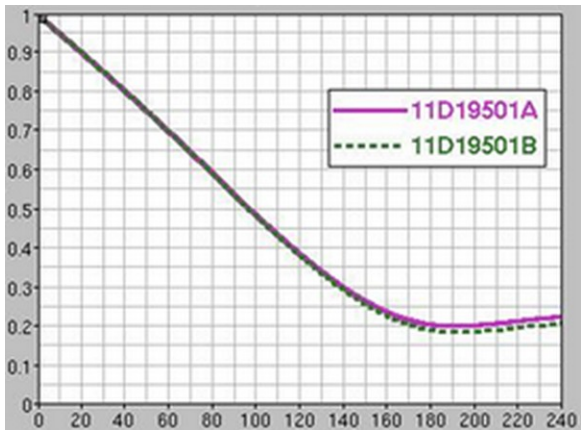

Impact Force (N) versus Time (ms)

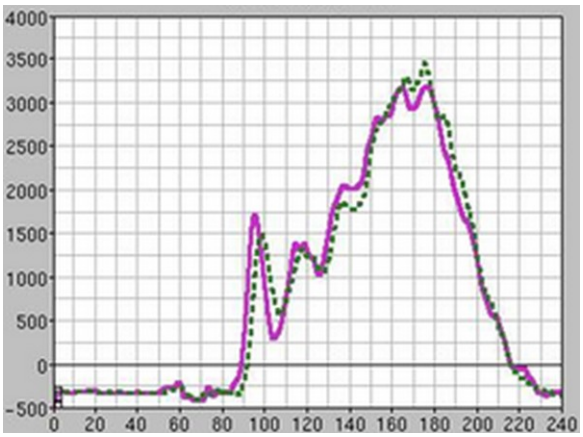

Force (N) versus Deflection (mm)

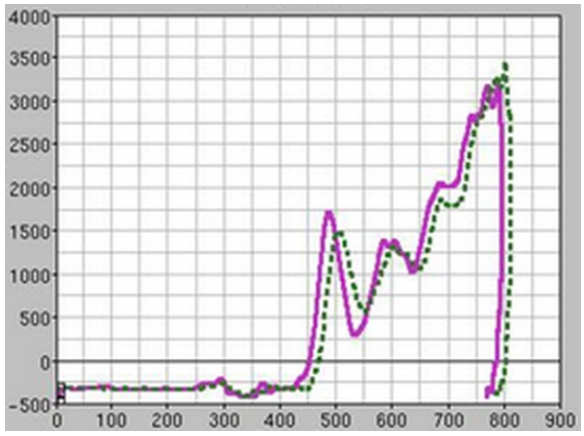

Kinetic Energy (Nm) versus Time (ms)

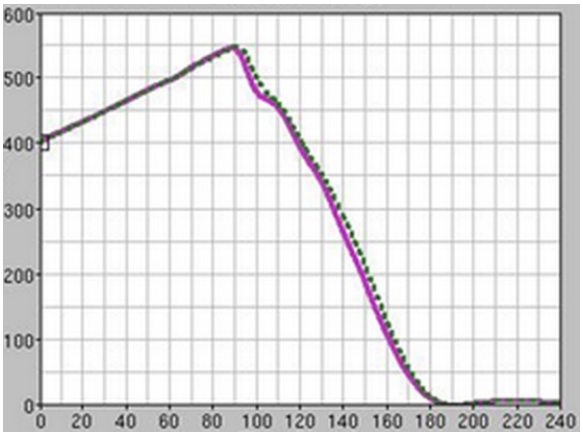

Figure 28. Measured and Computed Data – Drop Tower Test #2

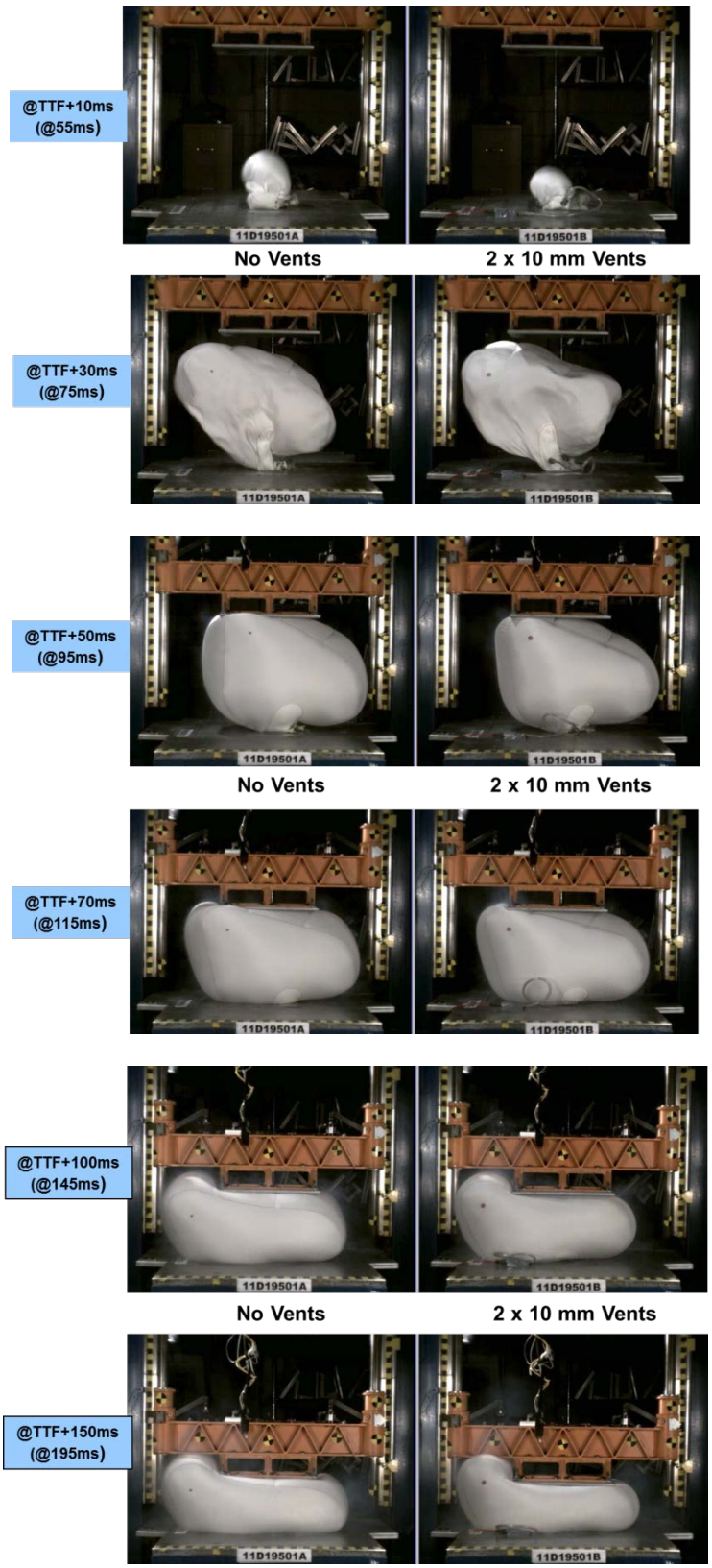

Figure 29. Cushion Kinematics – Drop Tower Test Series #2

7.1.3 Airbag Model Characterization

The intent of the airbag tests was to use the data to characterize the airbag submodel used in the RADIOSS sled test model. Prior to characterizing the data in the RADIOSS model, a characterized airbag model was prepared using MADYMO as an intermediate step.

For this effort, a MADYMO model of the drop tower test setup was prepared (see Figure 30). All appropriate test parameters (drop height, mass, etc.) and the PH-5 inflator characteristics were built into the model. Frictional losses at the guide rod were modeled using a simplified damping approach that has historically performed satisfactorily for KSS. Subsequently, airbag leakage parameters were adjusted to derive a performance (acceleration profile of the drop mass) that was comparable to the test data. Tuning of leakage was accomplished by changing the overall permeability factor for the airbag, and by defining an additional discharge function representing leakage through the airbag as a function of the internal pressure. Comparative results from the characterized MADYMO model and the corresponding test data are shown in Figure 31 (for the unvented airbag).

Characterized airbag data from the MADYMO model was transferred to RADIOSS where, with RADIOSS-specific adjustments (permeability, discharge, and vent size), the model matched test data reasonably well (see Figure 32), though some minor oscillations were noted. To some extent these oscillations are seen in the test data as well. The oscillatory behavior seen in the RADIOSS drop test simulations are not seen in sled test simulations, as evident in the head, chest, and neck acceleration and force data from the post-characterization runs. The differences between the MADYMO and RADIOSS models are likely due to minor variations in how damping of pressure waves within the airbag is implemented in the two programs, combined with the fact that the drop tower simulation has a very ‘mild’ crash pulse (essentially 1 g flat forcing function), thereby making the resulting oscillations appear more significant than they are. In a ‘real’ pulse, where the forcing magnitudes are several times higher, these oscillations, even if present, are not likely to have any notable effect on ATD kinematics or resultant injury indices.

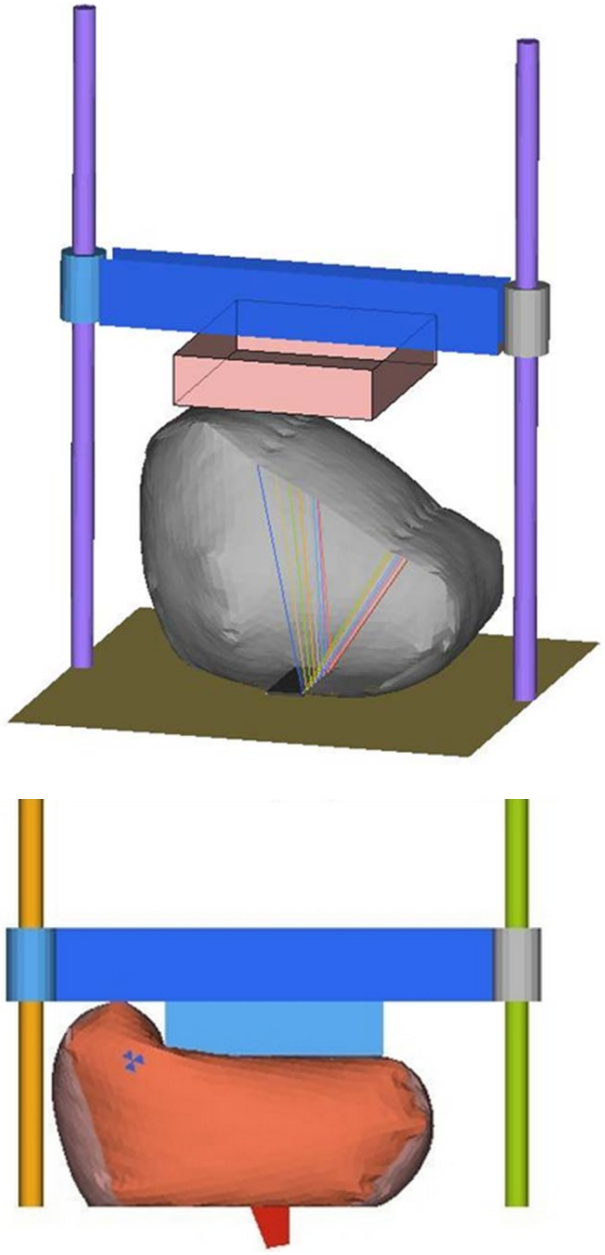

Figure 30. MADYMO Drop Tower Test Model

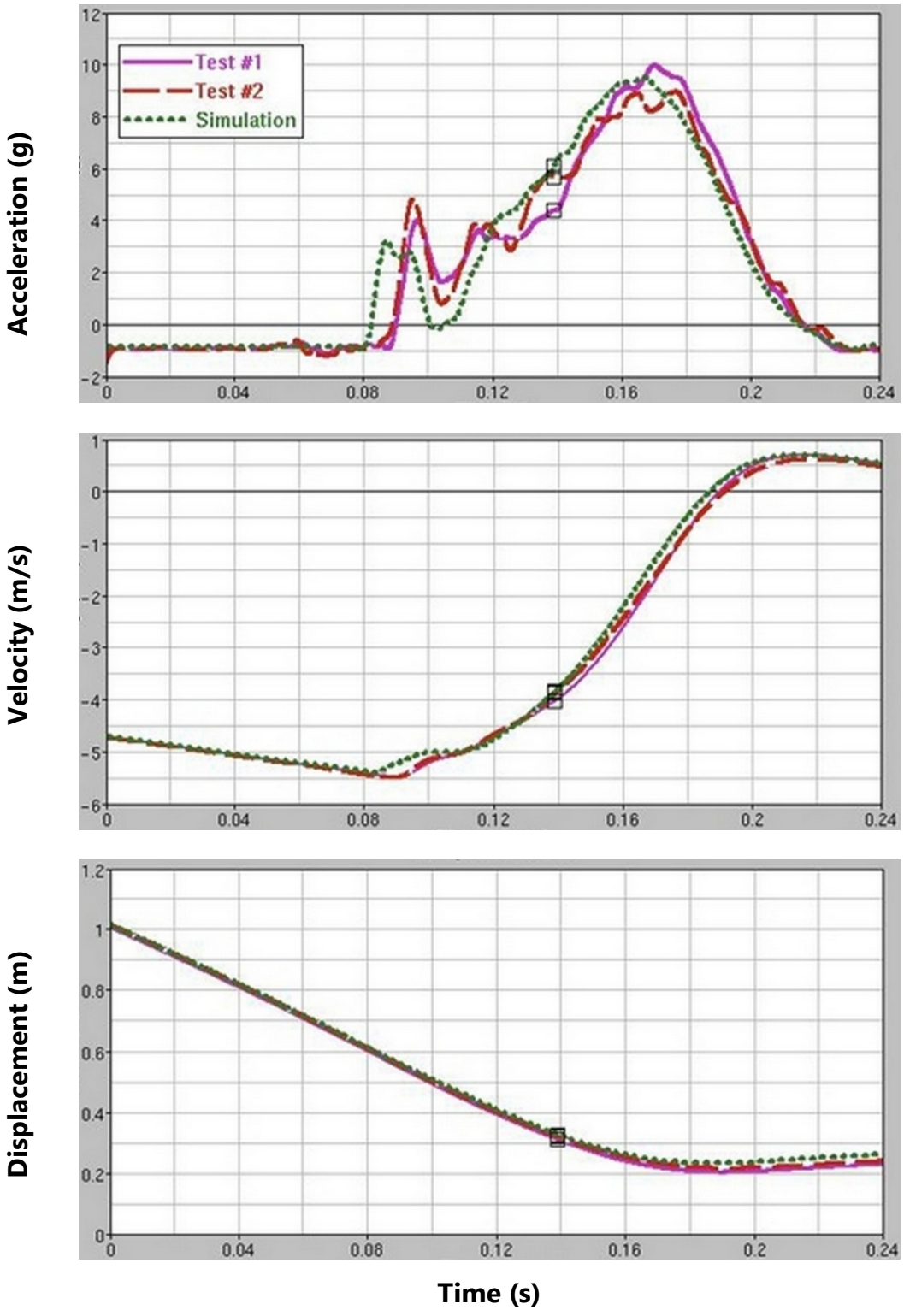

Figure 31. MADYMO Characterized Data – Unvented Airbag

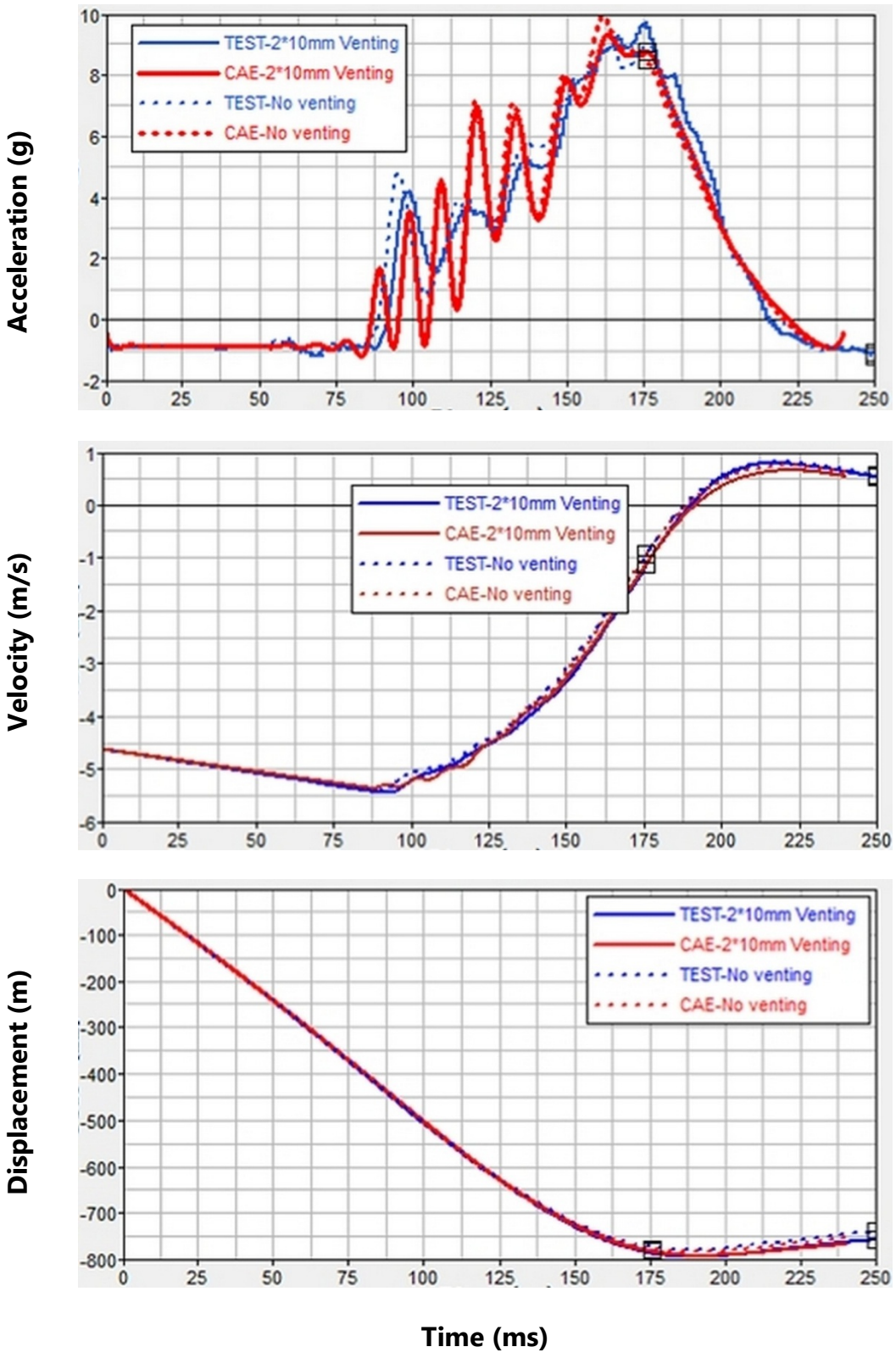

Figure 32. Characterization Data – RADIOSS Drop Test Model

7.2 Knee Bolster Testing

The proposed knee bolster K/B assembly consists of two deformable elements: a pair of brackets and a honeycomb element. The honeycomb element is sandwiched between the front plate (the plate facing the engineer) and the back plate, which is attached to deformable brackets.

From a simulation perspective, the characteristics of the K/B are defined using the following:

- Traditional material properties of the K/B bracket material—such as the yield strength, ultimate strength, and the elongation—in addition to the Young's modulus, Poisson's ratio, and density
- An aggregate stress-strain curve for the honeycomb material that represents the 'engineered' behavior of the material

Properties such as those defined above are traditionally measured through appropriate quasi-static and material characterization tests. The test procedures and the test results for these elements are described in the following sections.

7.2.1 Honeycomb Crush Tests

The intent of this effort was to test the honeycomb material used for the knee bolster system in a quasi-static manner in order to characterize its force-deflection characteristics. The test provided the force-deflection characteristics for input to the RADIOSS™ model of the EPS. The test also helped confirm the published crush values of the honeycomb material.

Test Input Parameters

A key input parameter set is the geometry and material of the specimen itself. The specimens consist of aluminum honeycomb sheets with a cross-section of a 4 x 4 in square with a height of 2.5 in. The honeycomb material is model # HexWeb CRIII-⅜-5052-0015N-2.3 (made by HexCel Corp), and the test specimen is composed of four stacked sheets of ⅝ in thickness each. The material is composed of ⅜ in hexagonal cells made of 5052 aluminum with a nominal foil thickness of 0.0015 in, and a published crush strength of 75 psi.

The other key input parameter is the loading condition; essentially, the test intent is to crush the honeycomb material along its loading axis with a quasi-statically applied load until the honeycomb is fully crushed (approximately 20 percent of its initial height).

Test Output Parameters

The key output parameters are the time histories of the loading and the crush (displacement) from which the F-D curve of the honeycomb material can be established, thereby characterizing the honeycomb material.

Test Description

Two specimens of the selected honeycomb sample were tested. Each specimen consisted of four 4 x 4 in honeycomb pieces cut out from a large sheet and stacked. The stack was backed with relatively rigid ⅛ in thick steel plates on both top and bottom.

The test frame and loading and instrumentation schematics are shown in Figure 33. The test setup consists of a frame, a hand-cranked hydraulic piston, a calibrated load cell, a string-

potentiometer for vertical displacement measurement, and a data collection system to record the applied load and deflection of the honeycomb specimen.

For each test, the specimen was mounted in the test frame with the hydraulic cylinder just touching the top cover plate (see Figure 34). The data collection system and the video recording were initiated, and a vertical load was slowly applied by hand cranking the hydraulic pump, with the load being continuously monitored on the data collection computer screen. Force and deflection data were collected continuously and saved for post-test analysis. The test was stopped when a sharp increase in the load was observed, indicating a complete crush of the honeycomb.

Honeycomb Test Results

In both tests, the honeycomb specimens crushed in a similar and consistent fashion. Images of a crushed test specimen and the four individual crushed pieces are shown in Figure 35. The individual pieces show that the honeycomb elements deformed as expected (i.e. the cell shape remained with walls buckling in place).

The crush load-deflection characteristics for both tests are shown in Figure 36. The test curves show a load peak before beginning to crush, and then the crushing occurred at a nearly constant load. The load peak near the deflection limit occurs as the honeycomb crushes to its solid height. In these tests, the stack was 2.5 in tall. The load begins to rise as deflection reaches 2.1 in (84 percent) and rises sharply at 2.25 in (88 percent).

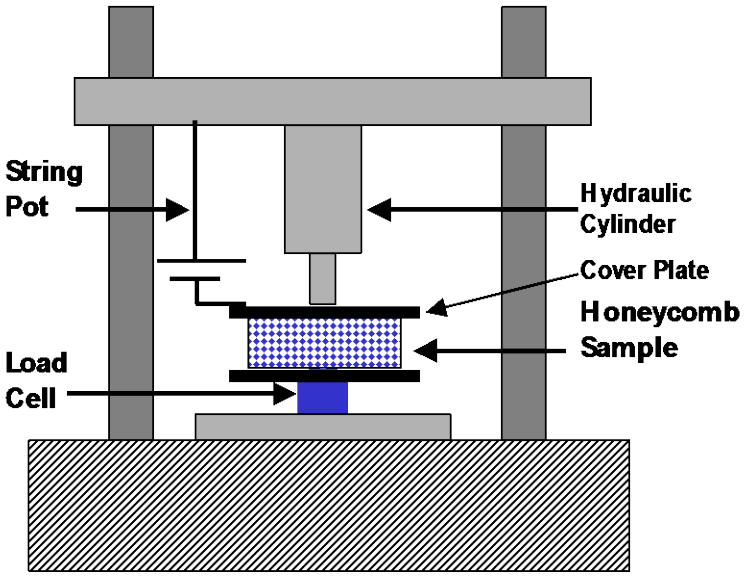

Figure 33. Schematic of the Honeycomb Sample Test Fixture

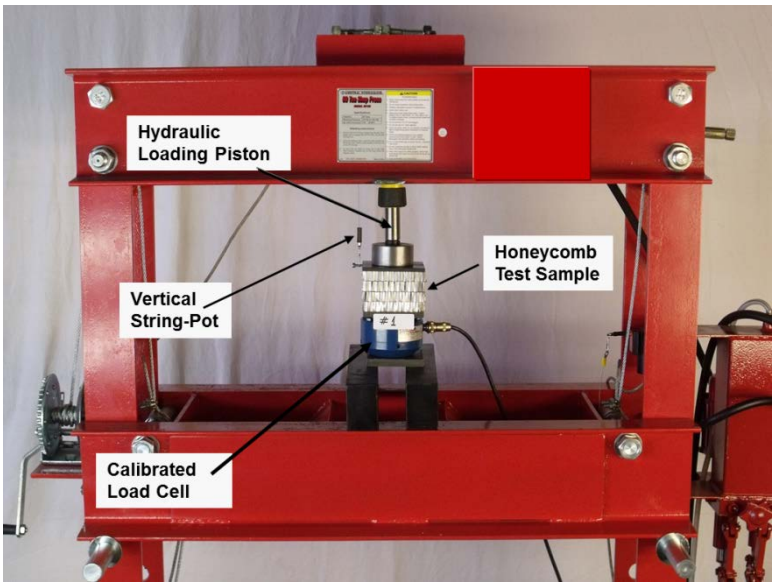

Figure 34. Honeycomb Sample in the Test Frame

For the honeycomb material used in these tests, the published crush strength is 75 psi with a +/-15 percent variance—i.e. the sample could provide crush stress between 63.75 and 86.25 psi. The two tested cases yield ~65 psi crush stress which is within the manufacturer's published range.

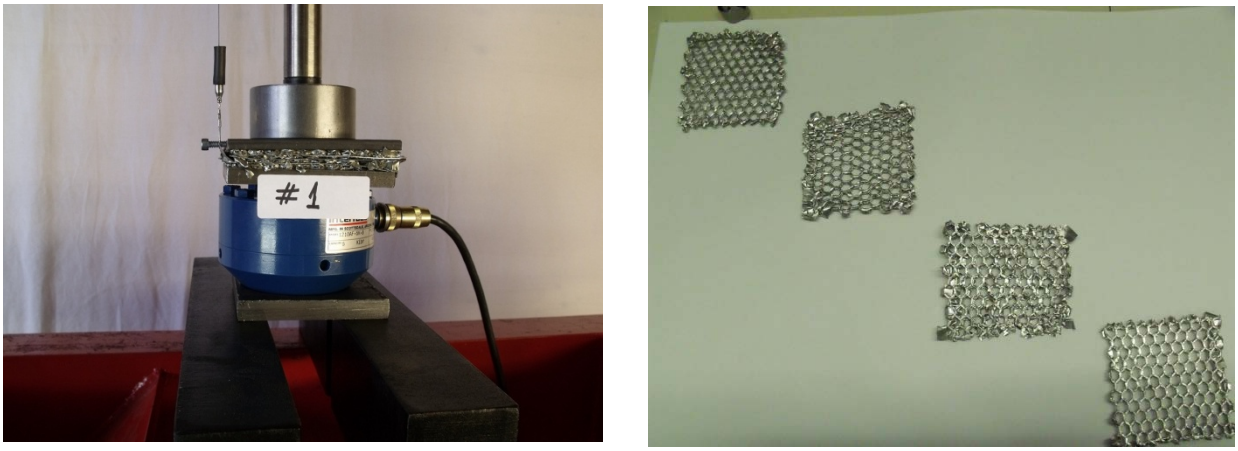

Figure 35. Crush Honeycomb Sample (Left) and Individual Layers in Crushed State (Right)

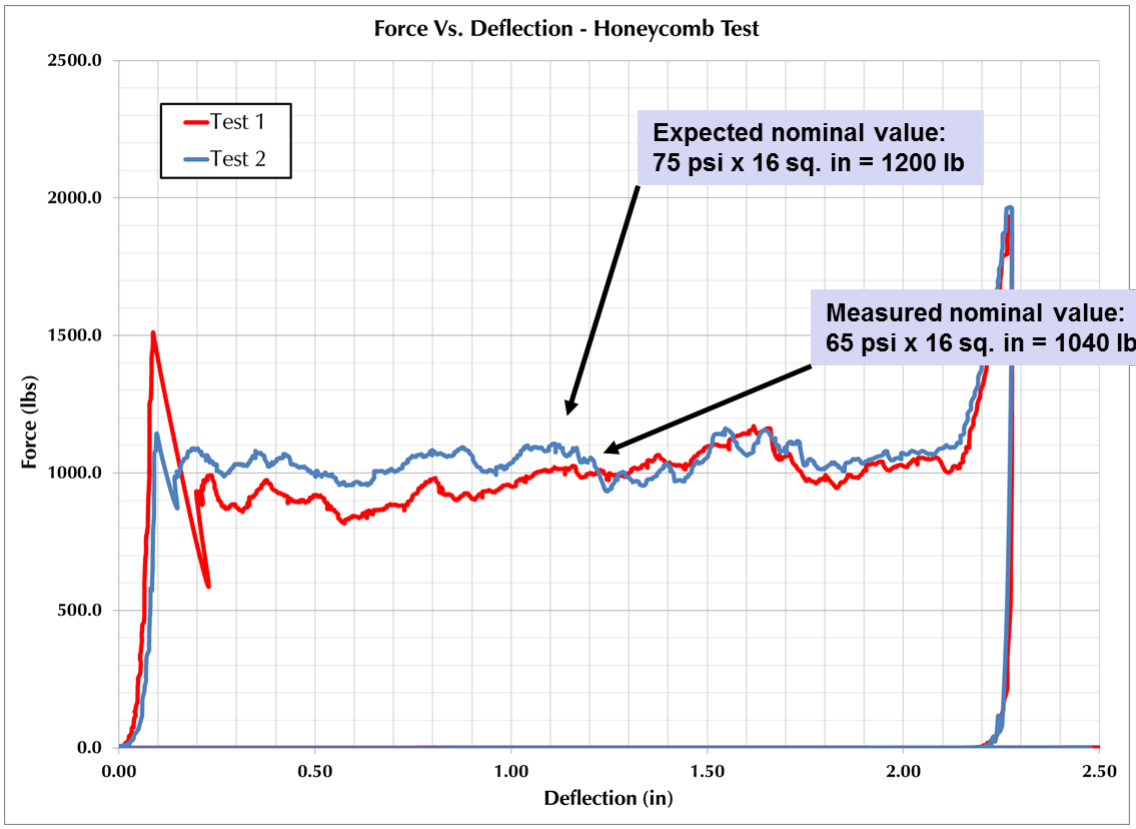

Figure 36. Crush Force versus Displacement Characteristics for the Honeycomb Sample

Characterization of Honeycomb Model

To ensure that the tested characteristics of the honeycomb were transferred to the FE model correctly, a RADIOSS model of the honeycomb block was prepared. The model consisted of a honeycomb block with dimensions (4 x 4 x 2.5 in) that reflected the test setup in terms of loading conditions, support conditions, and the displacement measurement points. In the simulation, the honeycomb block was squeezed between two rigid surfaces, and the F-D curve was extracted. Figure 37 shows that the response from the characterized honeycomb model was comparable to that from the tests. Properties in the secondary directions were taken from published manufacturer data.

After confirming proper characterization, the properties of the honeycomb block were transferred to the full FE sled test model.

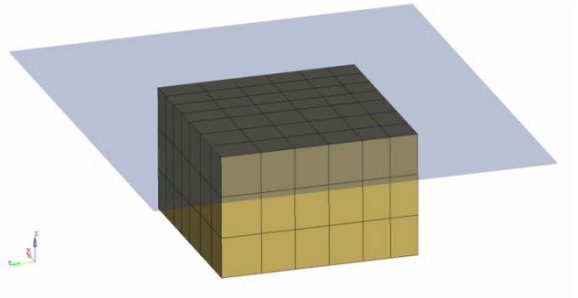

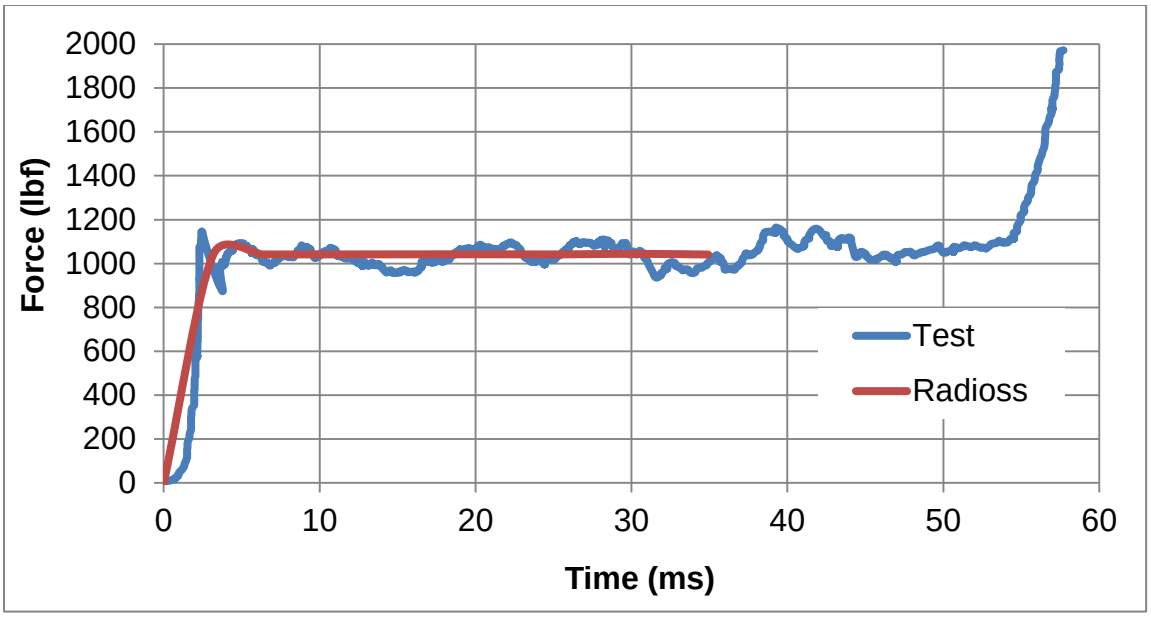

Figure 37. Model and Characterization of Honeycomb Block

Knee Bolster Bracket Tests

The intent of this test was to characterize the force-deflection characteristics of the knee bolster bracket in a quasi-static manner. The test data was used to characterize a bracket submodel in order to provide the basis for input to the RADIOSS™ full FE sled test model of the EPS.

Test Input Parameters

A key input parameter set for the knee bolster bracket is the geometry and material of the bracket specimen itself. The knee bolster brackets are made of ASTM A36 steel with a minimum yield strength of 36 ksi, a minimum ultimate strength of 50 ksi, and the dimensions noted in Figure 19. To confirm the material properties of the specimens, three coupon samples of the material were tested by an external laboratory in a standard test that measured the yield and ultimate strengths. The measured properties were as follows:

- Yield Point: 51 ksi (minimum); 54 ksi (average)
- Ultimate Stress: 75 ksi (minimum); 78 ksi (average)
- Elongation: 27 % (minimum); 28 % (average)

The other key input parameter is the loading condition; essentially, the intent of the test is to load the bracket along its loading axis with a quasi-statically applied load through ~ 4 in of deflection.

Test Output Parameters

The key output parameters are the time histories of the loading and displacement from which the F-D curve of the bracket can be established.

Test Description

Two bracket specimens were prepared and tested as part of this effort. The specimens were tested in the same frame as the honeycomb elements, but with the fixturing modified to suit the brackets. The fixture schematic is shown in Figure 38, and the complete setup with the bracket mounted in the fixture is shown in Figure 39. The load cell was mounted above the hydraulic cylinder and allowed appropriate positioning of the loading point on the bracket. A semicircular stock piece was attached to the bottom of the loading piston to minimize friction force at the loading interface and to maintain the loading position as the bracket went through relatively large displacement. Two string-potentiometers were used to measure the vertical and lateral displacements of the bracket at the gusset weld point. The load was applied through a hand-cranked pump. Load and displacements were measured continuously using a data acquisition system connected to the load cell and displacement sensors. Since the bracket experiences vertical and lateral deformation, the measurements from the vertical and lateral string-potentiometers were transformed to compute net vertical and lateral movement under the load point.

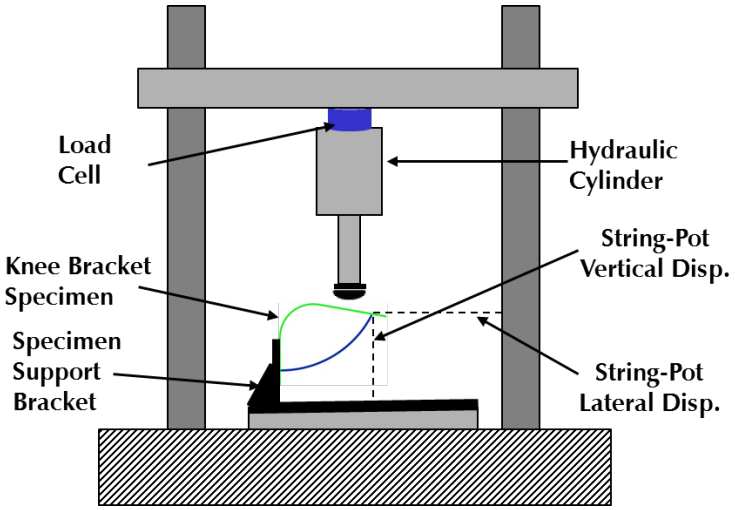

Figure 38. Schematic of the Knee Bracket Test Fixture

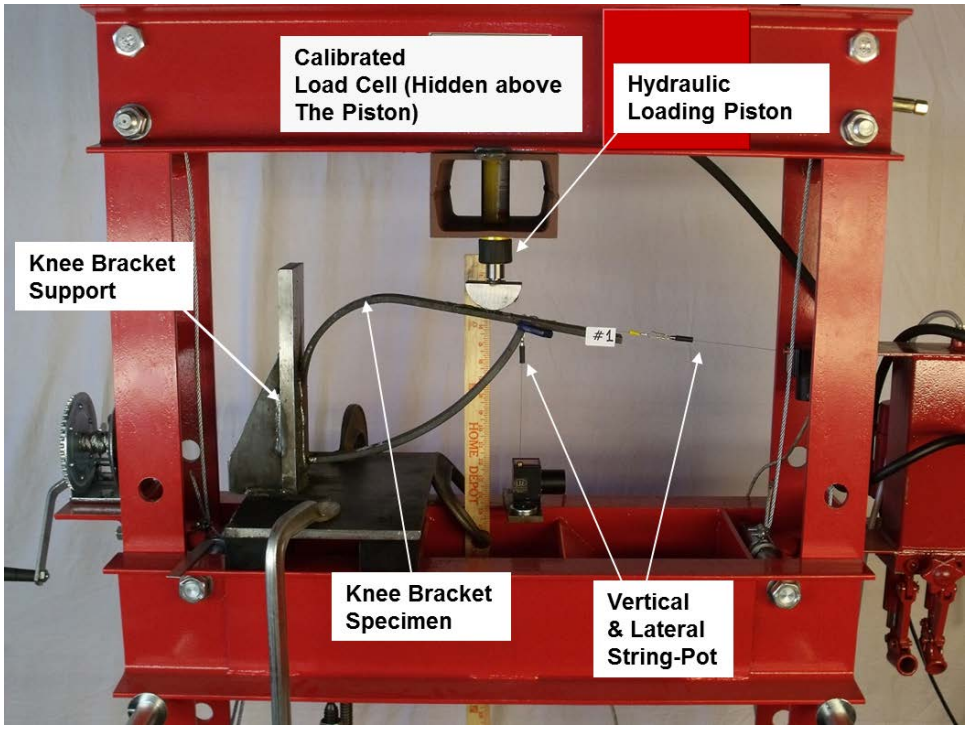

Figure 39. Knee Bracket Sample in the Load Test Frame

Bracket Test Results

The tests proceeded as expected and the behavior of the brackets was also as expected. The knee bracket was loaded to its peak load in a fairly linear fashion. Once the peak load was reached, the load level remained fairly constant, which is ideal behavior. The deformed shape was as expected.

The behavior of the two specimens was similar.

Figure 40 shows the final deformed shape of the bracket specimen after load removal. Figure 41 shows the same specimen before and after the load test. The bracket experienced a permanent deformation of 3.75 in in the vertical direction under the load point. Figure 42 shows the applied vertical load plotted against the computed vertical displacements for each bracket specimen.

Figure 40. Knee Bolster Bracket Specimen – Permanently Deformed Under Load

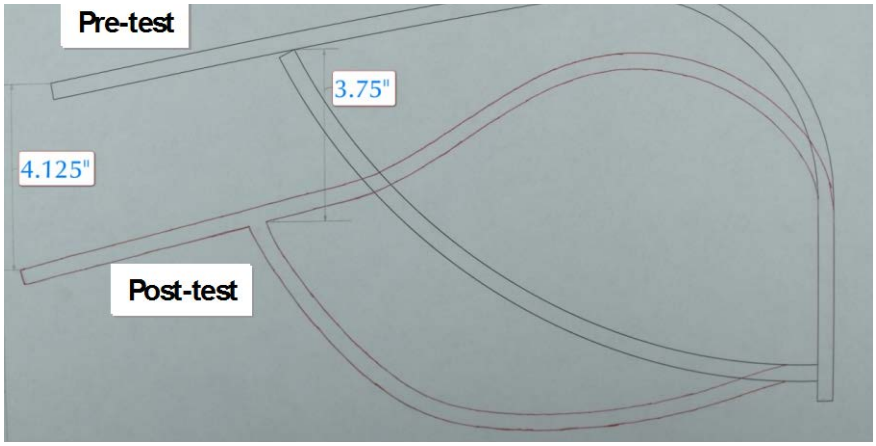

Figure 41. Knee Bolster Bracket Specimen – Pre- and Post-Test Traces

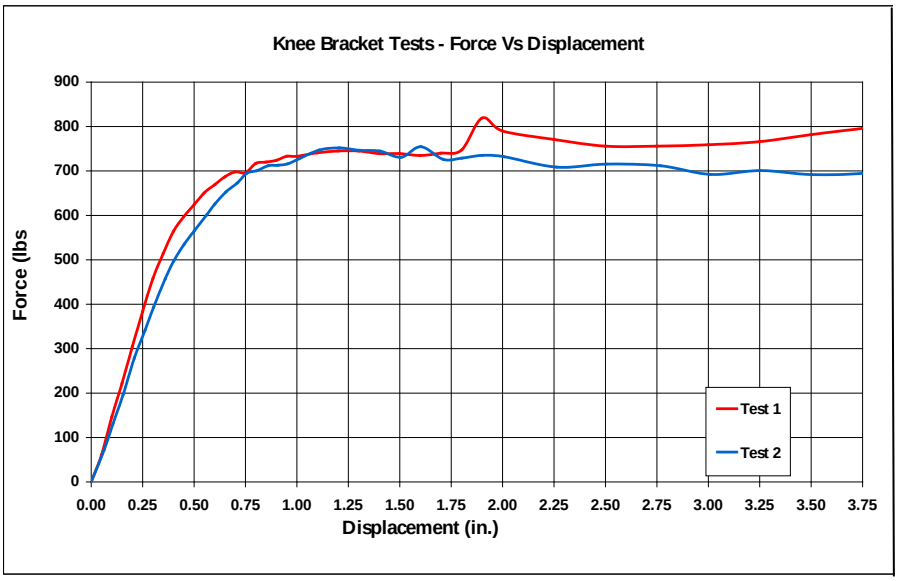

Figure 42. Knee Bolster Bracket Force Deflection Characteristics for the Two Specimens

Knee Bracket Characterization:

A RADIOSS submodel of the knee bracket was prepared for characterization (see Figure 43). The model reflected the test setup in terms of loading conditions, support conditions, and displacement measurement points. Given that RADIOSS is an explicit solver intended for dynamic analysis, the quasi-static nature of the test was simulated by using a loading time of 1000 ms. Subsequently, the material properties of the bracket (yield and ultimate strengths) were adjusted to derive an F-D curve that was comparable to the test data. Two sets of characterized data are presented in Figure 44. Data set 1 used a yield strength of 51 ksi and an ultimate strength of 75 ksi, mimicking the minimum values seen from the material tests. Data set 2 used a yield strength of 54 ksi and an ultimate strength of 78 ksi, mimicking the average values seen from the material tests. Close correlation is seen between the test data and the submodel data. Data set 2 (yield of 54 ksi and ultimate of 78 ksi), being the better match, was used as the final characterized set in the full sled model.

7.3 Summary

As part of the effort to better characterize the behavior of the deformable elements of the EPS, a series of tests were performed. These included static deployment and dynamic drop tower tests on the airbag system, and quasi-static tests of both the knee bracket and the honeycomb material. The test results were used to characterize the RADIOSS submodels of the airbag and the knee bolster. The post-characterization RADIOSS submodels' behavior matched the tested behavior well.

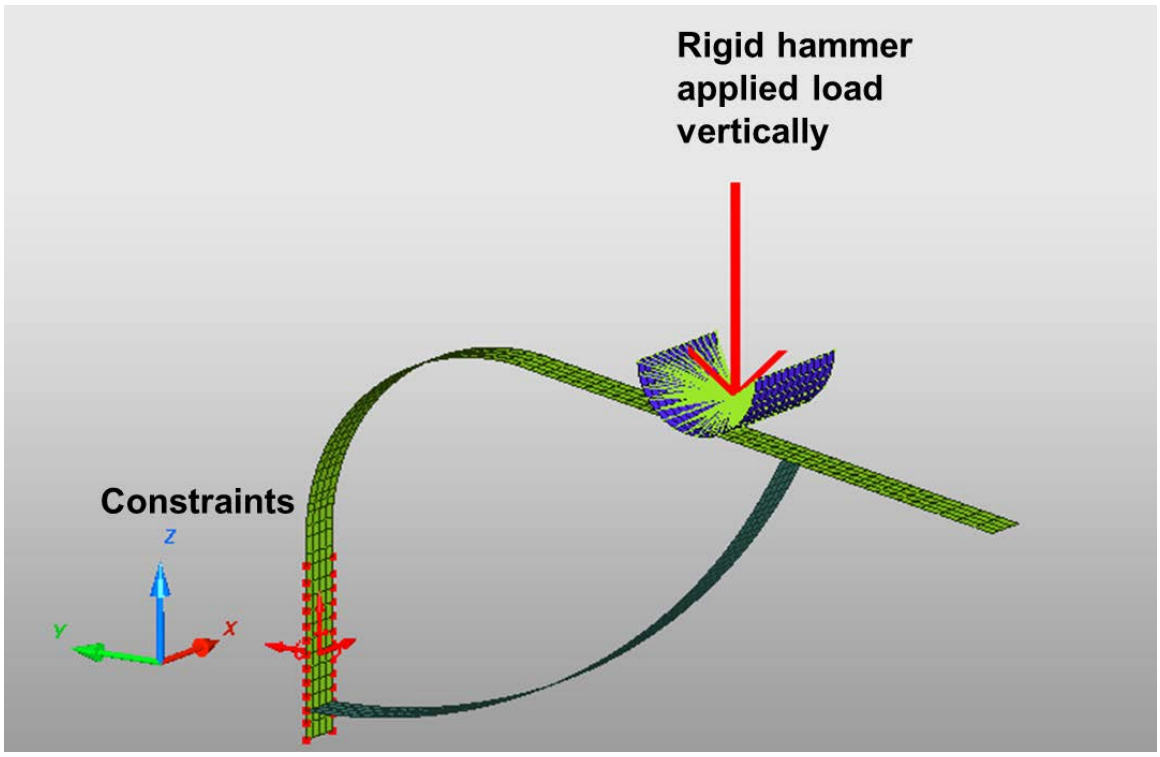

Figure 43. RADIOSS Model of Knee Bracket Test Setup

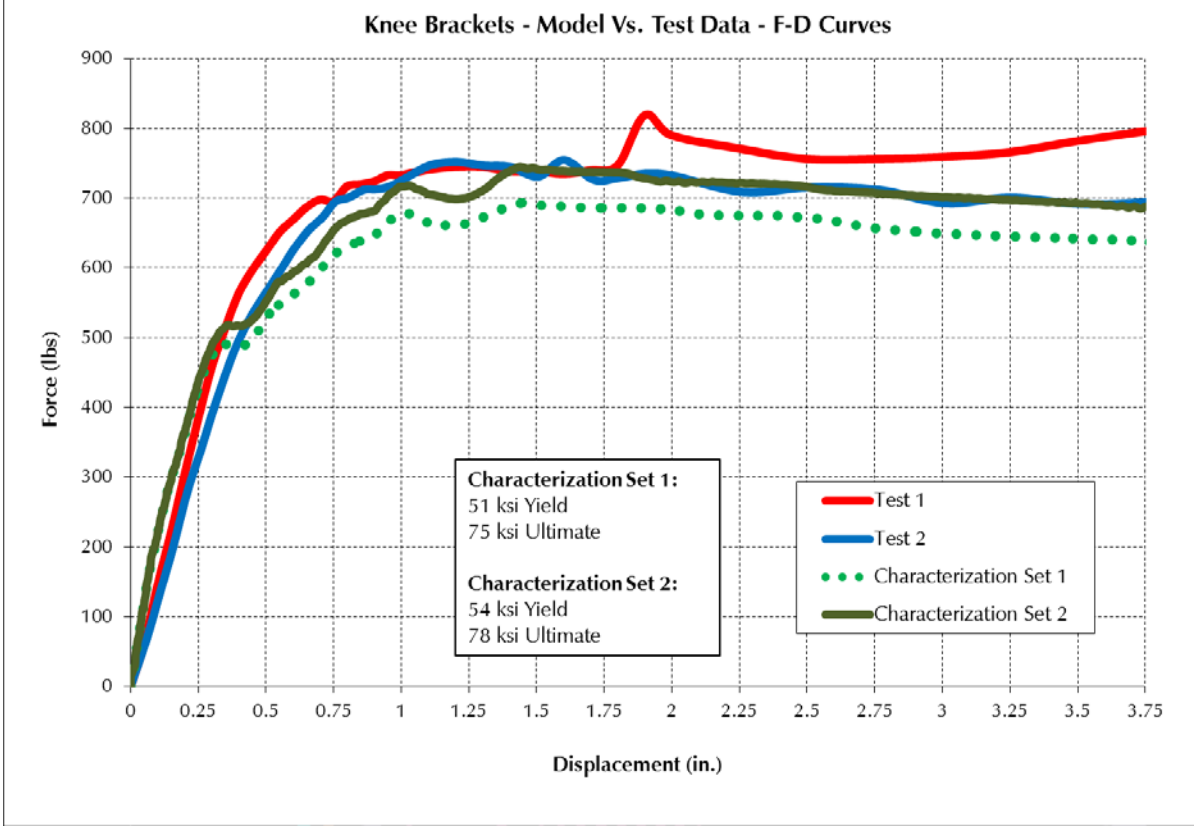

Figure 44. Test and RADIOSS Model Force-Deflection Results for the Knee Brackets

8. Post-Characterization System Performance

The project team updated the full sled test FE model using the post-test characteristics of individual components (see Chapter 7) and simulated a sled test. As part of this effort, characterized submodels of the airbag and knee bolster were integrated back into the RADIOSS model of the sled test, which had been used for prior simulations. The updated model is shown in Figure 45, and the key parameters are identified in Table 18. The EPS test pulse was applied to the system, with a 95^{th} percentile male ATD positioned in the seat. The model was set up to reflect a test in which the sled floor, ATD, and cab environment are all initially at rest and then the test pulse is applied to the sled floor, rather than the ATD. Initial results showed that the system performed well and that all injury criteria were comfortably met.

It was also clear that the results could be improved, from both an injury index perspective and ATD kinematics perspective, by implementing a small design change. The change involved modifying the bottom of the front knee plate by using a hinge connection that would allow the bottom to rotate rather than slide (see Figure 45).

Table 18. Final Model Parameters

Airbag	**Knee Bracket**
• 700 mm length cushion • 450 mm width cushion • PH-5 inflator, 700kPa • 10 ms time delay between the first and second stage trigger • 155 liters cushion volume • Upper/lower tether (510/400 mm) • No vents • Updated leakage properties based on drop tower test data	• L-shaped brackets with gussets – ASTM A36, ⅜ in thick • Young's Modulus: 30.45×10^6 psi • Yield Stress: 54 ksi • Ultimate Stress: 78 ksi • Elongation: 28 % **Honeycomb** • Crush strength of 65 psi

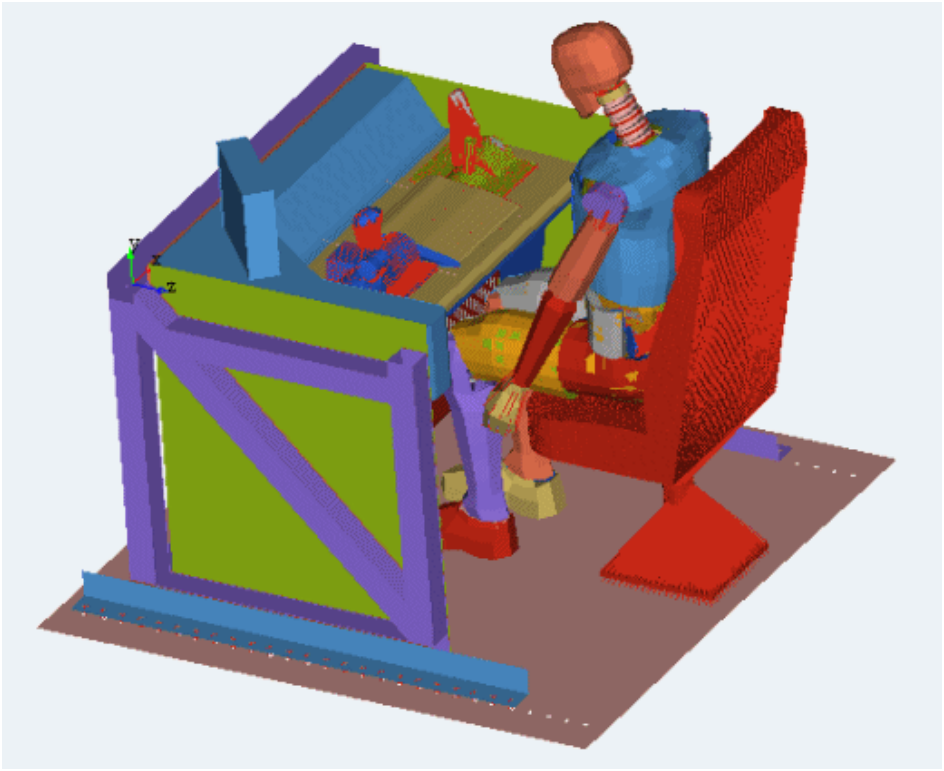

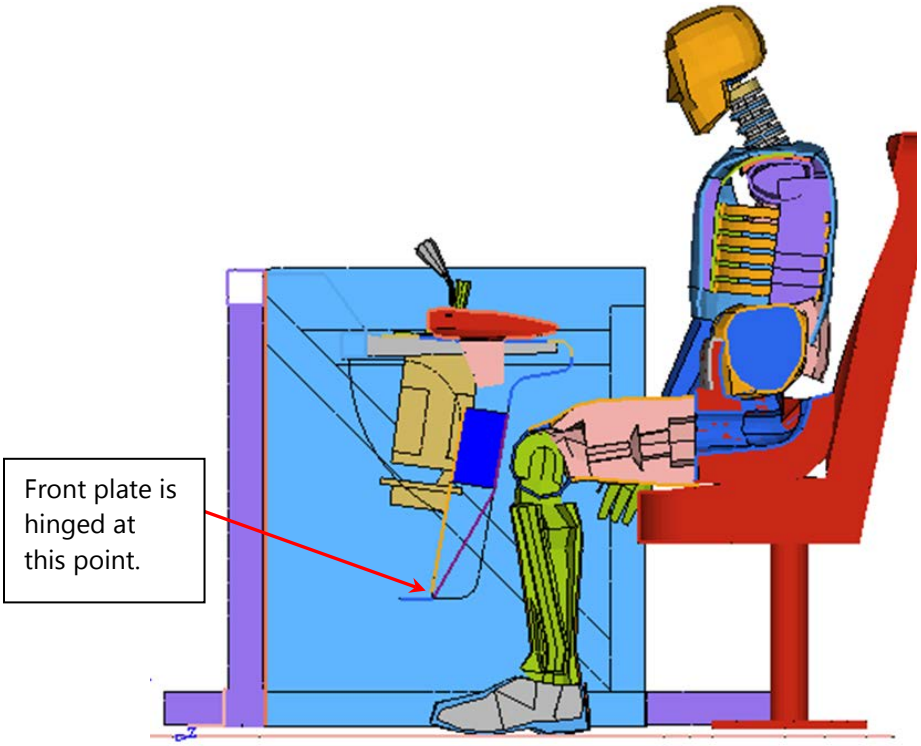

Figure 45. RADIOSS Model of Engineer Protection System Inclusive of Airbag and Knee Bolster Assembly-3-D View and a Sectional Side View

8.1 Results

Calculated injury indices from the final model are shown in Table 19, and normalized injury indices are shown in Figure 47. As shown, the predicted injury indices are lower than allowable limits with a comfortable margin, indicating that the proposed design is successful in meeting the design criteria. ATD kinematics from the proposed design are presented in Figure 46 and are similar to what was seen in the pre-characterization runs: initial contact is between the femur and the knee bolster; the hinged plate design reduced the femur loads and displacements—without notable detriment to ATD kinematics. As the knee bolster loads rise, the torso pitches forward slightly, followed by contact between the chest and the airbag, followed almost immediately after by contact between the head and the airbag—this being coincident with the rise in neck loads. The knees then start straightening out and the head and torso ride down with the airbag, avoiding a head strike and keeping the HIC values low.

Time histories of head acceleration, femur loads, thorax acceleration, chest deflection, chest viscous criterion, and neck forces and moments are presented in Appendix E.

Table 19. Performance of the EPS

Injury Parameter	Index Limit	Calculated Injury Indices (RADIOSS Model)		
		Base Case	Pre-Component Characterization Tests	Post-Component Characterization Tests
HIC_15	700	9,661	104	87
Chest 3 ms (g)	60	38	38	35
Femur Left (N)	10,000	20,307	7,611	7,318
Femur Right (N)	10,000	20,236	7,743	6,924
Neck Tension (N)	4,170	5,089	2,177	2,504
Neck Compression (N)	4,000	2,525	934	543
N_{te}	1.0	1.39	0.60	0.77
N_{tf}	1.0	1.07	0.25	0.29
N_{ce}	1.0	0.28	0.26	0.18
N_{cf}	1.0	0.82	0.26	0.25

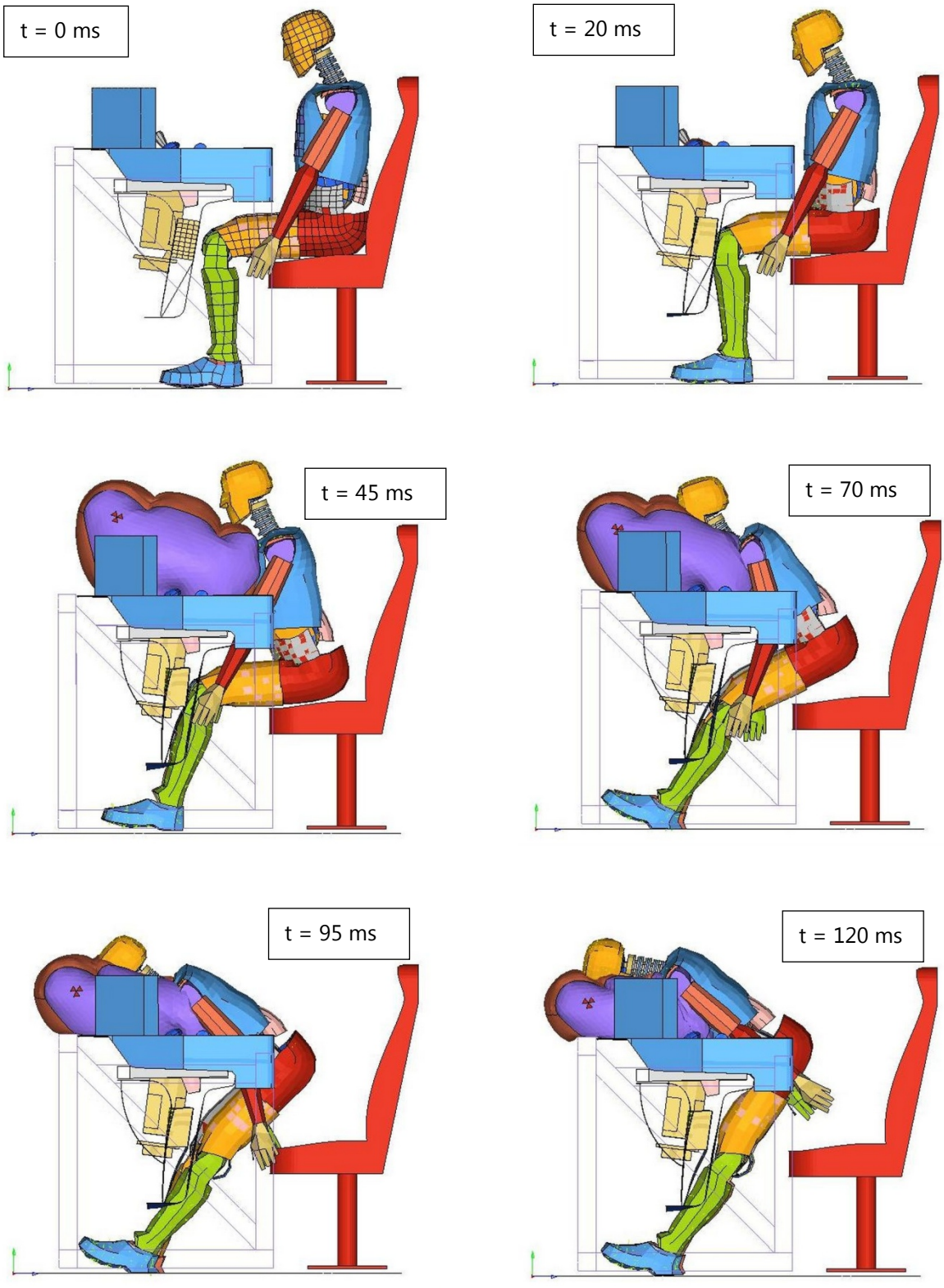

Figure 46. ATD Kinematics for the Proposed Design

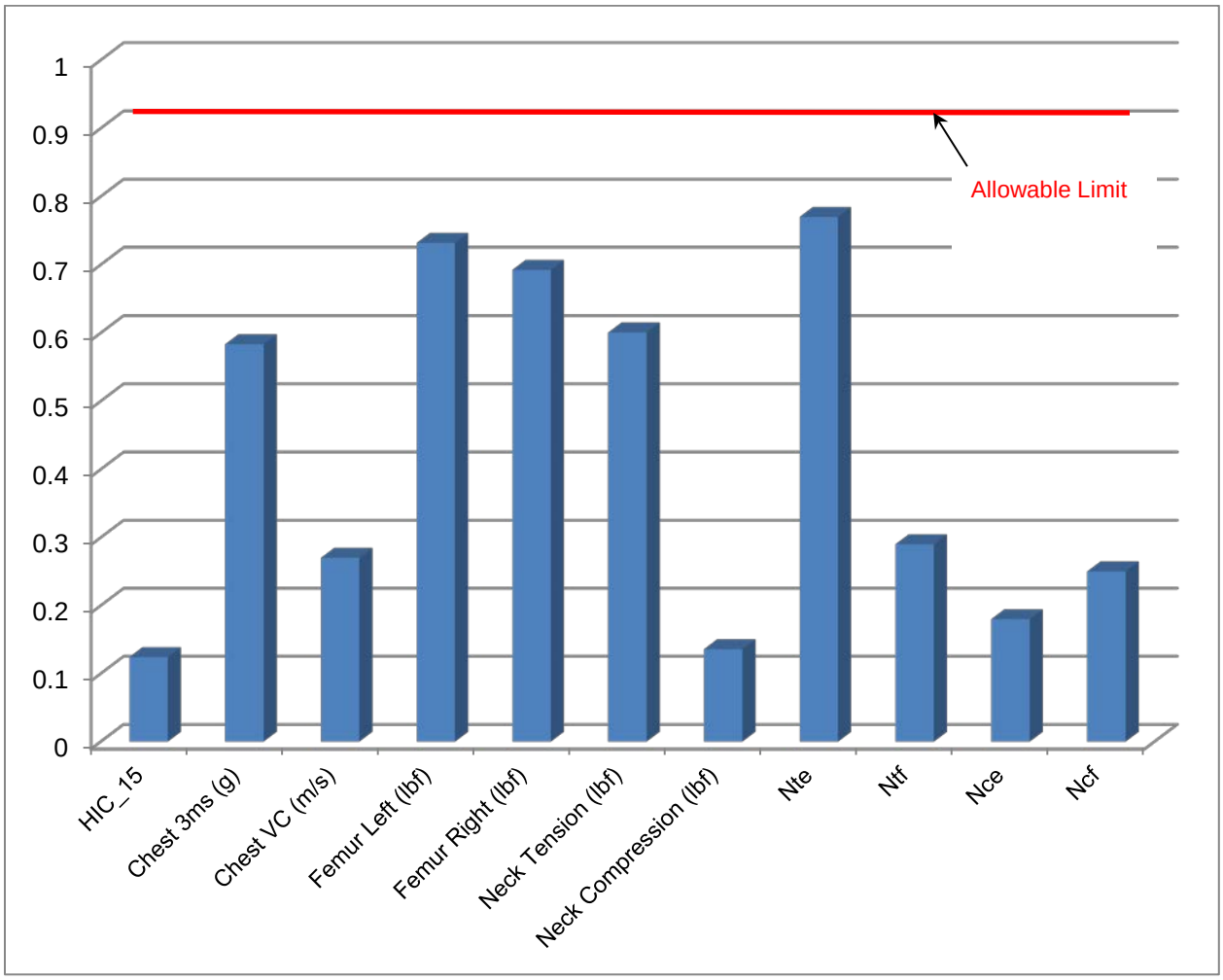

Figure 47. Predicted Normalized Injury Indices for Final Design of Engineer Protection System

9. Conclusions and Recommendations

This effort has resulted in the development of an EPS that effectively protects a cab engineer in the event of a moderate train collision (represented by the EPS test pulse, which is a 23 g, 130 ms trapezoidal crash pulse) and keeps all injury criteria within reasonable limits—without requiring input from the engineer, without restraining him or her, and without impeding egress.

The system is expected to add approximately 30 lb to the car weight, which is reasonable, considering the safety benefits offered. The cost of such a system is likely to vary significantly depending upon volume. For small volumes (100 or fewer units per year), initial estimates of material cost indicate that the system is likely to add approximately $3,000 per equipped cab.

The design was evaluated using a high fidelity, finite element simulation of a sled test, modeled upon a representative baseline cab geometry derived from widely used commuter cab styles in North American railroads. The model uses a detailed representation of a 95th percentile HYBRID III ATD and test-derived characteristics for an airbag and a knee bolster system designed to provide crash protection to the cab engineer without the use of seatbelts.

Simulations carried out using this model predict the injury indices to be much lower than respective allowable limits; these results provide reasonable confidence for proceeding to the next phase of the protection system development. Also, simulation results from various intermediate configurations indicate that the resulting injury indices are not overly sensitive to minor variations in properties of design elements. In other words, reasonable design flexibility is available to achieve the specified injury protection criteria; essentially, the protection system can be adjusted to accommodate other considerations, such as ATD categories, car designs, etc.

Following completion of the protection system evaluation, the final configuration was designed in detail and documented with engineering drawings.

In the next phase of the effort, we recommend that the performance of the proposed system be verified with a full-scale sled test and model validation.

10. References

1. Code of Federal Regulations, Title 49, Part 571, Section 208, Occupant Crash Protection, October 1, 2002.
2. Priante, M. “Review of a Single Car Test of Multilevel Passenger Equipment” American Society of Mechanical Engineers, Paper No. JRC2008-63053, April 2008.
3. MADYMO, Version 7.0, TNO Automotive, Delft, The Netherlands.
4. Radioss, Version 10, Altair Hyperworks, Troy Michigan, USA.

APPENDIX A. STRATEGY AND STANDARDS REVIEW

As noted in section 4, this Appendix presents the strategy and standards review that was conducted as part of this project. A key goal of this effort was to understand the approach, strategy, and protection system elements used in other industries—for example, the automobile industry—and to consider their potential applicability to this cab engineer protection effort. Sections A.1 and A.2 describe occupant protection strategies used in the automobile and heavy vehicle (truck/bus) industries, respectively. Section A.3 discusses how these strategies may be applied to the railroad context.

Another goal was to review the injury criteria and standards used for occupant protection to ensure that the appropriate index targets were used in this effort. Section A.4 discusses key findings from the standards review. Some elements from section 4 are repeated herein, so that this appendix can be a complete document by itself.

A.1 AUTOMOTIVE OCCUPANT PROTECTION STRATEGIES

Passenger safety regulations, other industry criteria (for example, the 'star' rating system), and a competitive marketplace have led automobile manufacturers to develop and deploy advanced crash protection strategies that protect automobile occupants in a variety of impact scenarios. Although crash protection takes several forms, the focus here is on mitigating injuries from secondary contact between the occupant and the vehicle.

A.1.1 Anatomy of a Frontal Crash Event

Automobile frontal crash protection strategies are designed for a standard impact of 35 mph against a rigid wall, as shown in Figure A-1. The resulting crash pulse (typical) to which a passenger is subjected is shown in Figure A-2. The crash pulse duration for such impacts is in the range of 60–80 ms, which is much shorter than the design deceleration pulses used in the railroad industry (APTA[1] or GM/RT2100[2] pulses), or the 130 ms pulse used for this effort. Upon impact, the automobile structure begins to decelerate almost immediately, but the occupant continues to move at the initial velocity of impact until he or she interacts with the vehicle safety system or vehicle interior. Once the occupant engages with the safety system/interior, his/her velocity is quickly reduced to match the vehicle velocity. The time from first contact of the structure with the barrier to the time the occupant reacts to the load varies depending on the severity of the impact and the size of the vehicle; however, a typical time range is 30–60 ms.

[1] TA SS-C&S-016-99, Standard for Passenger Seats in Passenger Rail Cars, The American Public Transportation Association, Washington, DC.

[2] Railway Group Standard GM/RT2100, Requirements for Rail Vehicle Structures, Vol. 4, Rail Safety Standards Board, London, UK, December 2010.

Figure A-1. Standard 35 mph Rigid Barrier Impact Test Used by the Automobile Industry

From first contact, the sequence is as follows:

- A crash sensor mounted on the front vehicle rails senses the impact around 2–4 ms.
- To determine the severity of the impact, that initial pulse is compared to the pulse from a secondary crash sensor located in the immediate vicinity of the occupant. This measurement and comparison takes approximately 5 to 8 ms.
- For an impact meeting the severity threshold, the airbags are triggered to deploy around 7–10 ms, and the airbags take 8–15 ms to fully inflate, depending on the inflator volume, airbag size, and design pressure. The airbags are fully inflated around 20–25 ms.

In a frontal crash, the passenger safety protection system applies key loads directly to the passenger's body. Optimization and adjustment of these forces through various restraint systems leads to minimization of passenger injury. In general,

- Seatbelts limit the translational motion of the occupant and transfer load to the hips and shoulders.
- Head, neck, and chest are decelerated by the primary airbag.
- Seat ramps (angularity of the seat base from the horizontal) can help transfer loading to the pelvis.
- Contact of the occupant's knees with the instrument panel or steering column transfers load onto the occupant's femurs through the knee bolsters or knee airbags which are housed behind the instrument panel or steering column.

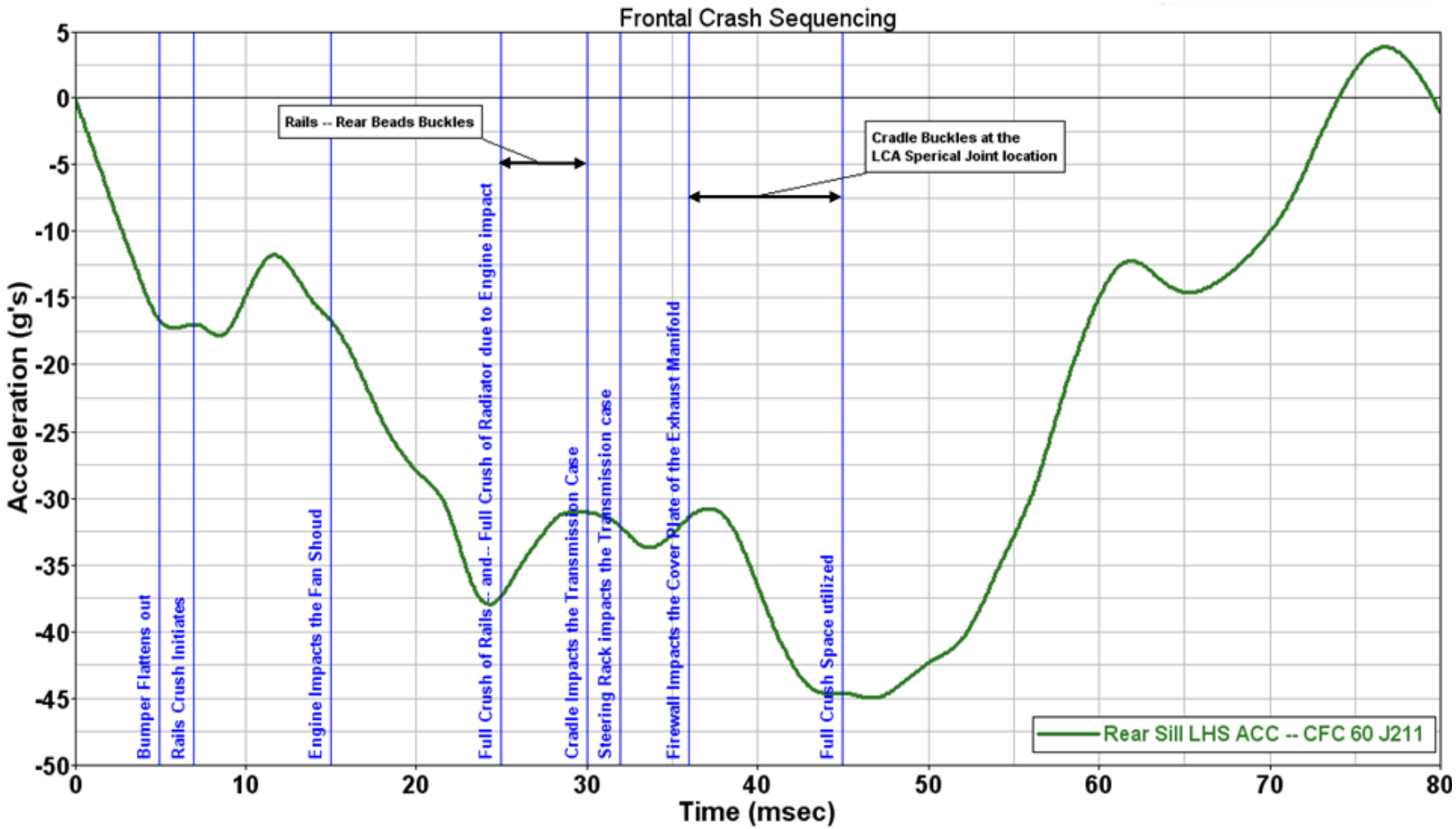

Figure A-2. Typical Automobile Crash Pulse Sequencing and Vehicle Response

A.1.2 Relevant Key Elements of an Automotive Protection System

Frontal Airbags

Frontal automotive airbags are designed to provide coverage for frontal as well as oblique frontal impacts and are sized to accommodate belted as well as unbelted (i.e., out of position) occupants. The driver airbag, which deploys from the steering wheel, is typically round since the actual position of the steering wheel during an accident would be unknown and a shaped airbag could not be controlled. The passenger airbag is typically rectangular or pillow shaped and may have additional protrusions to accommodate different occupant orientations. Both driver and passenger airbags may have specific chambers and differential internal pressures to account for multiple impact scenarios.

For unrestrained occupants, airbags significantly reduce injury to the head and chest—compared to safety belts alone. Airbags provide a well-proven means of controlling energy absorption for an unbelted occupant, which is a critical protective element for survival in a frontal impact. Most vehicles have had driver airbags since 1995 and passenger airbags since 1997. Airbag systems are constantly being improved, and some of these improvements include the following:

- Sensors and sensor grids that better detect the location, size, and weight of occupants
- Multiple stage airbags that deploy with just enough force for a particular impact and occupant

Figure A3. Airbag Protection for an Unbelted Automotive Driver Position Occupant

Knee Airbags

The main function of a knee airbag is to position the body to be more safely accepted by the main airbag. The knee airbag also helps to offload some of the impact force from the lap portion of the seatbelt which reduces abdomen forces. Knee airbags are designed to protect the occupant's knee and leg area, especially if the occupant is not using a seatbelt. Knee airbags typically inflate like normal airbags outside the instrument panel trim, but in some cases the knee airbags inflate beneath the trim.

Figure A-4. Knee Air Bag Deployment for Knee Injury Protection

When the driver is unbelted in a vehicle without a knee airbag installed, there is nothing to restrain the driver at the initial stage of the collision. The driver's knees hit the instrument panel and the driver moves forward until the knee impacts structure substantial enough to stop the forward movement.

A knee airbag can restrain the occupant's knees at the initial stage of a collision, and this in turn increases the efficiency of the ride-down effect (ride-down effect describes the coupling of occupant velocity with vehicle velocity to maximize secondary impact protection). This coupling essentially rotates the driver's upper extremities to face the steering wheel, similar to when the driver is belted, and this makes possible reductions in both chest deflection and chest acceleration.

Knee Energy Absorbers (Knee Bolsters)

Knee energy absorbers are designed to provide controlled loading of the femur in frontal impact scenarios and to limit maximum femur load. These absorbers can consist of specially designed brackets with a tailored force versus deflection response and/or special energy absorbing materials. Knee bolster performance can affect the kinematics of the occupant—particularly an unbelted one—and can have a significant effect on the other injury parameters (e.g. head injury criterion).

Knee bolster impact forces may be controlled by adjusting the stiffness of the energy absorbing brackets behind the knee bolster and/or modifying the stiffness of the lower trim panel. If the knee bolster stiffness is too low, the occupant's knees will not be restrained and this can contribute to the submarining of the occupant beneath the instrument panel; in addition, the knees might pass through the trim panel and make contact with the instrument panel support beam, which is a very stiff member inside most instrument panels, resulting in a very high femur load. If the knee bolster stiffness is too high, the femur loads will be too high and this could result in a broken femur or pelvis.

Impact Countermeasures

Impact countermeasures are the last line of defense after all other safety system components have been exhausted, though they are sometimes employed in combination with existing safety system components to soften the interior contact surfaces and reduce the potential for injury. In essence, impact countermeasures are soft padding or similar elements used to blunt the force of secondary impact.

A.2 HEAVY VEHICLE OCCUPANT PROTECTION STRATEGIES

Heavy vehicles require different safety strategies due to their mass and high center of gravity. Generally, heavy trucks and buses structurally fare better than passenger cars in a crash unless impacting a fixed rigid object or another heavy vehicle.

There are no federal requirements for airbags or other advanced safety systems for heavy vehicles. Unlike the competitive rating system of the automotive safety standards, heavy vehicles typically follow a minimum compliance approach—keeping cost to a minimum—to comply with government regulations that do exist. There are, however, a growing number of studies that promote the implementation of advanced seatbelt and airbag protection systems in trucks.

Several recent studies[3,4,5] have pointed to ejection from the cab and/or crushing of the cab structure as the primary reason for serious/fatal injuries observed in truck crashes; ejection was most frequently observed in frontal impacts (even at low speeds) and rollovers. Accordingly, a priority became retaining the occupant in the cab (prevent ejection). Seatbelts have been shown to be the single most important crash protection device for preventing ejection of truck occupants, but airbags also help to contain the occupant and prevent ejection.

A.3 APPLICABILITY OF AUTOMOTIVE STRATEGIES TO THE RAILROAD ENVIRONMENT

Protection strategies used in the automotive industry offer a number of possibilities for railroad application. Unlike the automobile occupant, the railroad cab occupant is unrestrained—current regulations, operating procedures, and crew preferences do not allow the use of any seatbelt or like restraints for the cab occupant. Furthermore, railroad cab design and construction methods lead to a highly confined space with densely populated equipment and limited space for new items. The desk layout includes protrusions, i.e., throttle and brake levers/handles that pose a special challenge in terms of being kept out of the kinematic path of the cab engineer/occupant. However, the above challenges can be addressed with existing protection technology measures, materials, and adaptable (software) strategies that are currently being implemented by the automotive industry.

The focus of this program is on frontal impact and injuries. Automotive frontal protection techniques provide potential application possibilities.

---

[3] "2006 Large Truck Crash Overview," Analysis Division of the Federal Motor Carrier Safety Administration, U.S. Department of Transportation, Publication No. FMCSA-RI-07-033, December 2007.

[4] Craft, R., Blower, D., "The US Large Truck Crash Causation Study," International Truck and Bus Safety Research and Policy Symposium, Knoxville, Tennessee, April 2002.

[5] Boyle, L., Meltzer, N., Hitz, J., Knipling, R., "Case-Control Study of Large Truck Crash Risk Factors," International Truck and Bus Safety Research and Policy Symposium, Knoxville, Tennessee, April 2002.

Large airbags—similar to those used on the passenger side of automobiles—offer excellent protection to a cab engineer's head and upper torso under frontal impact conditions. Furthermore, the knee airbag or knee bolster type arrangement used for automobile driver positions can also be adapted to protect the cab engineer's knee against impact forces resulting from the unbelted engineer moving against the desk and the knees impacting equipment protrusions under the desk.

A.4 REVIEW OF STANDARDS AND INJURY CRITERIA

A detailed review of crashworthiness standards and recommended practices in the automotive, heavy vehicle, and railway industries, worldwide, was conducted to better inform the project team, and to help define specific goals for the effort. This section presents a list of the documents reviewed and the key takeaway points from the review.

A.4.1 Railway Industry Standards

Key standards that referred to operator/occupant protection issues such as injury indices, sled test pulses, etc. were the American Public Transportation Association (APTA) standards in the United States, the Association of Train Operating Companies (ATOC) standards in the United Kingdom, and GM/RT standards in the United Kingdom/Europe. In the United Kingdom, safety of vehicle interiors has been controlled by the ATOC standards AV/ST9001, though this standard has been superseded by the newly approved GM/RT 2100. Table TA-1 presents the rail industry standards that were reviewed.

The sled test crash pulses specified under these standards have taken several forms. Figure A-5 below presents the crash pulses, or acceleration time histories. Figure A-6 below presents, for comparison, the SIV curves that would result from these different pulse definitions.

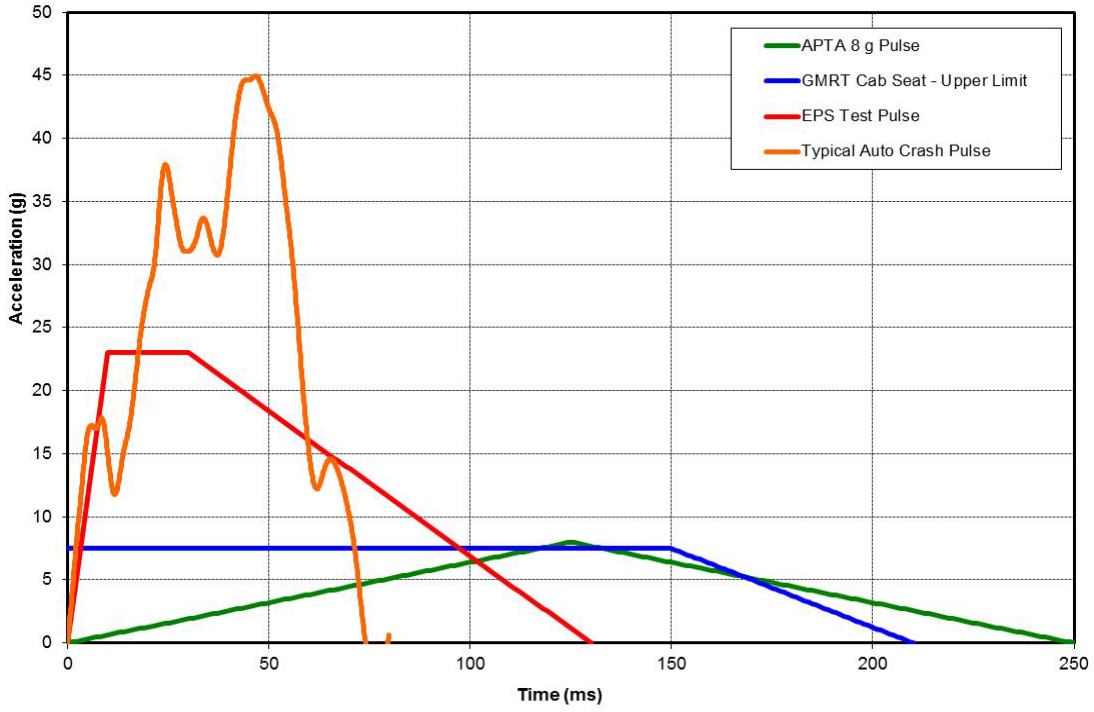

Figure A-5. Comparison of Crash Pulses

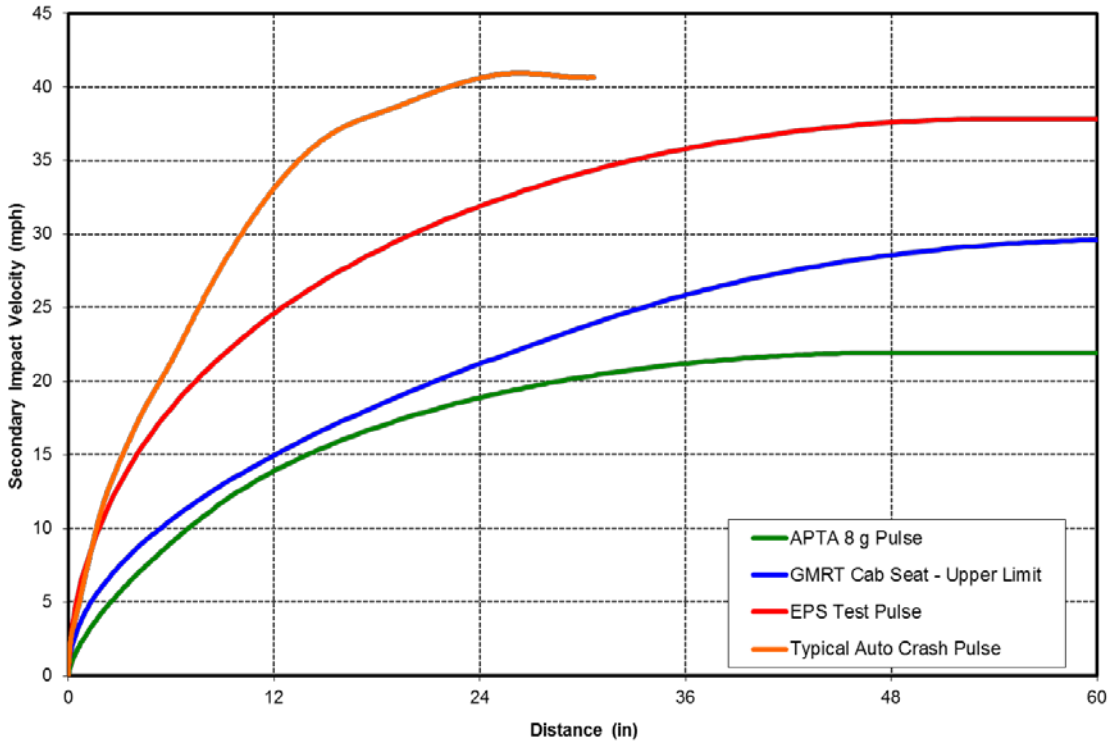

Figure A-6. Comparison of SIV Curves

Table TA-1. Summary of the Railway Vehicle Interior Design and Occupant Protection Recommended Practices and Standards

Document	Type	Description	Effective	Region/ Country	Governing Body
49 CFR PART 238		PASSENGER EQUIPMENT SAFETY STANDARDS		USA	U.S.-DOT-FRA
49 CFR PART 238.233	S	Subpart C – Specific Requirements for Tier I Passenger Equipment - Interior fittings and surfaces	1999	USA	U.S.-DOT-FRA
49 CFR PART 238.435	S	Subpart E – Specific Requirements for Tier II Passenger Equipment Section - Interior fittings and surfaces	1999		
49 CFR PART 238.447	S	Subpart E – Specific Requirements for Tier II Passenger Equipment	1999		
AAR-MSRP Section M - RP-5104	RP	Locomotive Cabs	1974		AAR
AAR-MSRP Section M - RP-5128	RP	Diesel Locomotive Control Stand for New Locomotives	1975		
AAR-MSRP Section M - RP-5132	RP	Rounding All Possible Exposed Convex Edges and Corners	1971		
APTA SS-C&S-011-99 Rev.1 (3-22-04)	S	Standard for Cab Crew Seating Design and Performance	1999		APTA
APTA SS-C&S-016-99 Rev.1 (3-22-04)	S	Standard for Row-to-Row Seating in Commuter Rail Cars	2004		
APTA SS-C&S-016-99 Rev.2	S	Standard for Passenger Seats in Passenger Rail Cars	2010		
EN12663, July 2000	S	Structural Requirements for Railway Vehicles	2000	Europe	European Committee for Standardization
EN15227 Final Draft 2007	S	Crashworthiness Requirements of Railway Vehicle Bodies	2009	Europe	European Committee for Standardization
AV/ST9001, Issue One, February 2002	S	Vehicle Interior Crashworthiness – ATOC Vehicle Standard	2002	UK	Association of Operating Companies
GM/RT2100, Issue One, July 1994	S	Structural Requirements for Railway Vehicles	1994		Safety & Standards Directorate
GM/RT2100, Issue Four	S	Requirements for Rail Vehicle Structures	2010		Railway Safety & Standards Board
SAF/STD/0057/RSK, Version 2.1, Dec. 2004	S	Rolling Stock Structural Requirements	2009	Australia	Queensland Railway Governance & Management Framework

S: Standards, RP: Recommended Practices

The injury indices specified in these documents, while not identical, are reasonably consistent and reflect ongoing biomedical research on what the human body can tolerate/survive, as well as mechanisms for best quantifying/measuring the key parameters. Table TA-2 below presents, for comparison, key injury indices from these standards. It should also be noted that injury criteria should be selected considering the input crash pulse; for example, some of the tighter injury criteria listed in the GM/RT2100[2] standard are also linked to a softer crash pulse than the APTA pulse (note crash pulses plotted in Figure A-5).

Table TA-2. Comparison of Injury Indices for APTA and GM/RT2100

Body Part	Criteria	APTA	GM/RT 2100
Head	HIC_{15}	<700	< 500
	3 ms Acceleration		< 80g
Neck	Bending in Flexion		< 310 Nm
	Bending in Extension		< 135 Nm
	Tension ($+F_z$)	<4,170 N	<4,170 N
	Compression ($-F_z$)	<4,000 N	<4,000 N
	N_{ij}	<1.0	< 1.0
Femur	Axial load	<10,000 N	< 4,300 N
Knee	Displacement		< 16 mm
Tibia	Index		< 0.75
Chest	3 ms Acceleration	<60 g	<60 g
	Deflection		< 63 mm
	Viscous		< 1m/sec
	Thoracic Index		<1.0
Abdomen	Compression		< 40 mm
	Viscous Criterion		<1.0

A.4.2 Automotive and Heavy Vehicle Standards

The project team also reviewed several automotive and heavy vehicle standards as part of this effort. A summary of the reviewed standards is included in Table TA-3.

United States injury indices for unbelted automobile drivers and passengers are based on a 50th percentile adult male for 25 mph (40 km/h) crash into a rigid barrier. The associated test procedures and the injury criteria are documented in the Federal Motor Vehicle Safety Standards (FMVSS) 208 – Occupant Crash Protection. Criteria for passengers in nonautomobile vehicles, such as vans and buses, are contained in FMVSS 201 and 222, respectively. Out of these three standards, FMVSS 208 has the greatest relevance to rail cab car crash protection since an automobile driver, like the cab engineer, is closest to impacting objects.

Table TA-3. Summary of Automotive Crashworthiness Standards

Document	Description	Effective	Region/ Country	Governing Body
ECE R-80	Seats of Large Passenger Vehicles	1989, 2009 (Rev 2)	Europe	Economic Commission for Europe (ECE)
ECE R-29	Protection of the Occupants of the Cab of Commercial Vehicles	1993, 2007 (Rev 1)	Europe	ECE
ECE R-33	Vehicle Structure in Head-On Collision	1995, 2008 (Rev 3)	Europe	ECE
ECE R-66	Strength of the Superstructure of Large Passenger Vehicles	1995, 2008 (Rev 1)	Europe	ECE
FMVSS 201	Occupant Protection in Interior Impact	1968, Rev. 2008	USA	U.S.-DOT
FMVSS 222	Passenger Protection in Commercial Vehicles (Used for School Buses)	1968, Rev. 2008	USA	U.S.-DOT
FMVSS 208	Occupant Crash Protection	1977, Rev. 2008	USA	U.S.-DOT
ADR 69	Vehicle Standard (Australian Design Rule 69/00 – Full Frontal Impact Occupant Protection) 2006 Compilation 1	2007	Australia	Australia DOT & Regional Services
ISO 3471	Rollover Protection in Construction Equipment	1986, Rev. 2008	Worldwide	

European standards ECE R29, R33, R66, and R80 pertain to crashworthiness and passenger protection. ECE R-80 includes the sled testing procedures and associated injury criteria. ECE R80 does not specify a shape to the sled test pulse, but aims for peak speed of 18.75–20 mph (30–32 km/h) with an average acceleration of 6.5–8.5 g. The ECE R80 injury criteria include only head, chest, and femur injury indices. The Australian standard ADR 69/00 specifies a 48 km/h rigid barrier impact test for motorized vehicles and defines required injury indices for head, neck, chest, and femur.

For comparative purposes, a summary of the automotive industry injury criteria from FMVSS 208, ECE R80, and ADR 69/00 is included in Table TA-4.

The HIC, chest, and femur injury criteria used in the automobile industry across the world are similar, perhaps underscoring the globalization of the automotive market. The European standards ECE R80 do not include any neck injury criterion.

Table TA-4. Summary of Automotive Injury Criteria

Body Part	Criteria	FMVSS 208	ECE R80	ADR69/00	
Head					No Head Contact
	HIC_{15}	<700	<500		<700
	HIC_{36}			<1000	
	3 ms Acceleration				<75 g
Neck	Tension	<937 lbf (4,170 N)			<3,300 N
	Compression	<899 lbf (4,000 N)			
	Nij	<1.0			
Femur	Axial load	<2,250 lbf (10,000 N)	<10,000 N <8,000 N (20 ms)	<10,000 N	<10,000 N
Chest	3 ms Acceleration	<60 g		<60 g	<60 g
	Deflection	<63 mm		<76.2 mm	<76.2 mm

A.4.3 Injury Index Summary

Although the impact and crash scenarios, resulting crash pulses, and sled test requirements between the automobile and railway environments—as well as within the railway industry—differ significantly, the injury criteria used are quite similar. This fact confirms that regulatory identities around the world are adopting reasonably consistent standards; it also establishes that the set of limiting injury indices adopted for this effort was reasonable and consistent with other efforts, thereby providing additional confidence in the requirements laid out.

APPENDIX B. BRAINSTORM SESSION TO GENERATE CONCEPTS FOR THE PROTECTION SYSTEM

Table TB-1. Concepts for Head Area

No.	Component/ Technique	Description	Feasibility + Acceptability	Development Timeframe	Likelihood of Success	Comment
1	Passenger Style Airbag	Large airbag using desk top surface and console surface for reaction loads	High	Short	High	Will also be helpful in torso protection (may have multiple chambers to control shape)
2	Deployable Net	Deploy from top, sides or bottom	Medium	Long	Medium	Based on pyrotechnic (pyro) deployment (a controlled explosion/inflation used for positioning a device)
3	Local Softening	HIC Cartridge concept; localized application of energy absorbing material(s)	High	Short	High	May not be effective if ATD/Engineer does not impact the surface
4	Friendly Controls	Breakaway or compliant controls that move away from the operation during impact	Medium	Long	High	May not be effective if ATD/Engineer does not impact the surface
5	Recessed Controls		Low	Short	High	
6	Dropdown Bolster	Swung down from ceiling to arrest upper body	High	Medium	Medium-High	Hinged and deployed using pyro; from the ceiling
7	Cantilevered Bolster	Swung from either side	High	Medium	Medium-High	
8	Neck Brace		Low	Short	High	

Table TB-2. Concepts for Torso Area

No.	Component/ Technique	Description	Feasibility + Acceptability	Development Timeframe	Likelihood of Success	Comment
1	Shaping the Console	Contoured shape + variable crush behavior	High	Short	High	
2	Honeycomb or Foam	Applied at the desk edge	High	Short	Small	
3	Airbag for Torso	Designed to engage torso + pelvis only	High	Short	Small	
4	Extended Desk	Extend desk edge to be permanently closer to the operator's torso when the operator is in the normal operating position; will most likely require the operator to push back/rotate the chair to get out of the chair	Medium	Short	Small	Highly feasible if it does not impede operator egress
5	Stroking Desk	Energy absorption elements behind the desk; entire desk moves forward and away from the operator during impact	Medium	Medium	Small	
6	Inclined Seat	Seat pan and back tilted back slightly	Medium	Short	Small	Needs Human Factors input, AAR MSRP S-5104 requires 3–6 degree tilt back of the seat pan and 95–115 degree tilt back of the seat back
7	Rotating Seat Base	Mechanism in the seat base to allow the seat pan and back to rotate up (pitch backward) during impact	Medium	Long	Medium	
8	Seat Base Plastic Deformation	Rear side of seat base collapses to allow the seat to pitch backwards during impact	Medium	Medium	Medium-High	

No.	Component/ Technique	Description	Feasibility + Acceptability	Development Timeframe	Likelihood of Success	Comment
9	Knee Activated Torso Bolster	Knee pushes the knee bolster plate which is hinged to the torso bolster and in turn pushes the torso bolster up to engage operator torso	Medium	Long	Medium	Torso bolster will be part of the desktop surface in normal usage.
10	Movable Controls and Under-Desk Devices	Controls and under-desk devices are mounted in rails; they move forward and away from the operator during impact	Medium	Medium	High	
11	Deployable Seatbelts		Low	Long	Low	
12	Concept No. 1 + Inflatable Tube Structure (ITS, Braided Tube)		High	Medium	High	
13	ITS + Sidewall Tethers		High	Medium	High	
14	Rotating Frame + Net		High	Medium	High	Frame hinged at the floor; needs pyro; how would the net deploy?
15	Rotating Frame + ITS		High	Medium	High	Frame hinged at the floor; needs pyro; ITS will be part of the desk edge
16	Dynamically Extending Desk	Move desk edge closer to engineer using pyro	High	Medium	High	Desk edge could be shaped dynamically to provide larger reaction area
17	Deploying ITS from Desk Mounted Arms		High	Medium	High	Arms swing up from the desk; hinged at the front desk edge?
18	Relocating Controls		Medium	Short	High	Need Human Factors input

Table TB-3. Concepts for Femur Area

No.	Component/ Technique	Description	Feasibility + Acceptability	Development Timeframe	Likelihood of Success	Comment
1	Beam/Bracket + Honeycomb	Knee bolster backed by a deformable beam/bracket and crushable honeycomb	High	Short	High	
2	Hydraulic Damper	Knee bolster backed by rotary or linear damper	High	Short-Medium	High	
3	Honeycomb Only		High	Short	High	
4	Knee Airbag	Deployed in front of or behind the knee panel	High	Medium	High	
5	Inflatable Tube/Braided Tube	Generally known as Inflatable Tube Structures (ITS)	High	Medium	High	
6	Buckling/Deforming Structures	Structures designed to take plastic deformation during impact	High	Short	High	
7	Tube in Tube/Cutting Head	Concentric, telescoping tubes in which the inner tube has a cutting edge that tears the outer tube during the stroke to absorb energy	High	Medium	Medium	
8	Structural Foam		High	Short	High	

APPENDIX C. EVALUATION OF POTENTIAL CONCEPTS FOR THE PROTECTION SYSTEM

Table TC-1. Evaluation of Concepts for Head and Torso Protection

No.	Concept Description	Injury Index Reduction	Compartmentalization	Affect Egress	Development Timeframe	Simplicity of Design	Maintenance	Comfort & Ergonomics	Weight Concerns	Material Costs	Manufacturing Costs	
	Weighting Factor	**5.0**	**5.0**	**5.0**	**4.0**	**3.0**	**3.0**	**3.0**	**1.0**	**1.0**	**1.0**	**SUM**
1	Passenger Style Airbag	4.75	4.50	4.50	3.88	3.63	4.25	4.50	4.25	3.50	3.50	**133**
2	Shaping the Console	2.75	3.50	4.25	4.25	4.25	4.75	4.25	4.63	4.38	4.25	**123**
3	Local Softening	2.63	1.50	4.88	4.13	4.50	4.50	4.75	4.75	3.88	3.88	**115**
4	ITS	3.88	4.00	3.88	3.38	3.25	4.00	4.63	4.13	3.13	3.25	**118**
5	Passenger Style Airbag + Tethers	4.88	4.88	3.75	3.50	3.00	3.88	4.50	4.25	3.25	3.25	**126**
6	Crushable Console (Honeycomb or Foam)	3.38	3.38	4.25	4.00	4.25	4.25	4.50	4.50	3.38	3.50	**121**
7	Dropdown Bolster + Shaping the Console	3.88	4.25	3.50	3.13	2.75	3.25	4.38	3.25	3.38	3.13	**112**
8	Cantilevered Bolster	3.50	3.75	3.88	3.13	3.25	3.50	4.38	3.50	3.38	3.50	**112**
9	Rotating Frame + ITS	4.00	4.25	3.13	2.75	2.75	3.13	4.25	3.00	2.88	2.88	**107**

Table TC-2. Evaluation of Concepts for Femur Protection

No.	Concept Description	Injury Index Reduction	Compartmentalization	Affect Egress	Development Timeframe	Simplicity of Design	Maintenance	Comfort & Ergonomics	Weight Concerns	Material Costs	Manufacturing Costs	
	Weighting Factor	**5.0**	**5.0**	**5.0**	**4.0**	**3.0**	**3.0**	**3.0**	**1.0**	**1.0**	**1.0**	**SUM**
1	Honeycomb or Foam	3.88	3.88	4.88	4.50	4.63	4.50	4.38	4.50	4.13	4.25	**135**
2	ITS	4.25	3.75	4.63	3.50	3.50	4.00	4.75	4.00	3.38	3.38	**125**
3	Knee Airbag	4.75	4.63	4.63	3.63	3.88	4.00	4.75	4.13	3.25	3.38	**133**
4	Hydraulic Damper	3.50	3.75	4.50	3.50	3.88	3.50	4.13	3.75	3.38	3.50	**118**
5	Tube in Tube	3.63	4.00	4.50	3.38	3.75	4.00	4.25	3.88	3.88	3.75	**122**
6	Deformable Beam Bracket + Honeycomb/Foam	4.38	4.38	4.50	4.00	4.13	4.38	4.25	4.25	4.00	4.00	**133**

APPENDIX D. PRELIMINARY EVALUATION OF CONCEPT VIABILITY

Prior project effort generated the following two promising concepts for an Engineer Protection System (EPS):

1. Automotive passenger-style airbag with a crushable knee bolster
2. ITS with a knee airbag or crushable knee bolster

The intent of the preliminary simulations described herein was to identify the strengths and weakness of the two concepts, thereby helping to select a configuration for further development and detailed design. MADYMO™ models of the two concepts were developed, including the ATD in cab seat and a desk with the deployable elements. For this initial modeling, typical passenger style airbag and knee bolster properties from an automotive application were used. The initial properties were intended to serve as starting points for the analysis, not design targets. The EPS test pulse shown in Figure 1 (main body) and a 95th percentile adult male ATD were used. A baseline run was made with no head, torso, or knee protection system.

Several variants of the two concepts were investigated, including airbags and ITS with different venting characteristics, multiple cab front wall configurations, etc. Concept 2 was evaluated with both knee airbag and knee bolster configurations. The airbag, knee bolster, ITS, and knee airbag characteristics used in the two concepts are shown in Figures D-1 through D-4. The investigated scenarios are summarized in Table TD-1.

For both concepts, injury indices for head, chest, neck, and femur were computed and are shown in Table TD-2 and Table TD-3. Also shown in those tables are injury indices for the baseline case (i.e., no protection system).

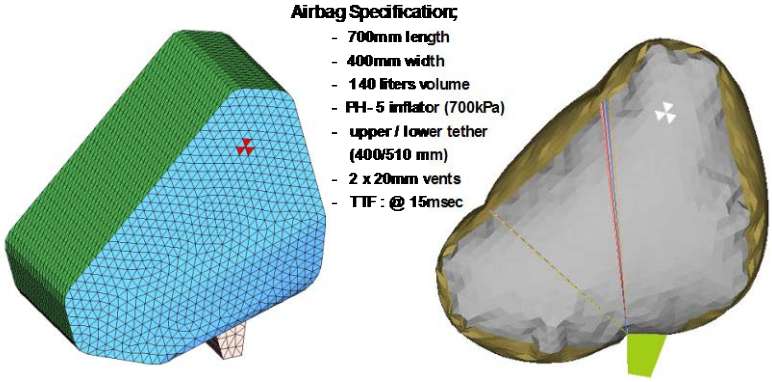

Figure D-1. Airbag Model Characteristics for Concept 1

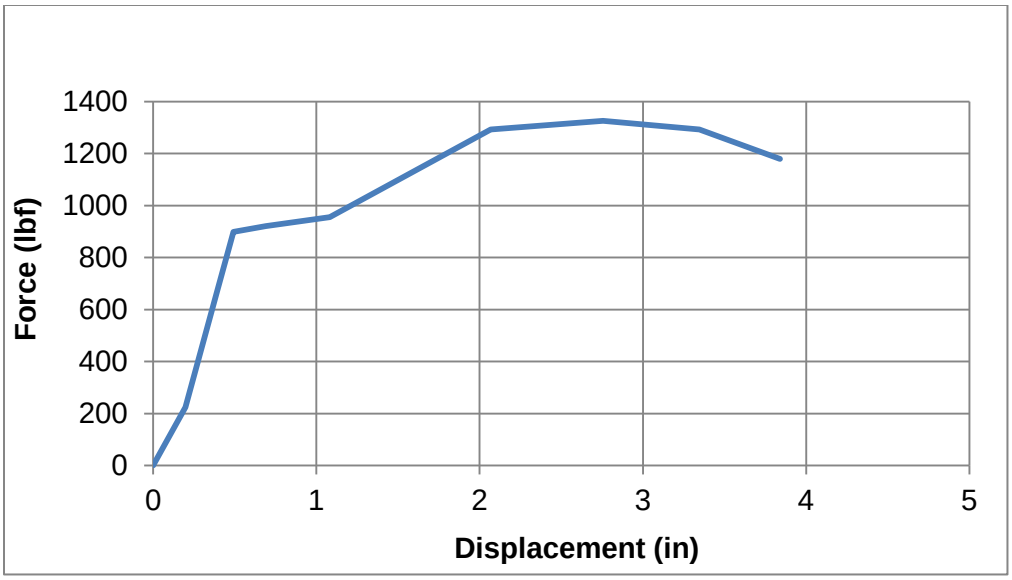

Figure D-2. Knee Bolster Force-Deflection Characteristics Assumed for Concept 1

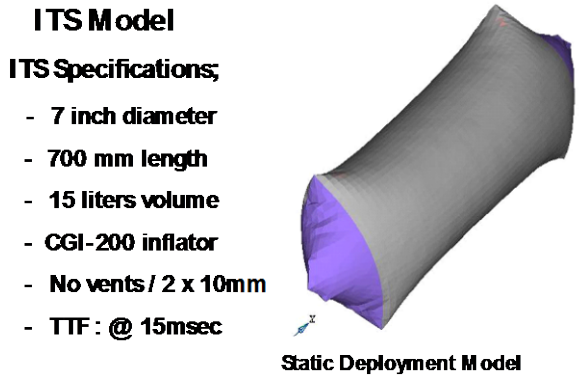

Figure D-3. Inflatable Tubular Structure (ITS) characteristics for Concept 2

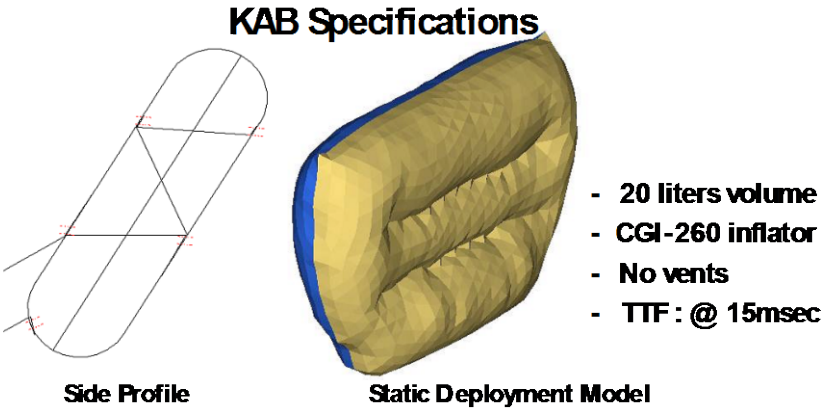

Figure D-4. Knee Airbag Characteristics for Concept 2

Table TD-1. Investigation Scenarios for Concepts 1 and 2

<table>
<tr><th>Item #</th><th>Model</th><th>Airbag</th><th>Front Wall</th><th>Airbag Vent</th><th>Knee Bolster</th><th>ITS</th><th>Knee Airbag</th><th>ITS Vent</th><th>ITS Location</th><th>Restraint Spec</th></tr>
<tr><td>1</td><td>Baseline
No Protection</td><td colspan="9">N/A</td></tr>
<tr><td>2</td><td rowspan="3">Concept 1</td><td>Y</td><td>Y</td><td>2x20mm</td><td>Y</td><td colspan="4" rowspan="3">N/A</td><td rowspan="4">Airbag:
630D fabric
400mm width
Upper/lower tethers (510/400mm)
140 liters volume
PH5 inflator
TTF: 15 ms</td></tr>
<tr><td>3</td><td>Y</td><td>N</td><td>2x20mm</td><td>Y</td></tr>
<tr><td>4</td><td>Y</td><td>N</td><td>2x10mm</td><td>Y</td></tr>
<tr><td>5</td><td>Y</td><td>N</td><td>No vents</td><td>Y</td></tr>
<tr><td>6</td><td rowspan="7">Concept 2</td><td colspan="4" rowspan="7">N/A</td><td>N</td><td>Y</td><td>Y</td><td>No vents</td><td rowspan="4">Base Location</td><td rowspan="7">ITS Configuration:
7” diameter
700 mm length
15 liters volume
CGI-200 inflator
No vents
TTF: 15 ms
KAB Configuration:
20 liters volume
CGI-260 inflator
No vents
TTF: 15 ms</td></tr>
<tr><td>7</td><td>Y</td><td>Y</td><td>N</td><td>No vents</td></tr>
<tr><td>8</td><td>Y</td><td>Y</td><td>N</td><td>2x10mm</td></tr>
<tr><td>9</td><td>Y</td><td>Y</td><td>N</td><td>2x20mm</td></tr>
<tr><td>10</td><td>Y</td><td>Y</td><td>N</td><td>No vents</td><td rowspan="3">Moved 4” back</td></tr>
<tr><td>11</td><td>Y</td><td>Y</td><td>N</td><td>2x10mm</td></tr>
<tr><td>12</td><td>Y</td><td>Y</td><td>N</td><td>2x20mm</td></tr>
</table>

Table TD-2. MADYMO™ Simulation Results for Concept 1 and Baseline

Injury Response	Requirements 95th% ATD	Baseline		Concept 1 System (Airbag + Knee Bolster)							
		No Protection	%	W/ Front Wall Contact & 2x20 mm Vents	%	W/O Front Wall Contact & 2x20 mm Vents	%	W/O Front Wall Contact & 2x10 mm Vents	%	W/O Front Wall Contact & No Vents	%
HIC_15	700	84,318	**12,045%**	433	62%	1,215	**174%**	**625**	89%	531	76%
Chest 3 ms (g)	60.0	75.3	**126%**	41.2	69%	41.2	69%	38.4	74%	43.3	72%
V*C (m/s)	1.0	0.44	44%	0.39	39%	0.39	39%	0.47	47%	0.45	45%
Femur Left (N)	10,000	15,556	**156%**	5,825	58%	5,825	58%	5,825	58%	5,825	58%
Femur Right (N)	10,000	15,554	**156%**	5,826	58%	5,826	58%	5,826	58%	5,826	58%
Neck Tension (N)	4,170	11,262	**270%**	2,495	60%	4,434	**106%**	2,953	71%	2,495	60%
Neck Comp. (N)	4,000	4,509	**113%**	113	3%	113	3%	113	3%	113	3%
N_{te}	1.00	3.44	**344%**	0.72	72%	0.72	72%	0.52	52%	0.75	75%
N_{tf}	1.00	1.95	**195%**	0.65	65%	1.16	**116%**	0.56	56%	0.70	70%
N_{ce}	1.00	0.27	27%	0.11	11%	0.00	0%	0.10	10%	0.13	13%
N_{cf}	1.00	2.15	**215%**	0.03	3%	0.03	3%	0.03	3%	0.03	3%

xx Exceeds design requirements
x Exceeds target (80 % of design requirements)

Table TD-3. MADYMO™ Simulation Results for Concept 2 and Baseline

Injury Response	Requirements 95th% ATD	Baseline		Concept 2 System													
				ITS + Knee Airbag		ITS + Knee Bolster						ITS (Moved Back 4 Inch) + Knee Bolster					
		No Prot.	%	No Vents	%	No Vents	%	2 x 10 mm Vents	%	2 x 20 mm Vents	%	No Vents	%	2 x 10 mm Vents	%	2 x 20 mm Vents	%
HIC_15	700	84,318	**12,045%**	275	39%	302	43%	305	44%	298	43%	617	**88%**	654	**93%**	917	**131%**
Chest 3 ms (g)	60.0	75.3	**126%**	62.6	**104%**	56.0	**93%**	55.7	**93%**	55.8	**93%**	60.0	**100%**	60.4	**101%**	58.7	**98%**
V*C (m/s)	1.0	0.44	**44%**	0.74	74%	0.62	62%	0.63	63%	0.65	65%	0.70	70%	0.69	69%	0.67	67%
Femur Left (N)	10,000	15,556	**156%**	18,015	**180%**	8,504	**85%**	8,334	**83%**	7,902	79%	6,308	63%	6,157	62%	5,858	59%
Femur Right (N)	10,000	15,554	**156%**	17,939	**179%**	9,055	**91%**	8,808	**88%**	8,318	**83%**	6,919	69%	6,751	68%	5,854	59%
Neck Tension (N)	4,170	11,262	**270%**	2,426	58%	2193	53%	1,911	46%	4,341	**104%**	1,210	29%	1,206	29%	1,693	41%
Neck Comp. (N)	4,000	4,509	**113%**	118	3%	115	3%	114	3%	239	6%	473	12%	465	12%	278	7%
N_{te}	1.00	3.44	**344%**	0.53	53%	0.74	74%	0.54	54%	1.26	**126%**	0.62	62%	0.85	**85%**	0.53	53%
N_{tf}	1.00	1.95	**195%**	0.78	78%	0.62	62%	0.56	56%	0.73	73%	0.43	43%	0.33	33%	0.41	41%
N_{ce}	1.00	0.27	**27%**	0.01	1%	0.00	0%	0.00	0%	0.00	0%	0.04	4%	0.00	0%	0.14	14%
N_{cf}	1.00	2.15	**215%**	0.05	5%	0.03	3%	0.03	3%	0.39	39%	0.32	32%	0.27	27%	0.32	32%

xx Exceeds design requirements
x Exceeds target (80 % of design requirements)

The results showed that the baseline case (no occupant protection system) produces injury indices for head, chest, neck, and femur, which are significantly greater than the requirements.

Concept 1 (airbag +knee bolster) generally met the specified criteria, except for the case where 2 x 20 mm vents were used and there was no front wall ahead of the airbag. Such a condition allows the inflated bag to move away from the occupant, thus reducing the overall resistance the airbag would offer against forward/downward acceleration of occupant's upper body (i.e. the head and chest). Normalized injury index plots for Concept 1 simulations are shown in Figure D-5.

When the front wall was introduced to constrain airbag expansion longitudinally, or if airbag venting was eliminated, the airbag provided improved resistance to occupant head travel. The kinematics show an initial knee hit against the deformable knee bolster with nominal femur loads, followed by pitching of the upper torso and head about the pelvis, with the head and torso striking the airbag and riding down with it with low acceleration; the moderate HIC values were the result of a late head strike against the console (see figure D-6). As the design was further developed, improved airbag design and deployment was implemented, eliminating the head strike, and resulting in improved HIC values (under 200). The peak neck injury values, while within limits, were also observed during the late head strike.

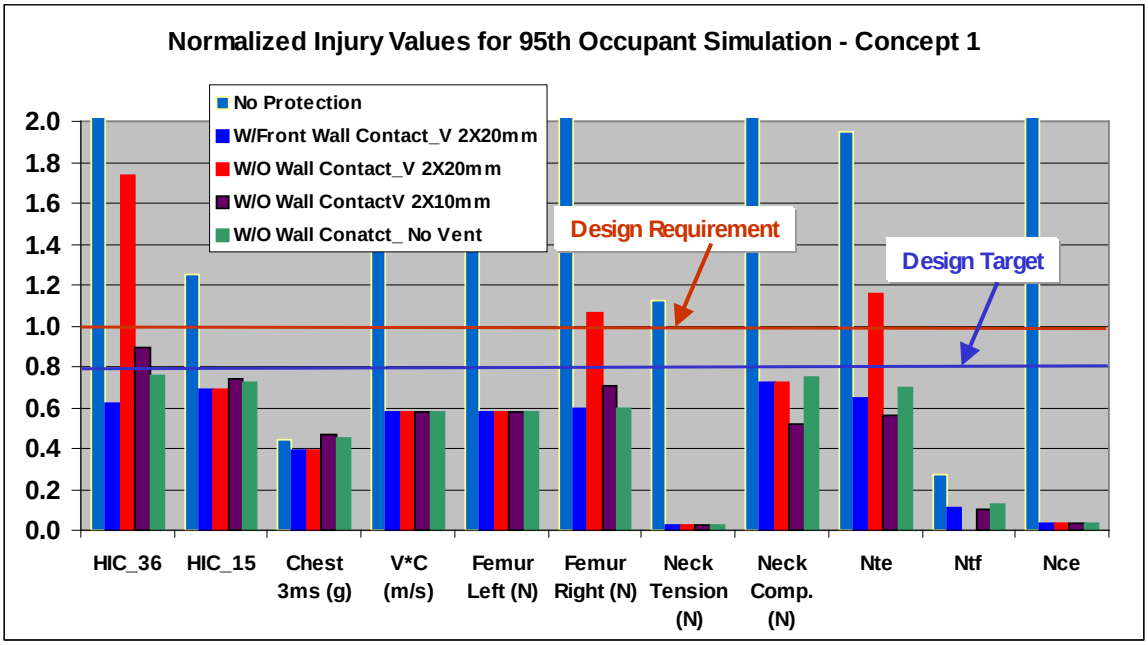

Figure D-5. Normalized Required and Design Target Injury Indices for Concept 1 Configurations

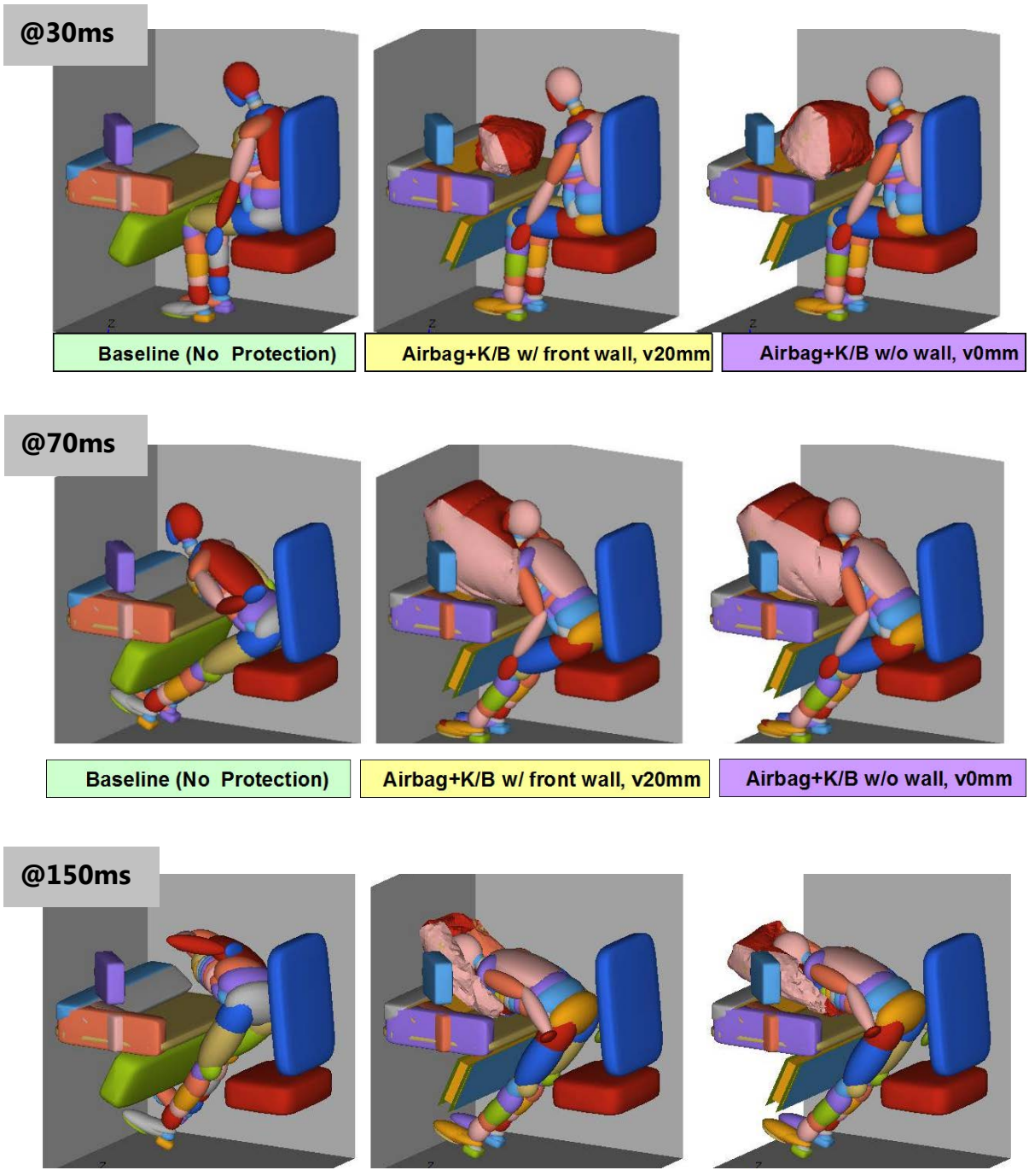

Figure D-6. ATD Kinematics for Baseline, Concept 1 with Front Wall and 20 mm Vents, and Concept 1 without Front Wall and without Vents Configurations @ 30 ms, 70 ms, and 150 ms of Crash Initiation

Results for Concept 2 for the various configurations are shown in Table TD-3 and the normalized injury indices plots are shown in Figure D-7. From an injury index perspective, Concept 2 performed reasonably well, with the following observations:

- When knee airbags were used, chest acceleration and femur load criteria were exceeded.
- With the knee bolster and the ITS positioned close to the occupant, neck injury criteria were somewhat elevated.
- With the ITS moved back, and with the knee bolster, the HIC values approached or exceeded the limit, and the chest injury criteria were also high.

The kinematics generally consisted of initial knee contact with nominal femur loads followed by near simultaneous contact of the head and torso with the ITS systems with relatively high (but below the limit) HIC and chest accelerations (see figure D-8). It was felt that the kinematics of the ATD were less than ideal due to the post-impact rebounding observed.

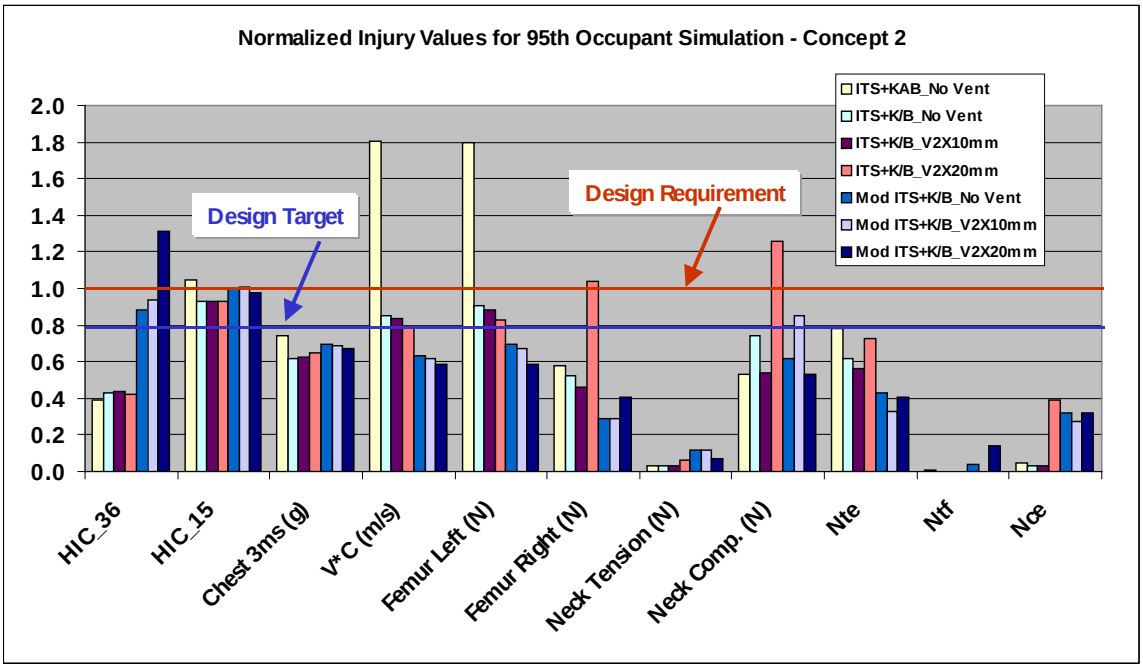

Figure D-7. Normalized Required and Design Target Injury Indices for Concept 2 Configurations

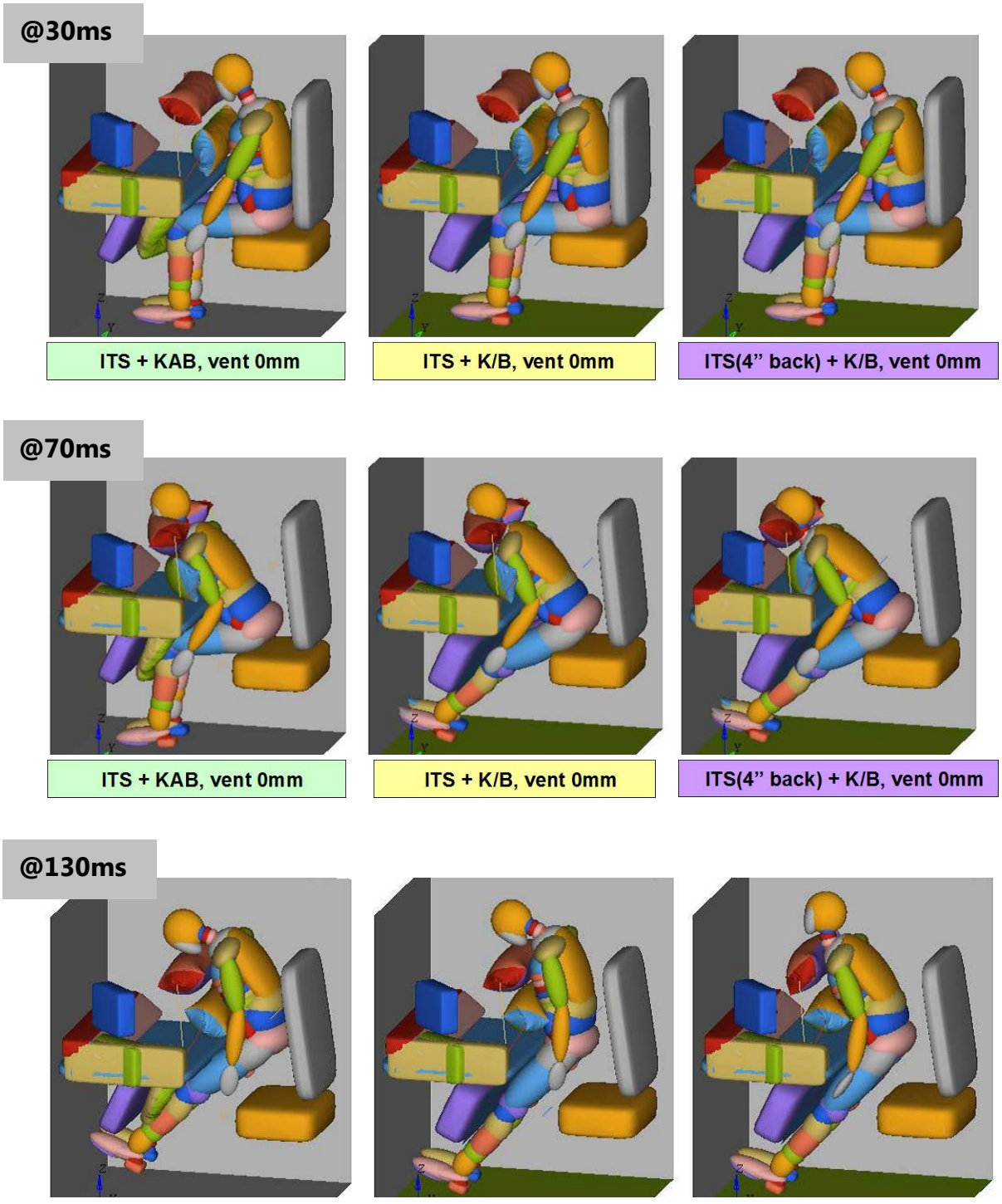

Figure D-8. ATD Kinematics for Concept 2 Configurations: Knee Airbag without Vents; Knee Airbag without Vents with ITS Moved Back by 4 in at 30 ms, 70 ms, and 130 ms After Crash Initiation

SUMMARY

Two concepts for cab engineer protection were developed using a rigorous process and with careful consideration of all design envelope and injury parameters. The developed concepts, as well as a baseline (no protection) version, were further evaluated using MADYMO™ simulations.

For the baseline case, the simulations predicted injury indices well in excess of the prescribed limits.

As expected, both protection concepts considered showed significant improvements for all injury indices compared with the baseline case. Concept 1 (passenger side airbag and knee bolster) showed better performance compared with Concept 2 (ITS with knee bolster), offering better ATD kinematics and the potential for all injury indices to be within 80 percent of the limits. For Concept 2 (ITS), chest injury index values were close to the limits, in addition to exhibiting unfavorable rebounding kinematics for the occupant due to the lack of upper torso energy absorption. Therefore, for this project, Concept 1 was selected for further design and development efforts.

APPENDIX E. Injury Index Plots – Final Run

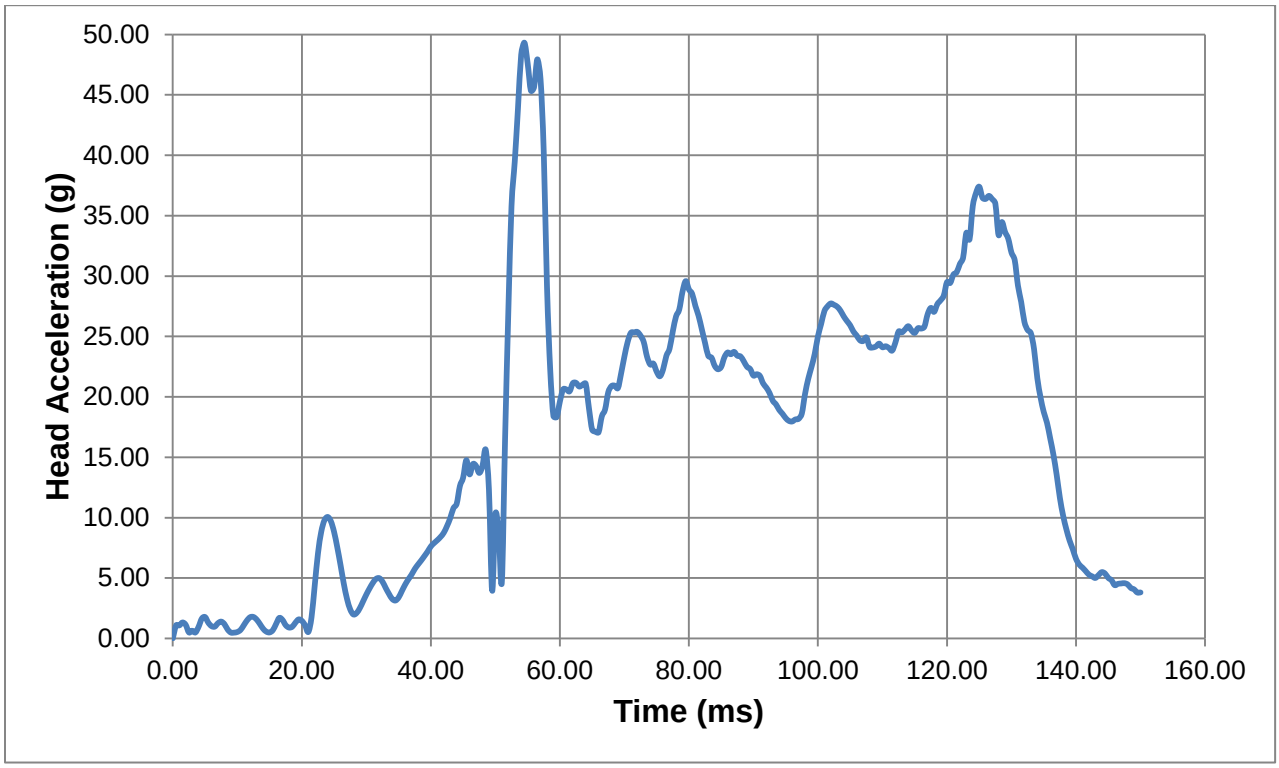

Figure E-1. Head Acceleration Time History

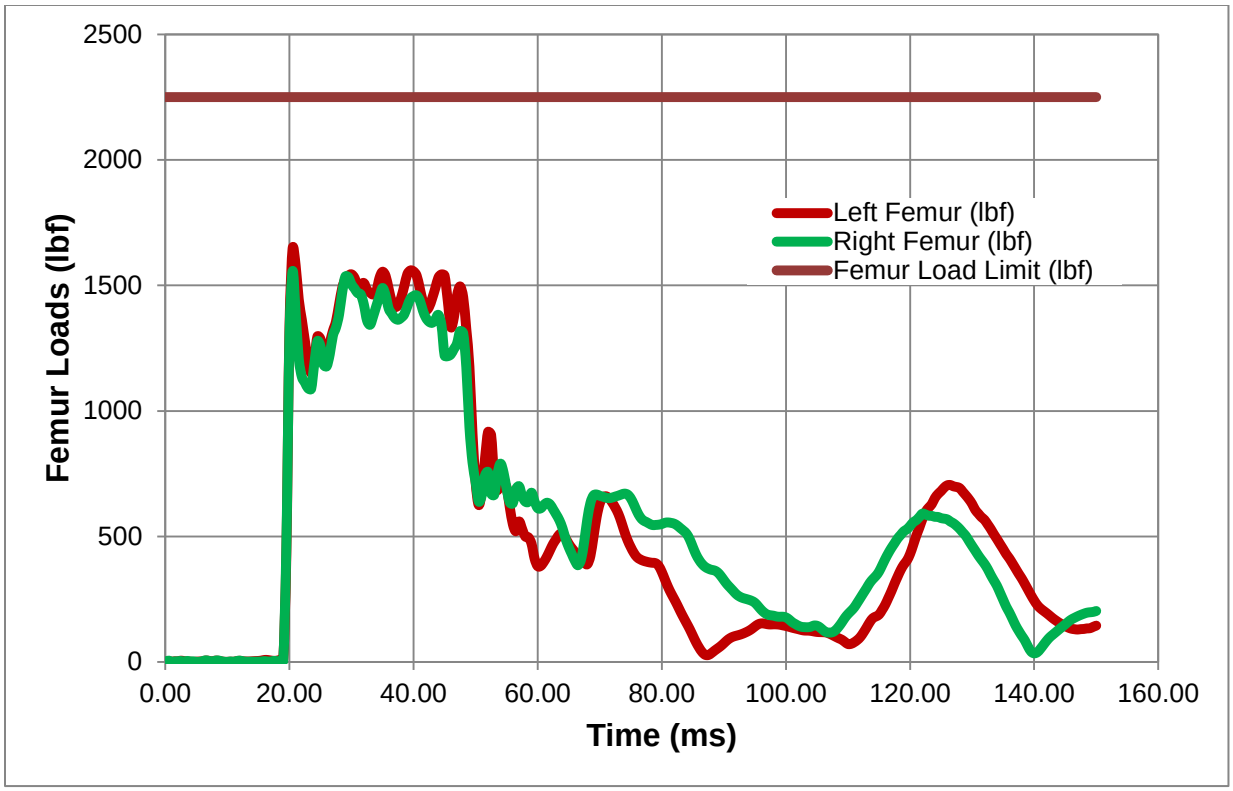

Figure E-2. Femur Loads Time History

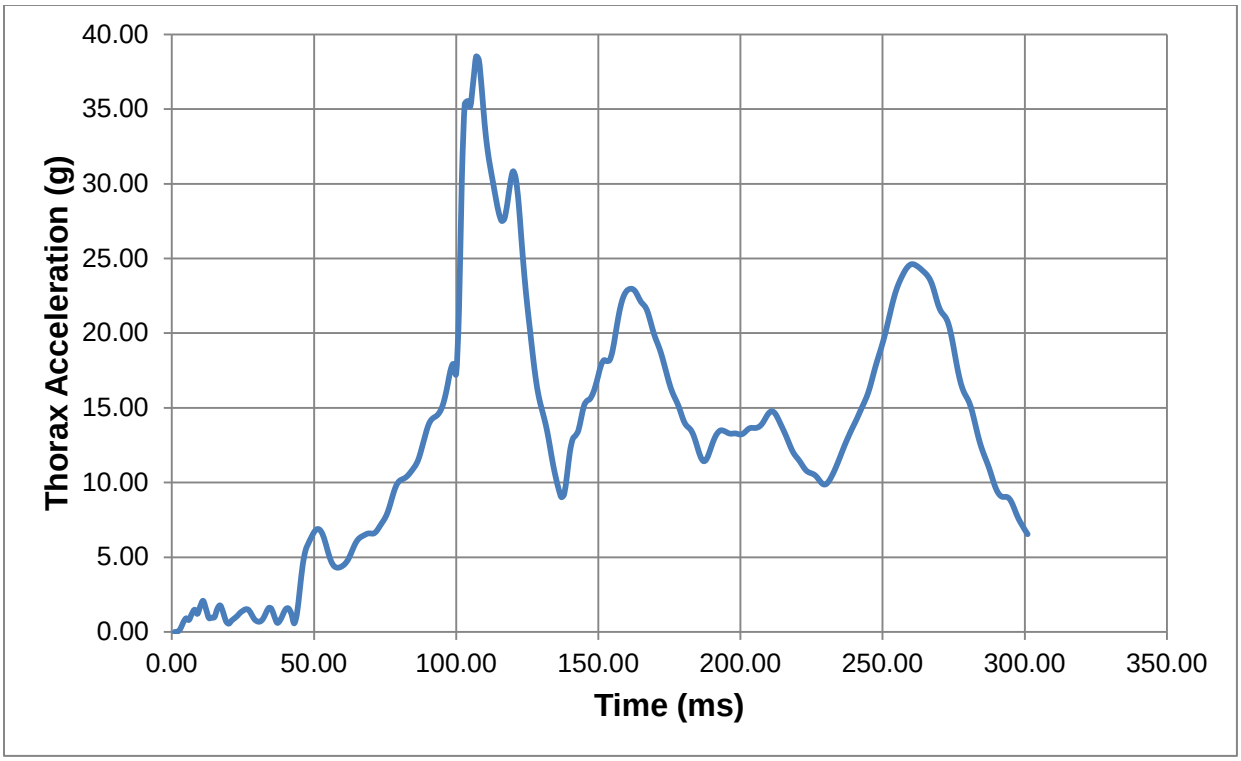

Figure E-3. Thorax Acceleration Time History

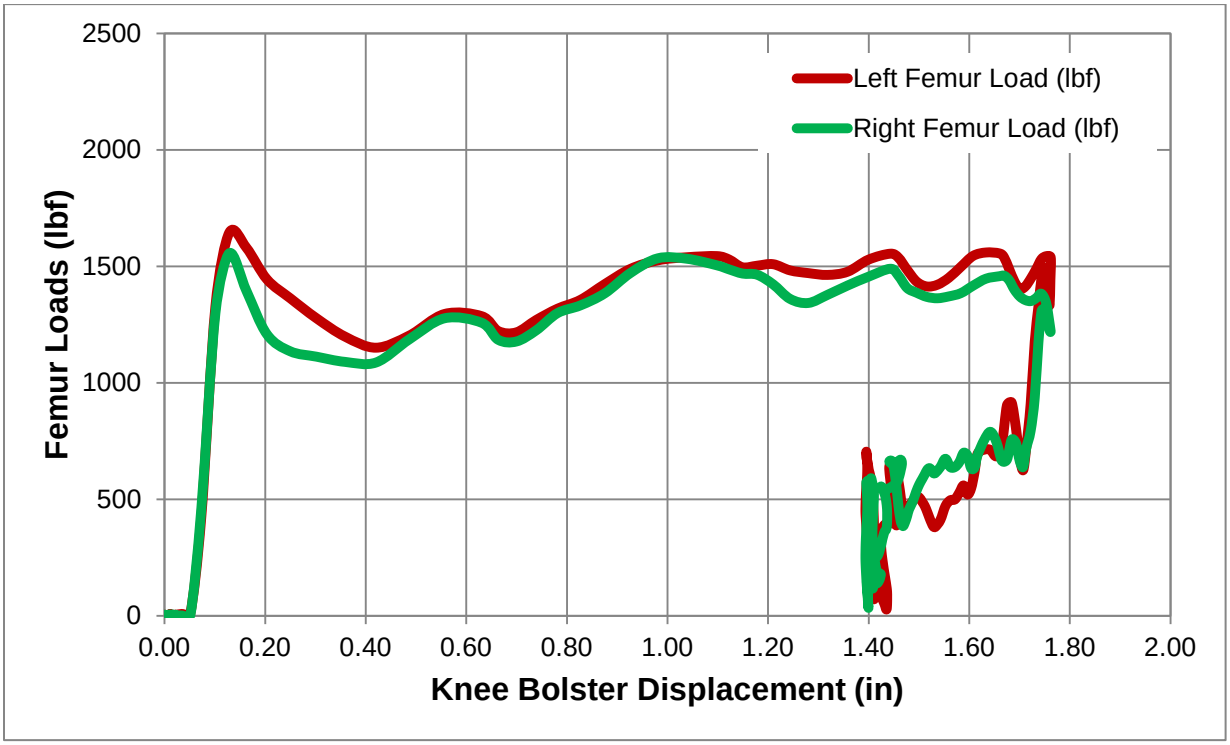

Figure E-4. Knee Bracket - Load versus Displacement

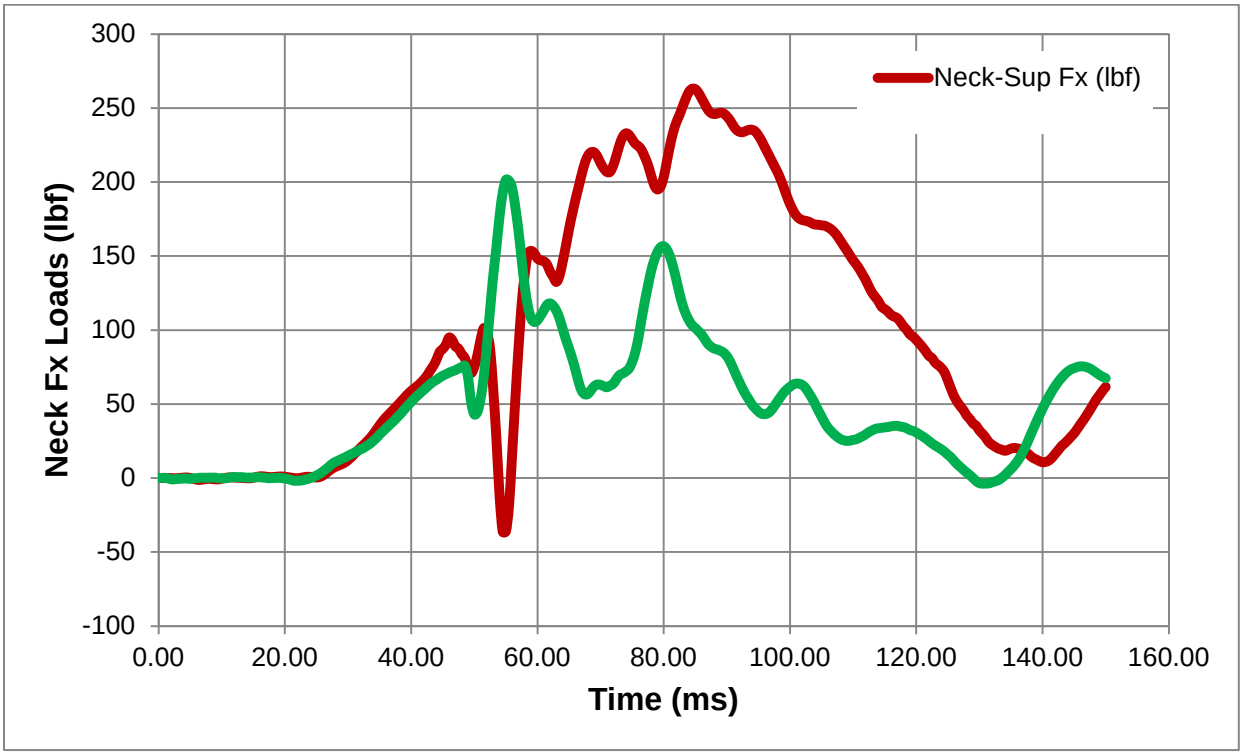

Figure E-5. Neck Fx Loads Time History

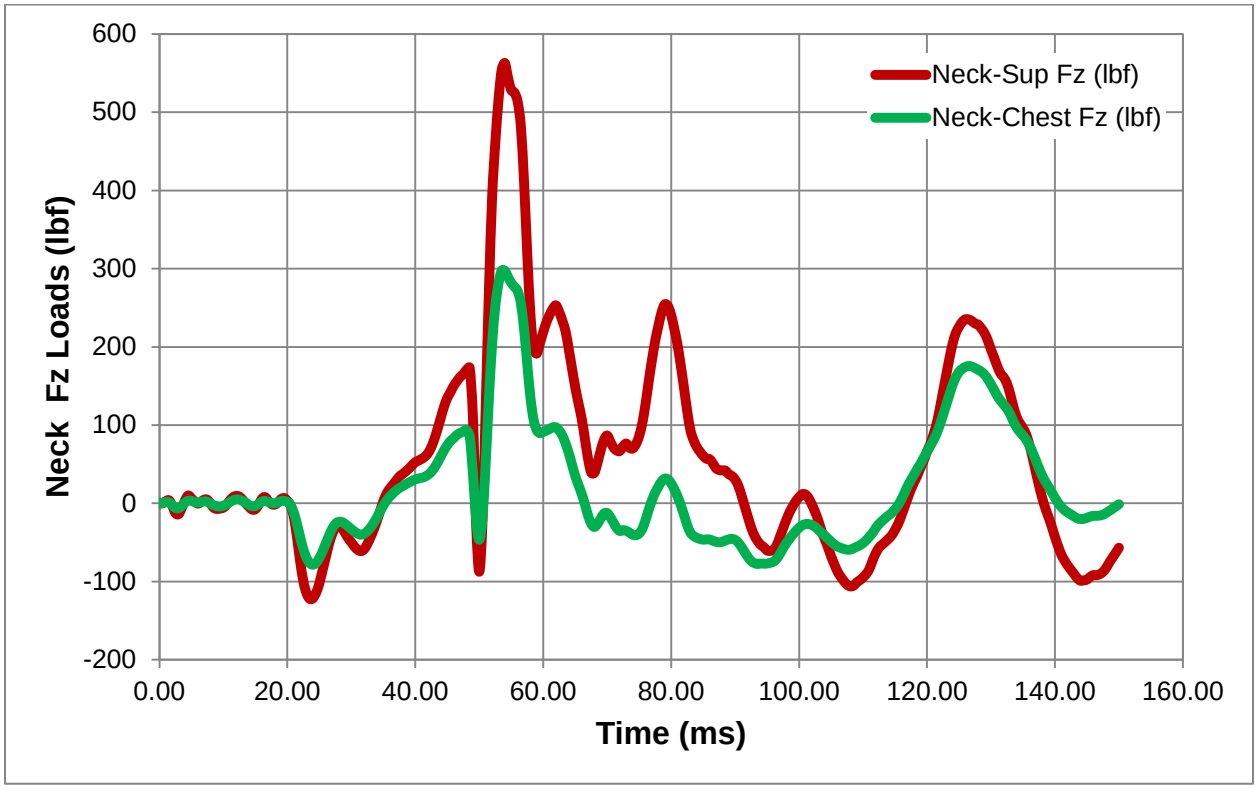

Figure E-6. Neck Fz Loads Time History

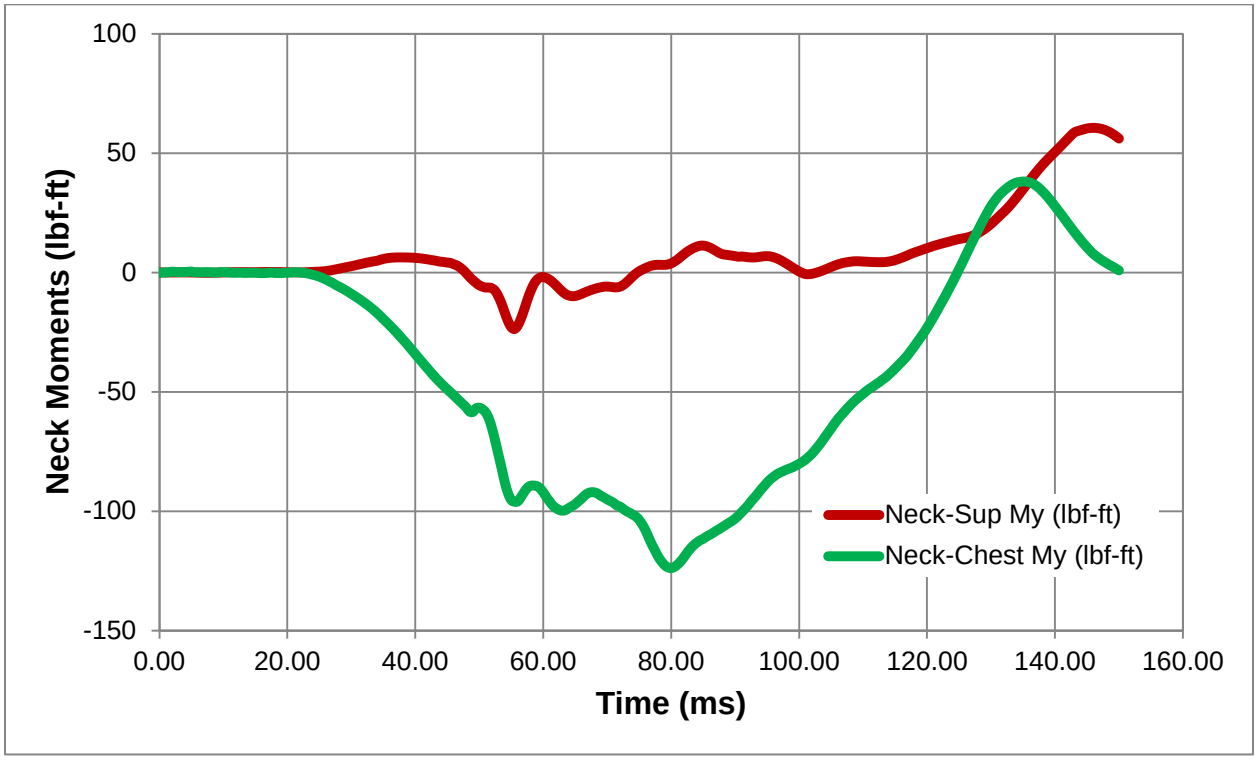

Figure E-7. Neck Moments Time History

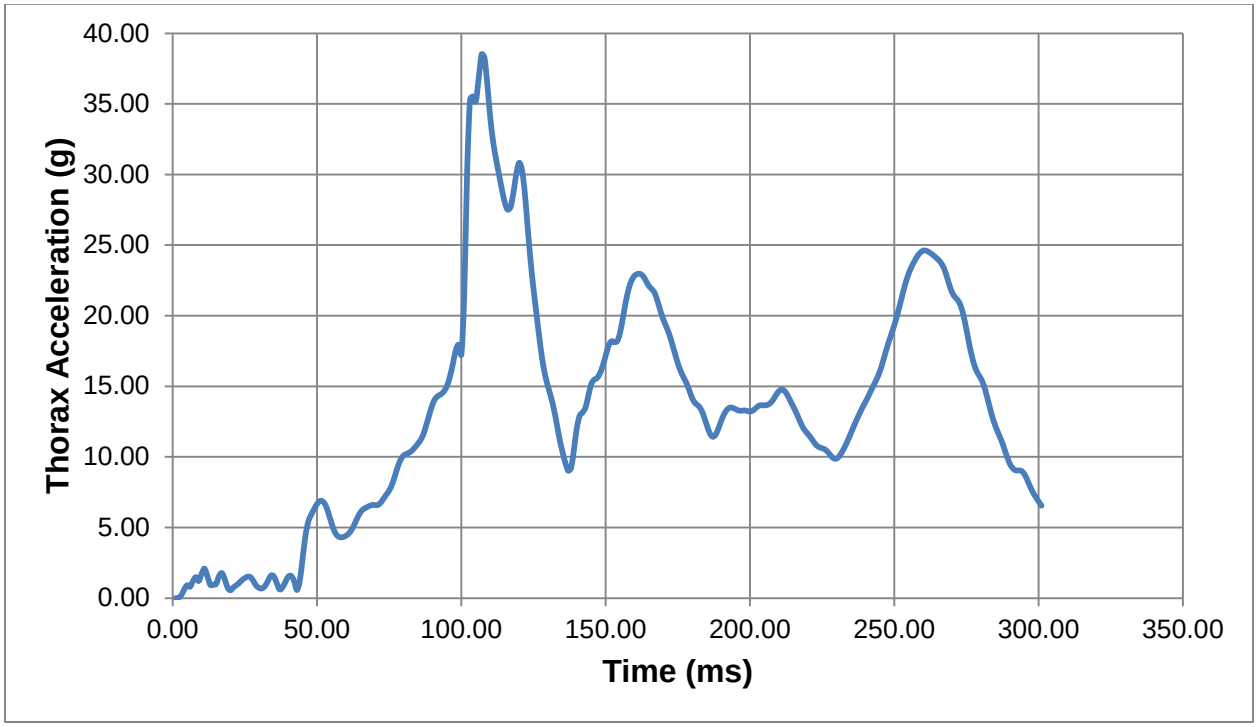

Figure E-8. Thorax Acceleration Time History

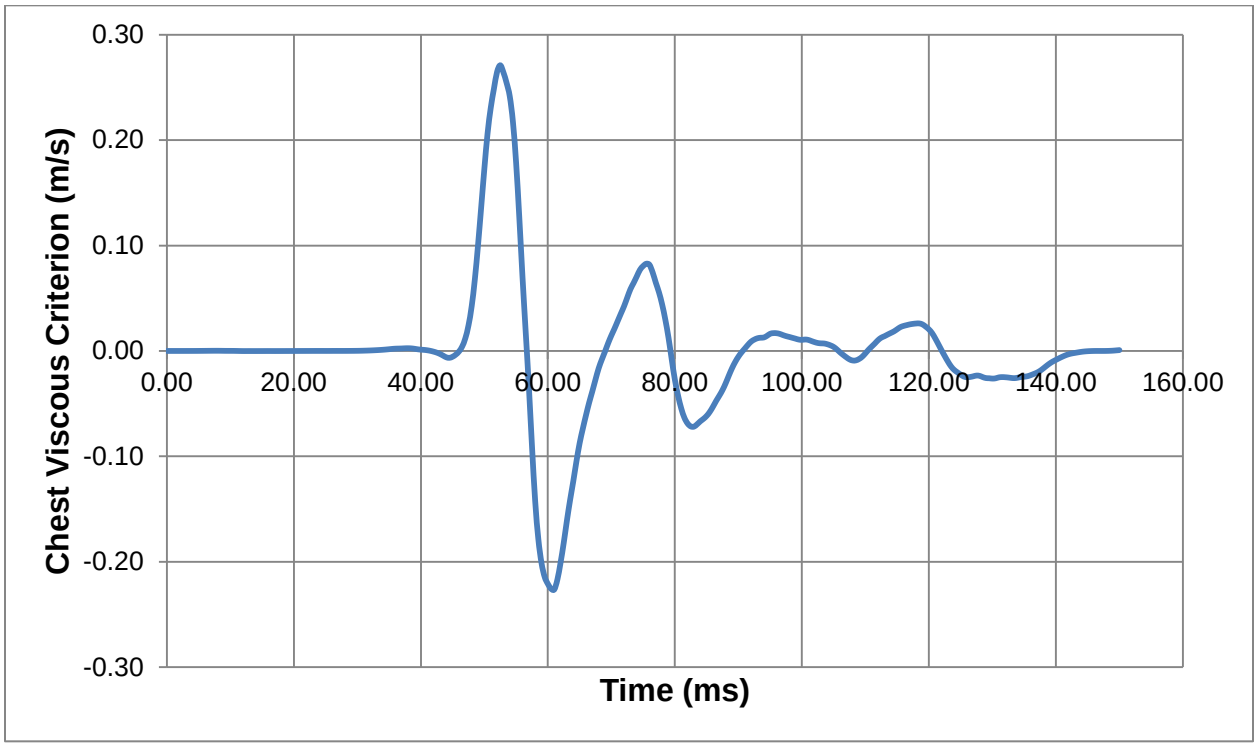

Figure E-9. Chest Viscous Criterion Time History

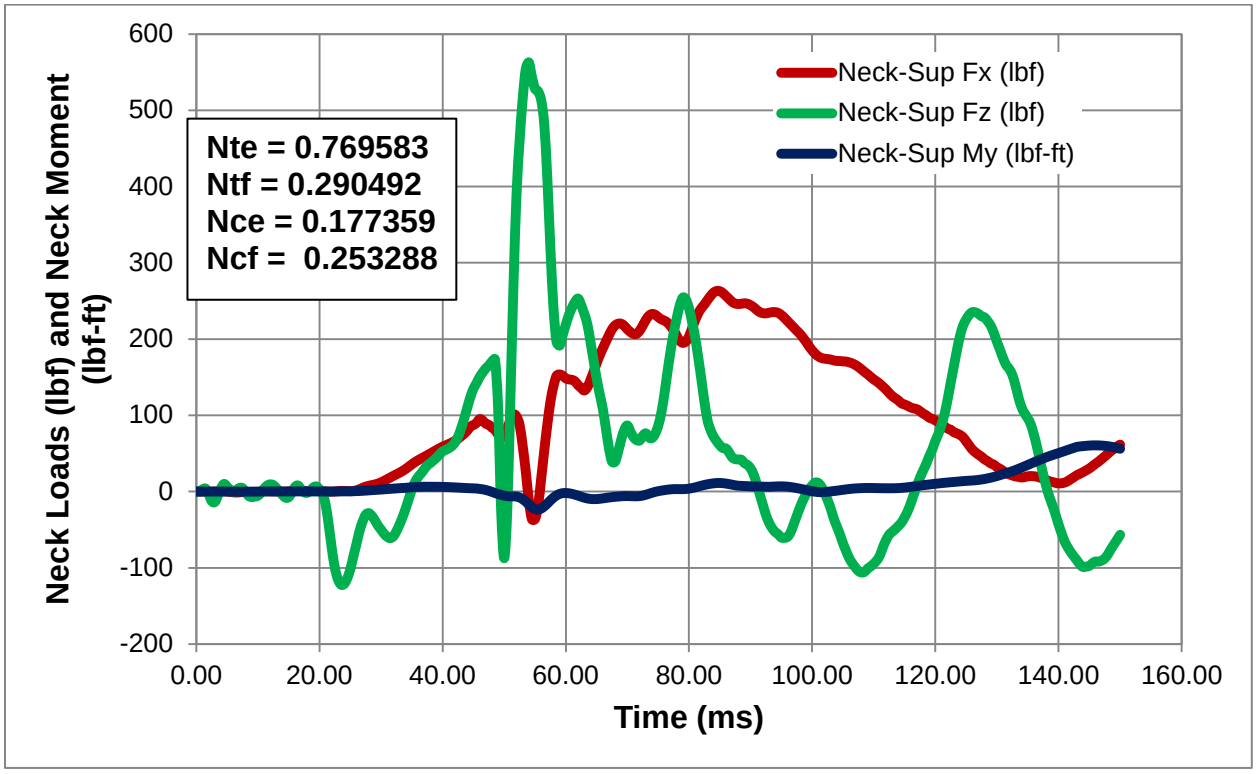

Figure E-10. Neck Injury Criteria (Nij) Summary